IMPACT OF CLIMATE CHANGE ON THE HYDROLOGY OF UPPER BLUE NILE RIVER BASIN: A CASE STUDY IN TANA SUB-BASIN, ETHIOPIA

MSc THESIS

SURAFEL ARAGAW LAMESGIN

HAWASSA UNIVERSITY

INSTITUTE OF TECHNOLOGY

HAWASSA, ETHIOPIA

August, 2020

IMPACT OF CLIMATE CHANGE ON THE HYDROLOGY OF UPPER BLUE NILE RIVER BASIN: A CASE STUDY IN TANA SUB-BASIN, ETHIOPIA

SUBMITTED BY:

SURAFEL ARAGAW LAMESGIN

A THESIS SUBMITTED TO HAWASSA UNIVERSITY DEPARTMENT OF HYDRAULIC AND WATER RESOURCES ENGINEERING,

INSTITUTE OF TECHNOLOGY, SCHOOL OF GRADUATE STUDIES,

HAWASSA UNIVERSITY

HAWASSA, ETHIOPIA

IN PARTIAL FULFILLMENT OF THE REQUIREMENTS FOR THE DEGREE OF

MASTER OF SCIENCE

IN

HYDRAULIC ENGINEERING

August, 2020

SCHOOL OF GRADUATE STUDIES

HAWASSA UNIVERSITY

ADVISORS' APPROVAL SHEET

This is to certify that the thesis entitled "**IMPACT OF CLIMATE CHANGE ON THE HYDROLOGY OF UPPER BLUE NILE RIVER BASIN: A CASE STUDY IN TANA SUB-BASIN, ETHIOPIA**" submitted in partial fulfillment of the requirements for degree of Masters with specialization in Hydraulic Engineering, the Graduate program department of Hydraulic and Water Resources Engineering, and has been carried out by **SURAFEL ARAGAW LAMESGIN, Id No PGHY /014 /10** under our supervision. Therefore, we recommend that the student has fulfilled the requirements and hence hereby can submit the thesis to the department.

ALEMAYEHU MULUNEH (Ph.D.)	----------	----------
Name of Major Advisor	Signature	Date
MIHRET DANANTO (Ph.D.)	----------	----------
Name of Co- Advisor	Signature	Date

SCHOOL OF GRADUATE STUDIES

HAWASSA UNIVERSITY

EXAMINERS' APPROVAL SHEET

We, the undersigned members of the board of examiners of the final open defense "**IMPACT OF CLIMATE CHANGE ON THE HYDROLOGY OF UPPER BLUE NILE RIVER BASIN: A CASE STUDY IN TANA SUB-BASIN, ETHIOPIA**" and examined the candidate. This is, therefore, to certify that the thesis has been accepted in partial fulfillment of the requirement for the degree of master of science.

---	---	---
Name of the Chairperson	Signature	Date
---	---	---
Name of the Internal Examiner	Signature	Date
---	---	---
Name of the External Examiner	Signature	Date
---	---	---
DGC/SGC	Signature	Date
---	---	---
SGS	Signature	Date

DEDICATION

I dedicated this thesis to **Likemenkrat Kessis Abebe (Abewa)** and his families, He scarifies for my success and for his kindness love and support me at all my life.

DECLARATION

I, SURAFEL ARAGAW declare that this thesis is my own original work and has not been presented for a degree award in any other University and HAWASSA University, and all material sources used in this study have been accordingly acknowledged.

Signature: - ---------- Date: - ----------

Email: surafael21@gmail.com

ACKNOWLEDGEMENT

Above all I thank the almighty of **GOD** for his mercy, grace, love and blessing with his mother St. Marry all his Angels and Saints for his helpful gifts to me, nothing could be achieving without his help, during all my works and in all my life.

I would like to express my sincere gratitude to my advisors Dr. Alemayehu Muluneh and Dr. Mihret Dananto for their giving me respected guidance, endless support and insightful comments extended throughout my work.

I would like to express my heartfelt thanks to Ethiopian Road Authority (ERA) for providing me a sponsorship to learn my MSc. Program and Hawassa University Institute of Technology.

I highly grateful to all offices and personalities who has provided me the necessary data for my-study: Ministry of Water, Irrigation and Energy, National Metrological Agency and International Water Management Institute.

I strongly extend my acknowledgement to Dr. Asres Tiku, Mrs. Abebech Abate, Mrs. Simegn Minuye and her Families, Dn-Ing Ermias Abebe, Mr. Liul Kassa (Bedlu) Mr. Muluken Ashagrie, Aba Mekonen Derese, Dr. Melaku Degife, Dr-Ing Netsanet Zelalem, Mr. Daniel Tamene, Mr. Tilksew Demeke, Mr. Workneh Tariku, Mr. Yabizot Aragaw, Mr. Wolde Chanie, Mr. Mebratu Esubalew, Mr. Adane Mezemr, Mr. Yitakel Asfaw, Mr. Tesfalem Abirham, Miss Seble Gizachew, Mr. Diriba Worku, Mr. Worku Nigussie, Mr. Bayu Atale and all my families, friends and classmates.

Finally, sincerest Thanks to Likemenkrat Kessis Abebe Lamesgin (Abewa) and his families, Indeed I have no wards can really express the degree of gratitude and appreciation I have for you. I know that I am nothing without your guidance, support and your continuous inspiration throughout my life.

TABLE OF CONTENTS

LIST OF TABLES

LIST OF FIGURES

LIST OF ACRONYMS/ ABBREVIATIONS

AR4	Fourth Assessment Report
AR5	Fifth Assessment Report
Arc GIS	Software for Geographic Information Systems
CFSR	Climate Forecast System Reanalysis
CMhyd	Climate Model data for hydrologic modeling
CMIP5	Coupled Model Inter comparison Project phase five
CORDEX	Coordinated Regional Climate down scaling Experiment
CV	Coefficient of Variation
DEM	Digital Elevation Model
ENMA	Ethiopian National Meteorological Agency
FAO	Food and Agricultural Organization
FCCC	Framework Convention Climate Change
GCMs	General Circulation Models
GHG	Greenhouse gas
GP	Grid Point
HadCM3	Hadley Centre coupled model version3
HadGEM2-ES	Hadley Global Environment Model 2 - Earth System
HRU	Hydrological Response Units
IPCC	International panel on climate change
IWMI	International Water Management Institution
MWIE	Ministry of Water, Irrigation and Energy
NCEP	National Center for Environmental Prediction

NMA	National Meteorology Agency
NSE	Nash and Sutcliffe Cofficient of Efficiency
PC	personal computer
RCM	Regional climate model
RCP	Representative Concentration Pathways
SDSM	Statistical Downscale Model
SWAT	The Soil and Water Assessment Tool
SWAT-CUP	Soil and Water Assessment Tool- Calibration and Uncertainty prediction
USCCP	United Nation Climate Change Science Program
UBNRB	Upper Blue Nile River Basin
USACE	United State Army Crops of Engineering
WCRP	World Climate Research Program
WLRC	Water and Land Resource Center

ABSTRACT

Climate change is one of the serious issues in the word including developed and developing countries like Ethiopia. Tana Sub-Basin is located in the upper Blue Nile River basin . The aims of this study was to evaluate the impact of climate change on the hydrology of Upper Blue Nile River basin of Tana sub-basin in the northwest of Ethiopia. Dynamically downscaled climate model precipitation and temperature outputs were obtained from CORDEX-Africa program RCP4.5 and RCP8.5 by Regional Climate Model. The climate data has significant bias and bias correction was done by using CMhyd tool before used as input to the impact analysis. The analysis was performed in two future projection, 2020-2049 and 2050-2079 considering the reference baseline period 1988-2017 with both RCPs. Minimum temperature changes for RCP 4.5 raised by 0.26°C to 1.10°C and 0.45°C to 2.77°C, and for RCP8.5 0.15°C to 1.58°C and 1.02°C to 2.68°C Mean monthly minimum temperature change for 2020 – 2049 and 2050 – 2079. and Maximum temperature changes for RCP 4.5 and increase by 0.25°C to 1.6°C and 0.1°C to 1.91°C and for RCP 8.5 0.11°C to 1.92°C and 0.19°C to 2.17°C for 2020 – 2049 and 2050 – 2079 time periods with reference to the baseline periods respectively. And also, the mean monthly precipitation change will be increased and decreased by 2.09% to 23.95 % and 30.73% to 47.46% for both RCP4.5 and RCP8.5 scenarios respectively. The SWAT models were used to assess the streamflow response to climate change. Calibration and validation of the model output were performed by comparing simulated streamflow with observed flows from Tana Sub-Basin (Blue Nile River outlet at Bahirdar gauging station) for the periods 1988-2001 for calibration and 2002-2008 for validation using SWAT-CUP(SUFI-2). The model calibration and validation result shows R^2 and NSE of 0.87 and 0.84 and 0.61 and 0.6 during calibration and validation respectively. Finally, climate change impact on monthly streamflow was evaluated by relating base period stream flow with the future flows for the 2020-2049 and 2050-2079 for both RCP4.5 and RCP8.5 scenarios. The future streamflow result shown increasing and decreasing change for both RCP4.5 and RCP8.5 scenarios. Hence, the increased and decreased stream flow in the basin may have a significant contribution for the sustainability of existed and undergoing water development projects.

Key words: Climate change, Tana sub-basin, RCPs, Bias correction, Trend analysis, Climate projection, SWAT2012

1. INTRODUCTION

1.1 Background

Water is an essential resource for all forms of life on our planet. Substantial effects of a changing climate are mediated through changes in the water cycle, because water resources are very sensitive to changing climate conditions. Thus, hydrological impacts of changing climate conditions are a potential threat to human societies as they often have serious consequences for agriculture, people living near water bodies, hydropower production and ecosystems. Therefore, it is necessary to provide information on potential future changes in the hydrological cycle to enable decision makers to develop possible mitigation and adaptation strategies (Teutschbein, and Seibert, 2012)

Climate change has emerged as one of the development challenges of the 21st century. There is high confidence and agreement among the global scientific community that climate change poses a serious threat to current and future sustainable development. In these days the awareness of the effect of climate change due to human activities has been accelerating. Climate change and variability has many significant effects on the hydrological cycle and thus also on hydrology and water resources system. The Intergovernmental panel on climate change has addressed this realization. Greenhouse gasses have played a great role in changing the climate change at global as well as regional level (IPCC,2014).

According to the International Panel on Climate Change (IPCC) report, by 2100 global average temperature would rise between 1.4 and 5.8°C and precipitation would vary up to ±20% from the 1990 level. Being one of the very sensitive sectors, climate change can cause significant impacts on water resources. Developing countries, such as Ethiopia, will be more vulnerable to climate change mainly because of the larger dependency of their economy on agriculture. Hence, assessing vulnerability of water resources to climate change at a watershed level is very crucial. This gives an opportunity to plan appropriate adaptation measures that must be taken ahead of time. Moreover, this will give enough area to consider possible future climate change effect on hydrology and water resource (IPCC, 2007).

Climate change will have a deep impact on the availability and variability of fresh water as the frequency of climatic extremes such as temperature, drought, and change in rainfall pattern increases in response to global warming. The uncertainty of the availability of water resources will affect agricultural production, challenge socio-economic systems, and threaten environmental sustainability by increasing use of non-recyclable resources to feed

the growing population. The effect of climate change will be significant particularly in developing countries where their economy is heavily dependent on agricultural production. The IPCC (2014) indicated Africa as one of the most vulnerable continents to climate change and climate variability. Ethiopia is one of the African countries whose economy is mainly dependent on agriculture. Therefore, the country's economy is subjected to a direct impact of climate change. A large portion of lands in Ethiopia is arid or semi-arid, in habited by poor and vulnerable communities wholly dependent on rainfall. In addition, poor land management coupled with increasing climate extremes is affecting the livelihoods of these communities. It is therefore important to understand the impact of climate change on Hydrology /water resources/ to implement appropriate climate change adaptation and mitigation strategies (IPCC,2014). Expansion of small-scale irrigation is one of the mitigation strategies under consideration where dry season streamflow is reliable. However, implementation of such strategies requires a thorough assessment of the impact of climate change on streamflow that is highly sensitive to climate, especially to changes in precipitation, snow regime and evapotranspiration. Climate change scenarios from either General Circulation Models (GCMs) or simple analog models are frequently used to assess the hydrological impacts of climate change. Since the impact of climate change can be significantly variable in different Regions, it is important to conduct such study at critical agro-ecological regions to develop and implement adaptation and mitigation strategies (IPCC, 2007).

1.2 Statement of the Problem

Water stress is one of several current and future critical issues facing Africa. About 25% of the contemporary African population experience water stress, while 69% live under conditions of relative water abundance (Vorosmarty et al., 2005). Water supplies from rivers, lakes and rainfall are characterized by their unequal natural geographical distribution and accessibility, and unsustainable water use. Climate change will amplify existing risks and create new risks for natural and human systems. Risks are unevenly distributed and are generally greater for disadvantaged people and communities in countries at all levels of development (IPCC,2014) and Climate change has the potential to impose additional pressures on water availability and accessibility (IPCC, 2007).

Therefore, the freshwater resource of the Upper Blue Nile River Basin is a fundamental basis for the economic growth and social development for communities in the basin and in

the riparian countries of East Africa. However; the ongoing global climate change puts further constraint on the already limited water resources in the basin. Due to high temporal and spatial variability in rainfall, prolonged dry season, global environmental changes and population growth, there is serious pressure on the water resources with consequences for the many rural poor in the basin.

Consequently, a number of studies were conducted on the Nile River. However, few studies investigated the impact of climate change on Upper Blue Nile River Basin (UBNRB). All studies focused on the whole basin and most of them used HEC-HMS and HBV models, while the water resources planning and managements were carried out at catchment level and sub basin level and SWAT models used for hydrological analysis.

Therefore, this study evaluates the effect of climate change on hydrology of lake Tana sub basin, which have important on socio economic activities carried throughout the country and also a big role on Sudan and Egypt.

1.3 Objective of the Study

1.3.1 Genral objective

The main objective of this research was to evaluate the effect of climate change on the hydrology of Tana Sub-Basin.

1.3.2 Specific objective

- To analysis the trends of the observed climate data.
- To assess climate change projection under different RCP Scenarios for near and midterm period.
- To evaluate climate change impact on the hydrology of Tana Sub-Basin by using SWAT model.

1.3.3 Research Questions

1. What are the trends of observed climate data?

2. How to asses climate change projection under different RCP Scenarios ?

3. How climate change affect the hydrology of Tana Sub-Basin?

1.4 Significance of the Research

This study mainly focus how climate change affect the hydrology of the Lake Tana sub basin to show local governments, nongovernmental organizations, policy makers to formulate and implement effective and appropriate response policies to minimize the undesirable effects of future climate change on the study areas.

The major significance of this study is to produce good understanding for planner, decision makers, stake-holders and any concerned bodies to the consequences of climate change on hydrological variables like precipitation, temperature and streamflow by using a recent technique of regional climate models under the two scenarios RCP 4.5 and RCP 8.5.

1.5 Scope of the Study

This research would add a value to understand the effect of climate change on hydrology in Tana Sub basin. The use of climate change scenarios will help to achieve new understanding about the hydrological problems and devising a harmonious solution.

This paper strongly links between climate change and hydrology but climate change links with: ecosystems and biodiversity, agriculture and food security, urbanization, land use and forestry, water supply and sanitation, health, infrastructure, and energy security which, in addition to climate, are strongly influenced by human interventions and actions. So it is impossible to cover those aspects with my specific objectives because of time and resource limitations.

1.6 Limitations of the Study

In this study, the impact of climate change on hydrology was evaluated as the land use/cover will remain constant for the future. however, in the real world, the land use/cover is dynamically changed due to natural and human influences. Moreover, the RCP scenarios were developed only for the three climatic elements: maximum temperature, minimum temperature and precipitation values. Whereas the other elements wind speed, relative humidity and sunshine hour are considered constant in the representative concertation pathway scenarios.

2. LITERATURE REVIEW

2.1 Climate Change

According to the IPCC (2007) definition and usage, the term 'climate change' refers to a change in the state of the climate that can be identified by changes in the mean and properties that persists for an extended period typically decades or longer (IPCC, 2007). in recent decades, changes in climate have caused impacts on natural and human systems on all continents and across the oceans. Impacts are due to observed climate change, irrespective of its cause, indicating the sensitivity of natural and human systems to changing climate (IPCC, 2014).

On a global scale, mean annual surface temperature has increased over the past century by 0.6°C (IPCC, 2001). In the scientific community, there is a general consensus that this increase during the past 50 years can be attributed partly to Greenhouse Gas (GHG) emissions from human activity. Global Climate Models (GCMs), which are capable of providing credible projections of climate changes into the next 100 years, use a coarse global grid scale (IPCC, 2001). Temperature and precipitation trends, however, differ on a regional scale due to different feedbacks appearing from synoptic to local scales. This results in differing impacts at different regional scales. To date, impacts researchers have only had GCM scale output to help determine the impacts of climate change to species and ecosystems on a 50 to 100-year time scale. In order to best assess the expected climate change impacts on a species, ecosystem or natural resource in a region, climate variables and climate change scenarios must be developed on regional or even site-specific scale (Wilby et al, 2001). To provide these values, projections of climate variables must be 'downscaled' from the GCM results, utilizing either dynamical or statistical methods (IPCC, 2001) Downscaling can be accomplished by using either a Regional Climate Model (RCM), or a statistical technique. Since RCM model output is not readily available for Atlantic Canada, a statistical technique will choose for this study. Statistical models are not only readily available. Thus most downscaling experiments can be run in minutes on a Personal Computer (PC) with a moderate processor speed (400-600 MHz), allowing for multiple computations to be run in real time, if required. Climate change refers to a change in the state of the climate that can be identified by changes in the mean and/or the variability of its properties and that persists for an extended period typically decides or longer (IPCC, 2007).

2.2 Climate Change in Ethiopia

Natural and human factors drive climate change by altering the Earth's energy budget. At present, there is a net uptake of the Sun's energy by the Earth system; that is, more energy is entering the Earth system than is being lost back to space. The outcome is an increase in heat energy stored by the Earth. This imbalance is driving the rise in global temperature (IPCC AR5/2014). The IPCC finding indicates that developing countries, such as Ethiopia will be more vulnerable to climate change. Because of the less flexibility to adjust the economic structure and being largely dependent on agriculture, the impact of climate change has far reach implication in Ethiopia.

Mainly, under the prevalent rain fed agricultural production system the progressive degradation of the natural resource base, especially in highly vulnerable areas of the highlands and lowlands coupled with climate variability have aggravated the incidence of poverty and food insecurity (NAPA, 2007).

Climate change is already taking place now, thus past and present changes help to indicate possible future changes (IPCC, 2014). Annual minimum temperature is expressed in terms of temperature differences from the mean and averaged for 40 stations. Over the last decades, the average annual temperature in Ethiopia has been increasing by 0.37^{o}C every ten years, which is slightly lower than the average global temperature rising (NAPA, 2007). The greater part of the temperature rise was observed during the second half of the 1990's and temperature rise is more pronounced in the dry and hot spots of the country, which are located in the northern, northeastern, and eastern parts of the country. The lowland areas are the most affected, as these areas are largely dry and exposed to flooding during extreme precipitation in the highlands.

Precipitation, on the other hand, remained fairly stable over the last 50 years when averaged over the country. However, the spatial and temporal variability of precipitation is high, thus large-scale trends do not necessarily reflect local conditions (NMSA, 2007).

Climate change over the next few decades is largely governed by levels of greenhouse gases already in the atmosphere. The amount of mitigation action assumed in scenarios has little impact in the near-term (IPCC,2013). However, in the middle term future temperature projections of the IPCC mid-range scenario shows that the mean annual temperature will increase in the range of 0.9^{o}C to 1.1^{o}C by 2030, in the range of 1.7^{o}C to 2.1^{o}C by 2050, and

in the range of 2.7ºC to 3.4ºC by 2080 in- Ethiopia compared to the 1961 to 1990 (Emerta, 2013). According to Netsanet, (2013) at UBNRB for the 2050s future time period the downscaled climate predictions indicate rise of 0.6℃ to2.70℃ for the seasonal maximum temperatures Tmax, and of 0.50℃ to 2.440℃ for the minimum temperatures Tmin. Similarly, during the 2090s the seasonal Tmax increases by 0.9℃ and Tmin by 10℃ to 4.6℃, whereby these increases are generally higher for the A2 than for the A1B scenario. And according to Feyissa, et al (2018) the maximum temperature increases were in the range of 0.9℃ (RCP4.5) in 2020 to 2.1℃ and in 2080 at Addis Ababa.

However, the country has both dry and wet periods over the past four decades, precipitation has a general decreasing trend since the 1990's (Abayneh,2011). The average change in annual rainfall is projected to be in the range of 1.4 to 4.5%, 3.1 to 8.4%, and 5.1 to 13.8% over 20, 30, and 50 years, respectively, compared to the 1961 to 1990 period of time. According to Abayneh, the trend analysis of rainfall shows that rainfall remained more or less constant when averaged over the whole country.

2.3 Meteorological Trend Analysis in Ethiopia

A trend refers to an association or correlation between concentration and time or spatial location, but can also refer to any population characteristic changing in some predictable manner with another variable. Trends take various forms, such as increasing, decreasing, or periodic. Detecting and assessing temporal and spatial trends is important for many environmental studies and monitoring programs (ITRC, 2013).

According to the National Metrological Agency (NMA, 2007) revealed that in Ethiopia climate variability and change in the country is mainly manifested through the variability and decreasing trend in rainfall and increasing trend in temperature. Besides, rainfall and temperature patterns show large regional differences. The Ethiopian climate is also characterized by a history of climate extremes, such as drought and flood, and increasing and decreasing trends in temperature and precipitation, respectively.

According to (Getachew, 2017) trend analysis of temperature and rainfall in the case of south Gonder zone. The analysis is based on the temperature and rainfall variation in south Gonder zone over three stations at Addis Zemen, Nefas Mewcha and Mekane Eyesu. The findings of the non-parametric Mann-Kendall test revealed that there was no significant trend in the

annual and seasonal rainfall data whereas monthly rainfall of April and November shown statistically significant increasing trend.

According to Hayelom et al., (2017) The coefficient of variation underlining the significant variability of precipitation. Though, recorded meteorological data analysis of temperature indicates that increasing trends detected. Regarding to the Mann-Kendall monotonic trend analysis test, the maximum temperature examination brings about in a general warming trend while the minimum mean temperature recorded cooling trend. To suggest that developing countries like Ethiopia in particular are more susceptible to the significant influences of climate variability. This is because of their low adaptive capacity and high sensitivity of their socio-economic systems to climate variability and change. Therefore, the concerned bodies should take in to consideration the precipitation and temperature variability of the area in to their climate change adaptation strategy.

According to Netsanet, (2013) Trends in one or another of the three climate variables mentioned. Thus, for the precipitation an increasing trend is observed in two sub-basins and decreasing one in two other sub-basins, but none in the remaining 10 sub-basins. Similarly, for the maximum temperature, the Mann-Kendal test indicates an increasing trend in only one sub-basin, but the seasonal Mann-Kendal test in two. For the minimum temperature, on the other hand, more significant trends are observed in both tests, than has been the case for the other two variables.

2.4 Climate Change and Hydrology

A changing climate and possible impacts on hydrology are currently intensely discussed issues. As the latest Fourth Assessment Report of the Intergovernmental Panel on Climate Change (IPCC 2007) stated, temperature, water vapor and precipitation patterns will significantly change by the end of the 21st century. With those variables being the main factors influencing the hydrologic cycle, climate change is therefore expected to have a major impact on watersheds and sub basins - at both global and local levels (Teutschbein and Seibert, 2012*).*

Since water is an essential resource, variations in the hydrologic cycle often have serious consequences. It is, thus, necessary to adjust future flood control concepts, hydropower production, agricultural irrigation, ecosystem preservation strategies and many more. To provide responsible decision makers with the best possible information, it is the scientists' job to apply reliable and accurate methods, especially in such a relatively uncertain domain

as climate modeling. To drive a hydrological model, reliable information on climatological variables (e.g. temperature, precipitation, evapotranspiration, etc.) and their distribution in space and time are required (Teutschbein and Seibert, 2012).
the role that temperature and water availability play in ecosystem function, climate change will influence aquatic ecosystems and biodiversity. In regions where precipitation is expected to increase, water levels in lakes, wetlands and rivers are also expected to increase in spite of increased evaporation, while the opposite will likely be the case elsewhere. In areas where precipitation and runoff are expected to decrease, drying of streams and lakes for extended periods could reduce productivity (FCCC, 2011).

While these hydrological changes are likely to occur, it is important to remember that ecosystems respond to changes in hydrology in complex and often non-linear ways through interactions between biotic and abiotic processes. This makes it difficult to project changes in aquatic biodiversity at the local level based solely on inferences derived from global climatic and hydrological assessments (FCCC,2011).

A growing body of information and knowledge pertaining to potential links between a changing climate and impacts on water resources is emerging. The graphical representation of the water cycle figure below traces the paths travelled through time and space by the fixed quantity of water found on the planet. By convention, it is often assumed that the cycle begins with evapotranspiration, or the transformation of liquid water into water vapor through the process of evaporation from open water and the transpiration of water through the processes of plant respiration (FCCC,2011).

Important climate control on evapotranspiration include temperature (positively correlated), relative humidity (negatively correlated) and wind speed (positively correlated). It is through the process of evapotranspiration that increasing global temperatures in the coming decades resulting from climate change would most directly affect water resources. Here it should be noted, however, that the increased levels of atmospheric carbon dioxide that will contribute to anticipated increases in greenhouse gas concentrations have the potential to counteract the effects of increasing temperatures. Uncertainty remains about potential future changes in evapotranspiration, as with much of the information on anticipated changes in the global climate system (FCCC,2011).

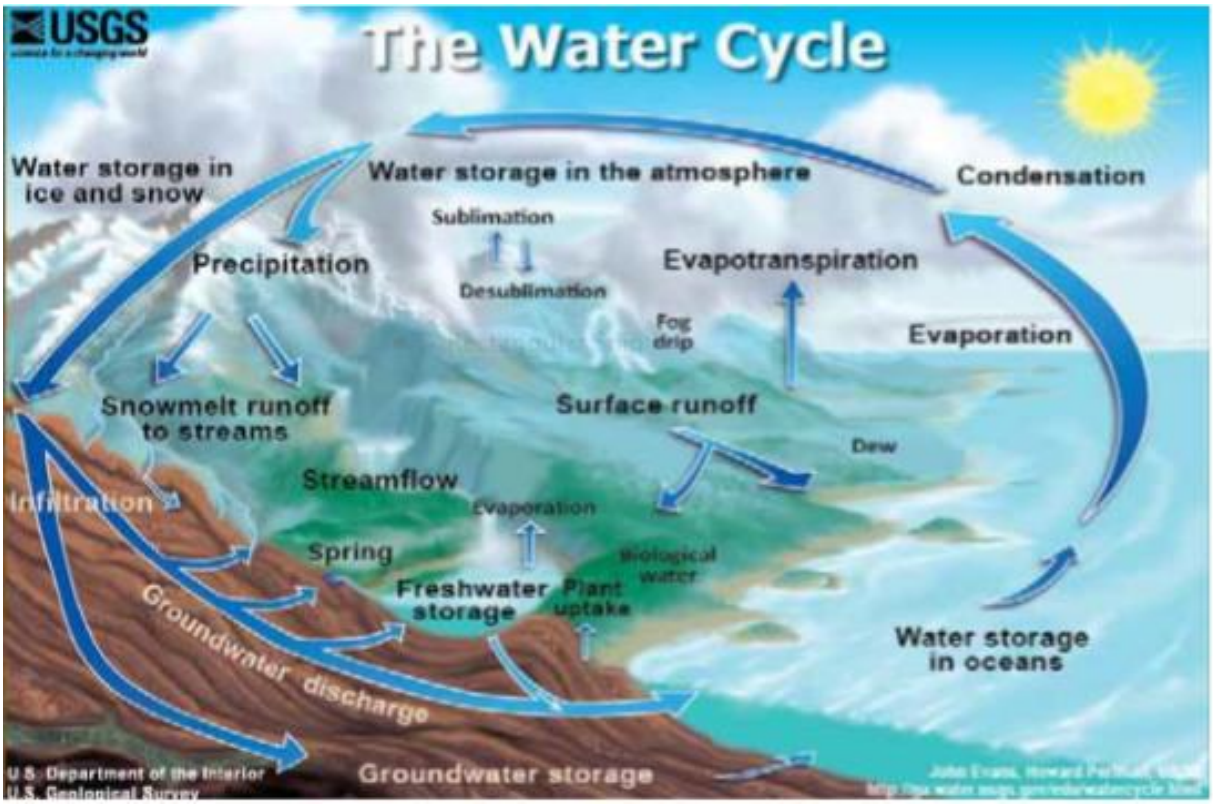

Figure 2. 1: Schematic Representation of Water cycle (U.S Geological Survey)

2.4.1 Impact of climate change on hydrology of Ethiopia

Access to water plays a key role in development. It sustains human life, both through direct consumption and use in agriculture and industrial activities. Availability of water for drinking purposes is also essential and it cannot be separated from wider water resource management issues. The competition between households, agriculture and industry on water can cause conflict over water availability and use. Today, more than one billion people still lack access to safe water, while over two billion lack safe sanitation (Solomon, 2016).

Water is involved in all components of the climate system. Therefore, climate change affects water through a number of mechanisms. Although climate change is expected to affect many sectors of the natural and man-made sectors of the environment, water is considered to be the most critical factor associated with climate change impacts. Therefore, it is very important to make evaluations of the expected impact on the hydrology and water resources due to expected climate changes regardless of the direction of the change (Ringius et al).

According to Gelete et al., (2019) It can be concluded that climate change is becoming a hot issue in the global environment because it affects water resources which humans rely on for drinking, crop production, and manufacturing. Climate change affects water resources in

many ways. It alters the spatial and temporal availability of water. It causes too much water in some areas while there is a drought in some other regions. Climate change increases the demand for water while diminishing the supply (availability). The Blue Nile river basin is one of the rivers which are severely affected by climate change. Even though it covers only 10% of the Nile basin, the Blue Nile generates about 85% of the water that reaches Egypt and Sudan. Therefore, any streamflow reduction in the Blue Nile river basin due to climate change affects water development in downstream countries. Climate change affects the water resources of the Blue Nile basin in many ways. The sediment yield in the basin is high and will increase by 21.3% in the 2080s due to high erosion. Evapotranspiration in the basin is also increasing by 19%, while rainfall is reducing by up to 25%.

According to Netsanet, (2013) on Downscaling and Modeling the Effects of Climate Change on Hydrology and Water Resources in the Upper Blue Nile River Basin. The results of the future simulations of streamflow in the basin, using both SDSM- and LARS-WG downscaled output in SWAT reveal a decline of -10% to -61% of the future Blue Nile streamflow, And, expectedly, these obviously adverse effects on the future UBNRB-water availability are more exacerbated for the 2090's than for the 2050's, regardless of the SRES. According to Melke, (2015) the monthly flow volume did not show systematic trends i.e. increases from month of April-September up to a maximum of 134.54% for A2a and 127.52% for B2a and decreases in the remaining months by 47.44% (A2a) and 46.62% (B2a). Seasonal and annual flow volume increases in all future time horizons as compared to the base period. Seasonally, the maximum increment was shown in the major parts of the rainy season (Kiremit) and small rainy season (Belg) in which the flow volume increases by 144.65% for A2a scenario and 101.58% for B2a scenario. Moreover, the annual increment showed systematic trends and the increment reaches up to 17.65% for both scenarios at the end of 21st century.

The impact of climate change on water resource of lake Tana sub-basin was assessed on the basis of CCCM and GFCD3 UK89 climate change prediction. The CCCM and GFCD3 GCMs predict a reduction of annual runoff by 18.2% and 12.6% respectively, while UKMo GCM predicts wetter condition and as result of an increase in 2.5% in annual runoff (Tarekegn and Tadege, 2006).

Study using dynamically downscaled RCP4.5 climate scenario for an input in HBV hydrological model, climate change is likely to have severe effect on water availability of Tana Belles sub basin. The annual rainfall will likely increase for Lake Tana near and Long

term by 7.6% to 21% while will decreased by 1.2% in medium term. The annual inflow to Lake Tana will likely be increased by 45.9%, 15.86% and 61.2% in near, medium and long term scenario (Belay, 2015).

2.5 Climate Change Scenarios

Climate scenarios are plausible representations of future climate conditions (temperature, precipitation and other climatological phenomena) based on assumptions including future trends in energy demand, emissions of greenhouse gases, land use change as well as assumption about the behavior of the climate system over long time scales. It is largely the uncertainty surrounding this assumption which determines the range of possible scenarios (Carter, 2007).

A scenario is a description of potential future conditions produced to in-form decision making under uncertainty. Scenarios use to make decisions that involve high stakes and poorly characterized uncertainty, which may thwart other, conventional forms of analysis or decision support. Originally developed to study military and security problems, scenarios are now widely used for strategic planning and assessment in businesses and other organizations, and increasingly to inform planning, analysis, and decision-making for environmental issues, including climate change. Scenarios can serve many purposes. They can inform specific decisions, or can provide inputs to assessments, models, or other decision-support activities when these activities need specification of potential future conditions. They can also provide various forms of indirect decision support, such as clarifying an issue's importance, framing a decision agenda, shaking up habitual thinking, stimulating creativity, clarifying points of agreement and disagreement, identifying and attractive needed participants or providing a structure for analysis of potential future decisions (U.S. CCSP, 2007). Future Climate Data Climate scenarios are used to understand the plausible future climate. They are also used to quantify the relative change in the current and future climate, which is often used as an input to the hydrological models to assess the impact of Climate change on hydrological (Wilby & Dawson, 2007).

When applied in climate change research, scenarios help to evaluate uncertainty about human contributions to climate change, the response of the Earth system to human activities, the impacts of a range of future climates, and the implications of different approaches to mitigation (measures to reduce net emissions) and adaptation (actions that facilitate response to new climate conditions). Emissions scenarios are descriptions of potential future

discharges to the atmosphere of substances that affect the Earth 's radiation balance, such as greenhouse gases and aerosols (Bjornaes, 2015).

According to Carter et al., (1999) notification, climate scenarios fall into three main classes which

1. Synthetic scenarios:

Synthetic scenarios describe techniques where particular climatic (or related) elements are changed by a realistic but arbitrary amount, often according to a qualitative interpretation of climate model simulations for a region. For example, adjustments of baseline temperatures by $\pm$1, 2, 3 and 4^{O}_{C} and baseline precipitation by $\pm$5, 10, 15 and 20 percent could represent various magnitudes of future change.

2. Analogue scenarios:

Analogue scenarios are constructed by identifying recorded climate regimes which may resemble the future climate in a given region. These records can be obtained either from the past (temporal analogues) or from another region at the present (spatial analogues).

3. Scenarios from general circulation model outputs.

Most commonly applied scenarios are from climate model outputs. Whereas, Synthetic scenario and analogue scenarios have been applied with reference to or in conjunction with model-based scenarios. (Bjornaes, 2015).

2.5.1 Representative concentration path way (RCPs) vs Emission scenarios

In preparation for the Fifth Assessment Report (AR5), researchers developed a new approach for creating and using scenarios in climate change research. This new approach was motivated by the changing information needs of policy makers. For example, the increasing interest in exploring different approaches to achieving specific climate change targets (such as limiting change to 2°), and growing interest in a "risk management" approach that combines reductions in emissions and adaptation to reduce climate change damages (IPCC,2014).

Scientific advances also dictated the need for new scenarios. Since the Fourth Assessment Report (AR4) important improvements in climate models have been made. As the climate models became more sophisticated, more detailed input was needed. Simultaneously, models that are used in the production of scenarios have improved and more advanced input can therefore be provided (IPCC,2013).

The new approach is built around the concept of Representative Concentration Pathways (RCPs). RCPs are time and space dependent trajectories of concentrations of greenhouse gases and pollutants resulting from human activities, including changes in land use. RCPs provide a quantitative description of concentrations of the climate change pollutants in the atmosphere over time, as well as their radiative forcing in 2100.

The main difference between the new RCPs and the previous scenarios is that there are no fixed sets of assumptions related to population growth, economic development, or technology associated with any RCP. Many different socioeconomic futures are possible leading to the same level of radiative forcing. This enables researchers to test various permutations of climate policies and social, technological, and economic circumstances.

Another key difference is that the RCPs are spatially explicit and provide information a global grid at a resolution of approximately 60 kilometers. This gives the spatial and temporal information about the location of various emissions and land use changes. This is an important improvement as the location of some emissions affects their warming potential.

2.5.2 Climate change observations and Climate change drivers

The Intergovernmental Panel on Climate Change report in IPCC, (2007) strongly confirmed that climate change due to human activities is happening and that its consequences are likely to be serious. Further, it broadly confirmed the findings of the UK Stern Review that the consequences of climate change under business-as-usual scenarios are likely to be far more expensive than efforts to limit climate change by reducing greenhouse gas emissions (Stern, 2006). It also pointed out that stabilizing concentrations of carbon dioxide equivalent (treating all greenhouse gases as if they were carbon dioxide) at 450 ppm still leaves more than 50% chance of global warming greater than 2°C relative to preindustrial conditions, and possibly as high as 3°C.

Climate observations from direct measurements and remote sensing platforms reveal unequivocal warming of the climate system. The atmosphere and ocean have warmed, the amounts of snow and ice have diminished, sea level has risen, and the concentrations of greenhouse gases have increased (IPCC, 2013). The global average surface temperature increased by 0.85 °C over the period 1880 to 2012. For the longest period when the calculation of regional trends is sufficiently complete (1901 to 2012), almost the entire globe has experienced surface warming. Averaged over the mid-latitude land areas of the Northern

Hemisphere, precipitation has increased since 1901 (medium confidence before and high confidence after 1951). For other latitudes area-averaged long-term positive or negative trends have low confidence. The global mean sea level rose by 0.19m between 1901 and 2010. Greenhouse gases emitted by human activities are believed to be the major causes of global warming. The atmospheric concentrations of these gases that include carbon dioxide (CO_2), methane (CH_4), and nitrous oxide (N_2O) have increased since 1750. In 2011 the concentrations of these greenhouse gases were 391 ppm, 1803 ppb, and 324 ppb, and exceeded the pre-industrial levels by about 40%, 150%, and 20%, respectively (IPCC, 2013). Climate change is caused by natural and anthropogenic substances and processes that alter the energy budget. The strength of drivers is quantified as Radiative Forcing (RF) in units of Watts per square meter ($W\ m^{-2}$). RF is the change in energy flux caused by a driver and can be positive or negative. Positive RF leads to surface warming, negative RF leads to surface cooling. The RF can be reported based on the concentration changes of each substance or the level of emission from different sources. The emission-based RF provides a more direct link to human activities. The total radiative forcing is positive with the largest contribution coming from the increase in the atmospheric concentration of CO_2.

2.5.3 Representative concentration pathways (RCP's) scenarios

The Representative Concentration Pathways (RCP) are based on selected scenarios from four modeling teams/models working on integrated assessment modeling, climate modeling, and modeling and analysis of impacts. In its name, the word "representative" signifies that this set of RCPs should be well matched with the full range of emission scenarios (with and without climate policy) available in the current scientific literature.The word "concentration" emphasizes that instead of emissions, concentrations are used as the primary product of the RCPs, designed- as input to climate models.

The RCPs are not new, fully integrated scenarios (i.e., they are not a complete package of socioeconomic, emissions, and climate projections). They are consistent sets of projections of only the components of radioactive forcing (the change in the balance between incoming and outgoing radiation to the atmosphere caused primarily by changes in atmospheric composition) that are meant to serve as input for climate modeling. Conceptually, the process begins with pathways of radioactive forcing, not detailed socioeconomic narratives or scenarios. Central to the process is the concept that any single radioactive forcing pathway can result from a diverse range of socioeconomic and technological development scenarios.

Four RCPs were selected, defined and named according to their total radioactive forcing in 2100. (Richard, 2007). The four RCPs (RCP 2.6, 4.5, 6.0 and 8.5) are consistent with certain socio-economic assumptions.

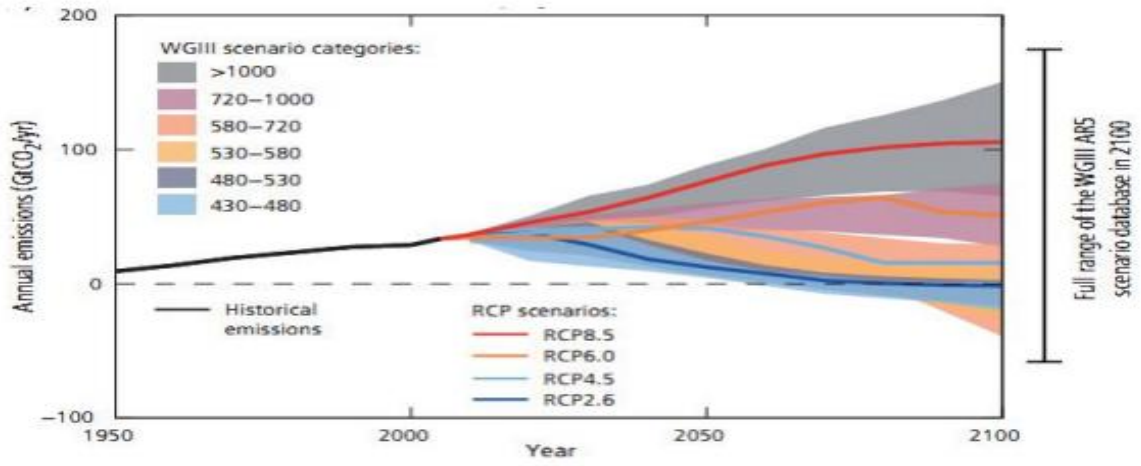

Figure 2. 2: RCPs scenarios annual anthropogenic CO2 emission (IPCC, 2014)

2.5.3.1 The selected representative concentration pathway scenarios (RCPs)

RCP8.5: A high emission pathway for which radiative forcing reaches more than 8.5 Wm-2 by 2100 and continues to rise thereafter. This RCP is consistent with a future no additional policy changes to reduce emissions and is characterized by rising GHG emissions. (The corresponding ECP assuming constant emissions after 2100 and constant concentrations after 2250) (developed by the International Institute for Applied System Analysis in Austria; (Riahi et al. 2011).

RCP6.0: Intermediate stabilization pathway in which radiative forcing is stabilized at approximately 6.0 Wm^{-2} after 2100 through the application of a range of technologies and strategies for reducing GHG emission. (The corresponding ECP assuming constant concentrations after 2150) (developed by the National Institute for Environmental studies in Japan; Masui et al. 2011)

RCP4.5: Intermediate stabilization pathway in which radiative forcing is stabilized at approximately 4.5 Wm^{-2} after 2100 through relatively ambitious emissions reductions. (The corresponding ECP assuming constant concentrations after 2150) (developed by the Pacific Northwest National Laboratory in the USA; Thomson et al. 2011).

RCP2.6: A pathway where radiative forcing peaks at approximately 3 Wm^{-2} before 2030 and then declines to 2.6 Wm^{-2} by 2100. This scenario is also called RCP3-PD (peak and decline). To reach such forcing levels, ambitious GHG emissions reductions would be required over time. (The corresponding ECP is assuming constant emissions after 2100) (developed by PBL Netherlands Environmental Assessment Agency; van Vuuren et al. 2011b)

Developing counters including Ethiopia was under middle/ intermediate emissions scenarios. Hence, for this study the intermediate emission scenarios RCP 4.5 and high emission RCP 8.5 were selected to analyze how driving forces may influence future emission outcomes and to estimate the associated impacts of future climate change on this study area of Tana sub basin.

2.6 Climate Models

Climate Models are the primary available tools for investigating the response of climate system for increasing greenhouse gas concentrations in the atmosphere with Global Circulation Models (GCMs) and attempt to project average temperature, precipitation and cloud cover over future decades or centuries (Goodess et al., 2007). Because of accepted physical principles inherent these models and their ability to reproduce present and past observed climate changes, there is considerable confidence that climate models provide plausible quantitative estimation of major features of climate change at present day (Randall et al., 2007).

Climate models are numerical solutions of a set of partial differential equations set up as an initial value problem. Generally, every GCM is formulated with some fundamental conservation laws, namely: the first law of thermodynamics (describing the movement of energy), Newton's second law of motion (it's about momentum of a particle), three continuity equations (the conservation of mass) and the ideal gas law (for the water vapor) (McGuffie and Sellers, 2005).

There are different climate scenarios for climate change studies. GCM based scenario and Synthetic scenario are often used to project future climate (Getnet et al,2018). This study used a general circulation model (GCM) based scenario to predicted the effect of future climate on the river flow. Scenario-based GCMs are the most common method of developing climate scenarios to quantify and assess the plausible impact of climate change (Abbasnia

and Toros,2016). GCMs are required to project and quantify the relative change of climate variables between the current and future time horizon. Several GCM models include atmosphere, ocean, land surface and sea ice components. This study used the Hadley Center Coupled Model version 3 (HadCM3), which is a coupled atmosphere–ocean model. HadCM3 is developed at the Hadley Center of the United Kingdom National Meteorological Service.

2.7 Climate Model downscaling

Global climate models (GCMs) are typically run at coarse spatial resolutions and result in a mismatch between available climate change projections and the scale of interest to most applications (Brown et al, 2008). Climate downscaling techniques are used to bridge the spatial and temporal resolution gaps between what climate modelers are currently able to provide and what impact assessors require (Wilby & Dawson, 2007a). There are two main types of downscaling techniques dynamical downscaling and statistical downscaling.

1. Dynamical Downscaling:

A Regional Climate Model (RCM) solving the same equation set as a GCM is driven at the lateral and surface boundaries by temporally evolving fields simulated by the GCM. The RCM tries to represent the transfer function F through the same 1st principle (solution methods) as the GCM using higher resolution over a limited geographical region (Wilby and Dawson, 2007).

Dynamical downscaling seeks to couple large-scale climate dynamics and local climate features. It does so by utilizing higher resolution regional climate models (RCMs) that respond to the output of GCMs. The GCM output is provided as boundary conditions, which are the values at the edges of the spatial domain of the RCM. Horizontal resolution for most RCMs is in the order of tens of kilometers which could capture important orographic and physical geography details to the simulations. In terms of temporal resolution, RCMs are usually most skillful at monthly or coarser timescales (Brown et al, 2008).

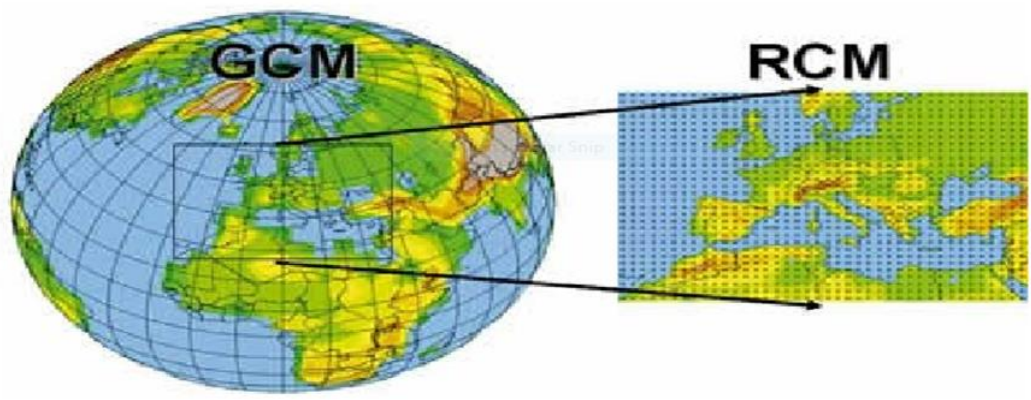

Figure 2. 3: Downscaling from GCM to RCM (Wilby and Dawson, 2007)

2.8 Uncertainties in Global Circulation Models

Uncertainties in climate models arise due to the formulation of climate models and adapted downscaling techniques. Studies show that there are marked differences between models, especially in the prediction of precipitation changes is often prone to a variety of uncertainties (Wilby et al., 2002. The best recommended approach to minimize such uncertainty and to gain- more confidence in the projection of climate change, is the inclusion of as many different types of global models. downscaling techniques and emission scenarios as possible (Goodess et al., 2007). For this study one global model with high and medium RCPs were used.

2.9 Climate Change Projection

Due to the inherent uncertainty of the climate system and the inevitable existence of model errors, the multi- model ensemble is the recommended approach for climate change projections. IPCC has used several models in its coupled model inter-comparison projects (e.g. CMIP3, CMIP5) to make the various projections. There are also regional model inter-comparison projects, like the Co-Ordinated Regional Climate Downscaling Experiment (CORDEX). The CORDEX project is an initiative of the World Climate Research Program (WCRP) performed with the intention of producing an ensemble of high-resolution climate change projections by dynamically downscaling GCM simulations from Coupled Model Inter-comparison Project Phase 5 (CMIP5) data archive (Jones et al., 2011).

The major aims of the CORDEX initiative are to provide a quality controlled dataset of downscaled information, coordinated model evaluation framework, and an interface to the

applicants of the climate simulations for further climate change impact, adaptation, and mitigation studies (Giorgi et al., 2009). Recent analyses in relation to CORDEX simulations over Africa can be found in Nikulin et al. (2012), Hernández-Díaz et al. (2013), and Jacob et al. (2012). Nikulin et al. (2012) evaluate the ability often RCMs over Africa and conclude that all RCMs simulate the seasonal mean and annual cycle quite accurately. Likewise, it is verified that the mean of multi- model outputs does better than individual simulation.
Downscaled rainfall and minimum & maximum temperature) projected climate data for the period 2020-2099 have been obtained from CORDEX-Africa database and is available at a spatial resolution of (approximately 50 km × 50 km). CORDEX is a program sponsored by World Climate Research Program (WCRP) for using the latest generation of regional climate models (RCMs). CORDEX data projections are presented showing possible future regional climate change scenarios on several domains of the worldwide including East Africa.

2.10 Hydrological Models

Hydrology is a science that deals with the occurrences and behavior of water in the atmosphere, on the ground and underground. Hydrological model is an approximation of the actual system with a structure that is a set of equations linking measured inputs and output variables (chow et al., 1988).

Hydrologic models are simplified, conceptual/physical representations of a part of the hydrologic cycle. Because of the limited range of hydrological measurements in space and time, it is necessary to develop a means of extrapolating rainfall-runoff processes from those of available measurements; that is from gauged sites to ungauged sites and from past/current time step into the future time span. This is off course the main function of hydrological models for detail study of water resources.

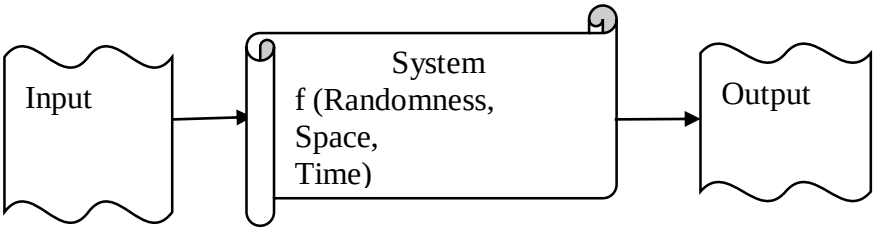

Figure 2. 4: Hydrological model processing

2.10.1 Classification of hydrologic models

Hydrological modeling is a great method of understanding hydrologic systems for the planning and development of integrated water resources management. The purpose of using a model is to establish baseline characteristics whenever data is not available and to simulate long-term impacts that are difficult to calculate, especially in ecological modeling (Lenhart et al. 2002).

There are many classification schemes of hydrologic models, such as short-term vs. long-term, small scale vs. large scale, forecasting vs. predicting, physical vs. mathematical, continuous vs. discrete, descriptive vs. conceptual, lumped vs. distributed, and deterministic vs. stochastic models. Classifications are generally based on the method of representation of the hydrologic cycle or a component of the hydrologic cycle (Zeray, 2006).

Hydrologic simulation models use mathematical equations to calculate results like runoff volume or peak flow. These models can be classified as either theoretical or empirical models. A theoretical model includes a set of general laws or theoretical principles. If all the governing physical laws were well known and could be described by equations of mathematical physics, the model would be physically based. However, all existing theoretical models simplify the physical system and often include obviously empirical components, so they are considered conceptual models. An empirical model omits the general laws and is, in reality, a representation of data (Zeray, 2006). Physically based models are based on our understanding of the physics of the hydrological processes which control catchment response and use physically based equations to describe these processes. Generally, physically based models are used to simulate a wide range of complex aspects (Lenhart et al. 2002).

Hydrologic models are broadly classified as physical model which describe the system as on a reduced scale and mathematical model in which the system operation links input and output variables with a set of equation (Chow et al., 1988).

Additionally, hydrological models are classified as deterministic and stochastic hydrological models. The deterministic hydrological model is the most common model approach in hydrology which can be further classified as lumped, distributed and semi-distributed (Chow et al., 1988).

Lumped hydrological models: Parameters of lumped hydrologic models do not vary spatially within the basin and thus, basin response is evaluated only at the outlet, without explicitly accounting for the response of individual sub-basins. Hence, do not represent physical features of hydrologic processes and usually involve certain degree of empiricism. The impact of spatial variability of model parameters is evaluated by using certain procedures for calculating effective values for the entire basin. The most commonly employed procedure is an area-weighted average (Haan et al., 1998). Example of such models are HBV, IHAC-RES, SRM, and WATBAL etc.

Distributed hydrological models: Such models require input data concerning the spatial distribution of parameter variations together with computational algorithms to evaluate the influence of this distribution on simulated precipitation-runoff behavior so as to model the physical process in detail for highest degree of accuracy in the output Example of such type of models are MIKE-SHE, VIC etc.

Semi-distributed hydrological models: These models are simplified form of distributed models where parameters are partially allowed to vary in space by dividing the basin into a number of smaller sub-basins. Sub division of sub-catchments in to a number of different homogeneous- zones can be accomplished based on various catchments characteristics (topographic elevation, soil type and land use). Examples of such type of models are SWAT, HEC-HMS etc.

2.10.2 Hydrological model selection

There are numerous criteria which can be used for choosing the "right" hydrologic model. These criteria are always project-dependent, since every project has its own specific requirements and needs. Further, some criteria are also user-depended (and therefore subjective), such as the personal preference for graphical user interface (GUI hereafter), computer operation system (OS), input-output (I/O) management user's.

Hydrologic model is generally dependent on the hydrologic components to be incorporated into the water balance system. There are a number of physically based semi-distributed hydrological models, one which is SWAT which is the most promising and computationally efficient model to operate on large basins in a reasonable time (Arnold and Allen,1996; Neitsch et al., 2005). The selection was based on the combined analysis of the above steps and the accessibility of the models from the cost and user kindliness aspects.

2.10.2.1 SWAT model introduction

The SWAT (Soil and Water Assessment Tool) watershed model is one of the most recent models developed at the USDA-ARS (Arnold et al., 1998) during the early 1970's. SWAT model is semi-distributed physically based simulation model and can predict the impacts of land use change and management practices on hydrological regimes in watersheds with varying soils, land use and management conditions over long periods and primarily as a strategic planning tool (Neitsch, et al, 2005).

The interface of SWAT model is compatible with ArcGIS that can integrate numerous available geospatial data to accurately represent the characteristics of the watershed. In SWAT model, the impacts of spatial heterogeneity in topography, land use, soil and other watershed characteristics on hydrology are described in subdivisions.

There are two scale levels of subdivisions; the first is that the watershed is divided into a number of sub-watersheds based upon drainage areas of the attributes, and the other one is that each sub-watershed is further divided in to a number of Hydrologic Response Units (HRUs) based on land use and land cover, soil and slope characteristics.

The SWAT model simulates eight major components: hydrology, weather, sedimentation, soil temperature, crop growth, nutrients, pesticides, and agricultural management (Neitsch, et al, 2005). Major hydrologic processes that can be simulated by this model include evapotranspiration, surface runoff, infiltration, percolation, shallow aquifer and deep aquifer flow, and channel routing (Arnold et al., 1998). Stream flow is determined by its components (surface runoff and ground water flow from shallow aquifer).

2.10.2.2 SWAT calibration and Uncertainty procedures (SWAT-CUP)

Distributed watershed models are increasingly being used to support decisions about alternative management strategies in the areas of land use change, climate change, and pollution control and water allocation. For this reason, it is important that these models pass through a careful calibration and uncertainty analysis. Furthermore, as calibration model parameters are always conditional in nature the meaning of a calibrated model, its domain of use and its uncertainty should be clear to both the analyst and the decision maker. Large-scale distributed models are particularly difficult to calibrate and to interpret the calibration because of large model uncertainty, input uncertainty, and parameter non-uniqueness. To perform calibration and uncertainty analysis, in recent years many procedures have become

available (Abbaspour, 2007). For this study, the hydrologic simulator SWAT under the same platform, SWAT-CUP (SWAT Calibration Uncertainty prediction).

2.10.2.3 SWAT model application in Ethiopia

The SWAT model application was calibrated and validated in some parts of Ethiopia, frequently in Blue Nile basin. Through modeling of Gummara watershed (in Tana basin), (Awulachew et al., 2008) indicated that stream flow and sediment yield simulated with SWAT were reasonable accurate. The same study reported that similar long-term data could be generated from ungauged watersheds using the SWAT model. A study conducted on modeling of the Lake Tana basin with SWAT model also showed that the SWAT model was successfully calibrated and validated (Setegn et al., 2008). This study reported that the model could produce reliable estimates of stream flow and sediment yield from complex watersheds. (Gessese, 2008) used the SWAT model performed to predict the Legedadi reservoir sedimentation. According to this study, the SWAT model performed well in predicting sediment yield to the Legedadi reservoir. The study further put that the model proved to be worthwhile in capturing the process of stream flow and sediment transport of the watersheds of the Legedadi reservoir. In addition to the above, the SWAT model was tested for prediction of sediment yield in Anjeni gauged watershed by Setegn et al., (2008). The study found that the observed values showed a good agreement at Nash-Sutcliff efficiency (ENS) of 80 percent. In light of this, the study suggested that the SWAT model could be used for further analysis of different management scenarios that could help different stakeholders to plan and implement appropriate soil and water conservation strategies.

Tekle (2010) through modeling of Bilate watershed also indicated that SWAT Model was able to simulate stream flow at reasonable accuracy. The literature reviewed and presented above showed that SWAT is capable of simulating hydrological and soil erosion process with reasonable accuracy and can be applied to large and complex watersheds.

2.10.3 Bias-correction method

Often, outputs of regional climate models cannot be directly used for impact assessment as the computed variables may differ systematically from the observed ones. Bias correction is therefore applied to compensate for any tendency to overestimate or underestimate the mean of downscaled variables. Bias correction factors are computed from the statistics of observed and simulated variables (CMhyd user manual, 2016).

2.10.3.1 CMhyd for extraction and bias correction

Watershed models are often used to simulate the impact of future climate conditions on hydrologic processes. However, (Teutschbein and Seibert, 2012) state that simulations of temperature and precipitation often show significant biases due to systematic model errors or discretization and spatial averaging within grid cells, which hampers the use of simulated climate data as direct input data for hydrological models. Bias correction procedures are used to minimize the discrepancy between observed and simulated climate variables on a daily time step so that hydrological simulations are driven by corrected simulated climate data match simulations using observed climate data reasonably well. CMhyd is a tool that can be used to extract and bias-correct data obtained from global and regional climate models. It is highly recommended to apply an ensemble approach, i.e. to use bias-corrected data provided by several climate models and downscaling methods (Teutschbein and Seibert, 2010, 2012).

2.10.3.2 Processing framework of CMhyd

CMhyd was designed to provide simulated climate data that can be considered representative of the location of the gauges used in a watershed model setup. Therefore, climate model data should be extracted and bias corrected for each of the gauge locations.

Bias correction procedures employ a transformation algorithm for adjusting climate model output. The underlying idea is to identify biases between observed and simulated historical climate variables to parametrize a bias correction algorithm that is used to correct simulated historical climate data (CMhyd user manual,2016).

Bias correction methods are assumed to be stationary, i.e. the correction algorithm and its parametrization for current climate conditions are assumed to be valid for future conditions as well. Thus, the same correction algorithm is applied to the future climate data. However, it is unknown how well a bias correction method performs for conditions different from those used for parametrization. A good performance during the evaluation period does not guarantee a good performance under changed future conditions. (Teutschbein and Seibert, 2012) provide a detailed discussion and state that a method that performs well for current conditions is likely to perform better for changed conditions than a method that already performs poorly for current conditions.

3. MATERIAL AND METHODS

3.1 Description of the Study Area

Tana sub-basin is located at the headwaters of Blue-Nile river basin. The drainage area of the lake is 15,319 square kilometers, of which 3100 is the lake area. The geographical location of the Tana sub-basin extends from 10.00ºN to 13.00ºN latitude and from 37.00ºE to 38.00ºE longitude (BCEOM, 1998). Based on the rainfall pattern, the year is divided into two seasons: a rainy season mainly centered on the months of June to September, and a dry season from October to March. In the southern parts of the basin the months of April and May is an intermediate season where slight rains often occur. Out of the total annual rainfall, 70% to 90% occurs in the June to September rainy season. The mean annual flow at the outlet of Lake Tana (Blue Nile river at Bahirdar gauging Station) is about 3.5 billion cubic meters and it varies from a maximum of 7 billion cubic meters to a minimum of 1 billion cubic meters in high and low water years respectively.in Tana sub basin there are four main rivers which are Megech, Ribb, Gummara and Gilgel Abay and all those rivers flows to Lake Tana from different directions.

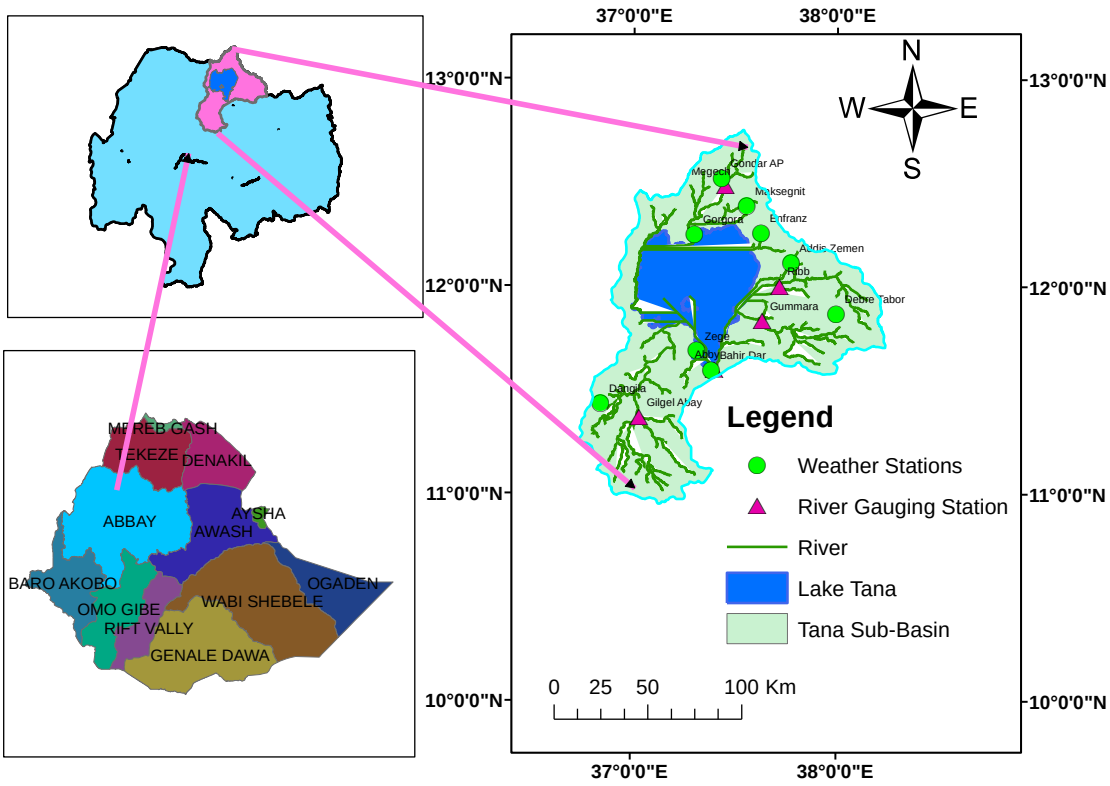

Figure 3. 1: Map of The Study Area

3.1.1 Soil of the study area

The soil data was collected in shape file format from the GIS department of EMWR. It has shown in details the figure. Soil in the Lake Tana sub basin are derived from the weathered basalt and highly variable. in low lying areas north to east of the Tana sub- basin, soil has been developed on alluvial sediment (SMEC, 2007). The figure and table below shown in detail.

Table 3. 1: Soil type and SWAT Code of Tana Sub-Basin

S/N	Soil Type	SWAT Code	S/N	LAND COVER	SWAT Code
1	chromic luvisols	LVx	7	Eutric Vertisols	VRe
2	Eutric cambisols	CMe	8	Lithic Leptosol	LPq
3	Eutric Regosols	RGe	9	Haplic Luvisoil	LVh
4	WATER	WATR	10	URBAN	URMD
5	Eutric Leptosol	LPe	11	Haplic Nitisols	NTh
6	Eutric Fluvisol	FLe	12	Haplic Alisols	ALh

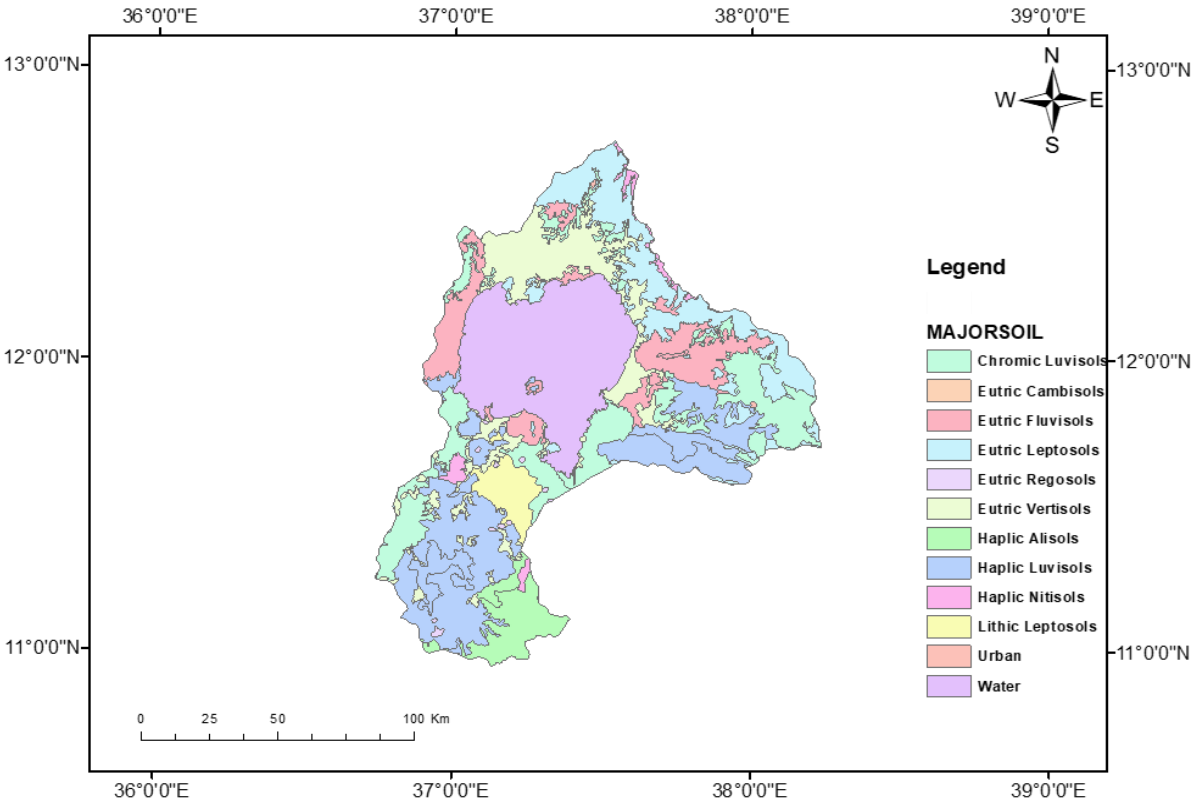

Figure 3. 2: Soil of The Tana sub-Sasin

3.1.2 Land use / Land cover

The land use data is collected from GIS department of EMWR in shape file format. The land use condition in the of the Tana sub-basin includes mainly of intensively cultivated agricultural land, moderately cultivated agricultural land, grassland, Woodland, Water body and forest land, rural and urban settlements. Land use refers to the actual economic activity for which the land is used for, for example, food production, commercial forestry, etc. land cover refers to the sole cover of the earth's surface. The table and figure below shown in detail.

Table 3. 2: Land Cover and SWAT Code of Tana Sub-Basin

S/S	Land Cover	SWAT Code
1	A: Afro alpine	FRST
2	C1: Dominantly cultivated	AGRL
3	C2: Moderately cultivated	AGRR
4	F2: Forest	FRSE
5	G2: Grassland	RNGE
6	H1: water body	WATR
7	H2: Swamp	WETF
8	P1.1: Plantations	AGRC
9	S1: Shrub land	RNGB
10	U: Urban	URMD
11	WO: Woodland open	FRSD

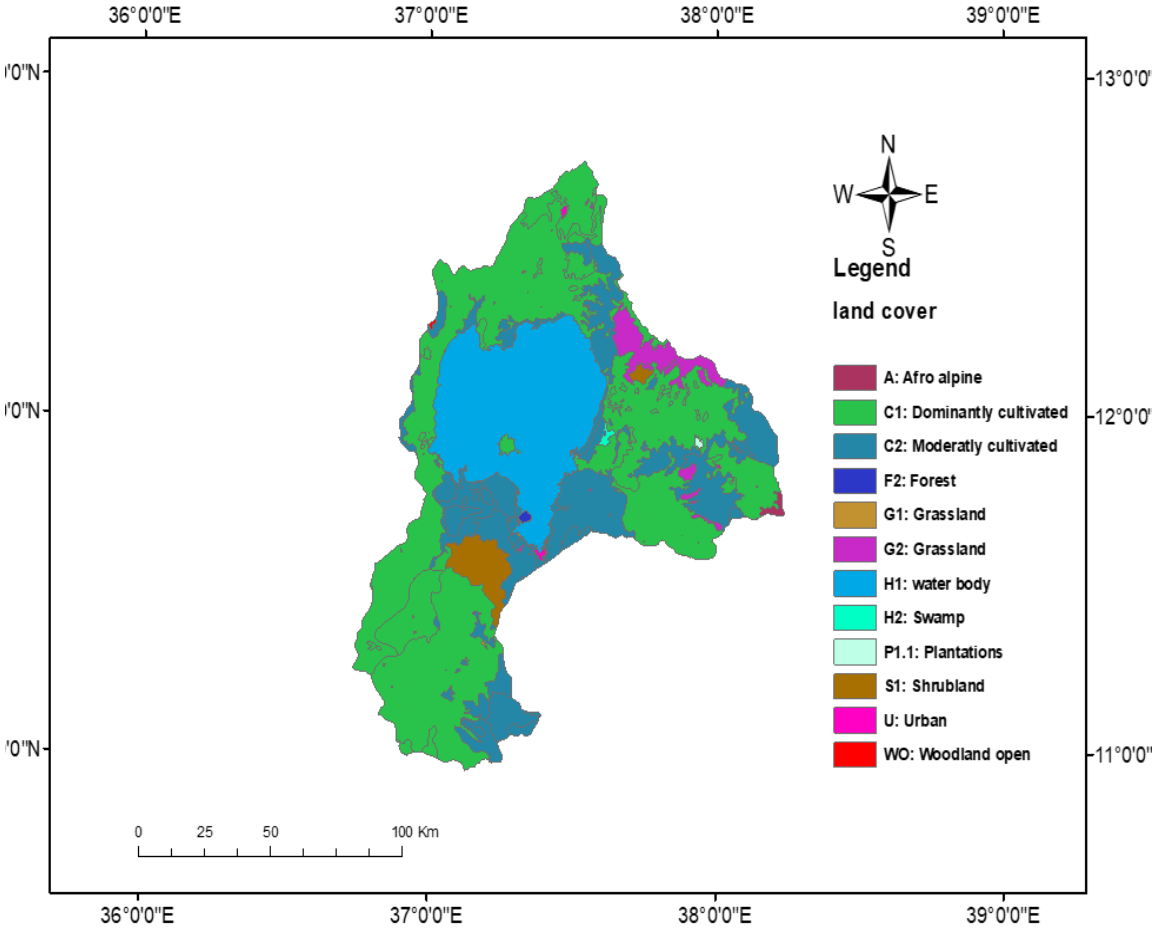

Figure 3. 3: Land use /Land cover of Tana Sub-Basin

3.1.3 Hydrology of the study area

Lake Tana has more than forty tributaries, but the major rivers feeding the Lake are Gilgel Abay (the largest river from the south direction), Gummara, and Ribb from the east and Megech from the north, these four main rivers accounts about 93% of inflow. The only river flowing out of the Lake Tana is the Blue Nile River (Abbay River). The Blue Nile river flow approximately reaches annually about 4 billion meter cubic at the out let of the Lake Tana (BCEOM, 1998)

3.1.4 Climate of the study area

The highlands and high plateaus of Ethiopia greatly influence the climate. In Ethiopia, three seasons can be distinguished based upon the distribution of rainfall (Belete, 2013). The strongly varying topography of Ethiopia leads to three distinct climate zones across the country, namely, Dega (cool zone), Woina-Dega (temperate zone) and Kolla (hot zone); Within each climatic zone, seasonal variations and changing atmospheric pressure systems

contribute to the creation of three seasons, which are known as the Kiremt, Belg, and Bega (Cheung et al., 2008).

The climate of Upper Blue Nile River basin (Tana basin), is dominated by highland tropical monsoon. Even if the basin is located near to equator the climate is comparatively mild due to high elevation. Most of the rainfall (70-90% total rainfall) occurs from June to September (Schipper,2011). April and March are intermediate seasons with some rainfall.

Generally, the climate of Ethiopia is mainly controlled by seasonal migration of Intertropical Convergence Zone (ITCZ) and its associated atmospheric circulation but the topography has also an effect on the local climate. The traditional classification of the country is based on altitude and temperature shows the presence of five climate zones namely, Wurch (cold climate more than 3000m altitude), Dega (temperate like climate-highland with 2500-3000m altitude), Woina-Dega (warm with the altitude of 1500-2500m), Kola (hot and arid type less than 1500m altitude) and Berha (hot and hyper-arid type) climate (NMA, 2001). According to this classification, the majority part of the study area falls in woina dega and the small part of the study area falls in dega and wurch. The climate of lake Tana basin is dominated by an altitude ranging from 1777m to more than 4089m.

3.1.5 Temperature of the study area

The temperature varies considerably in the basin within altitude. According to the data of the seven stations, the mean annual minimum temperature varies from 5.05℃ to 15.49℃ at Dangila and Maksegnit stations and the mean annual maximum temperature varies from 24.38℃ to 31.36℃ at maksegnit and Addis Zemen stations.

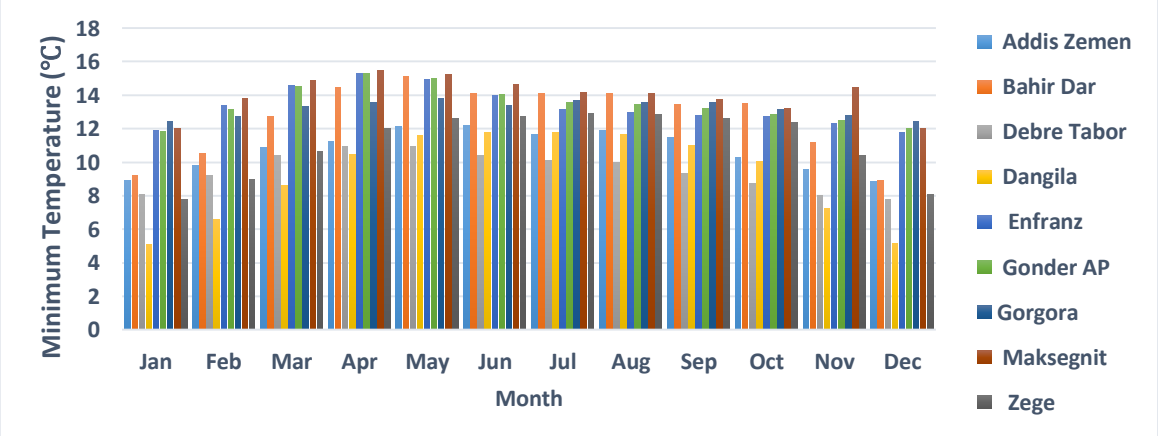

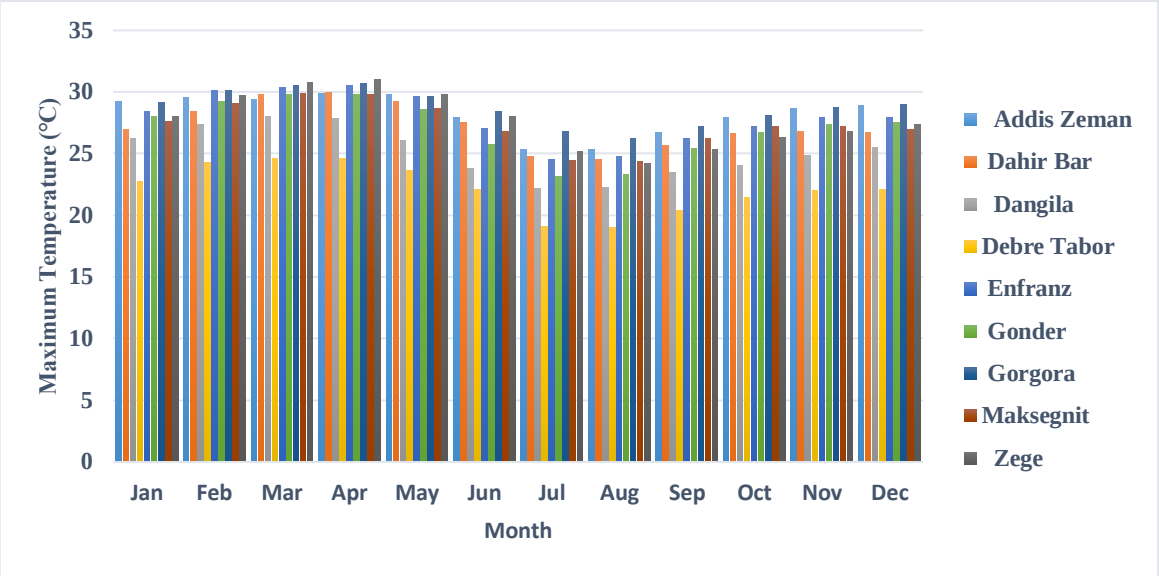

Figure 3. 4: Maximum and Minimum Temperature of selected stations in Tana sub-basin

3.1.6 Rainfall of Tana sub basin

The mean annual rainfall of the study is about 1473.1mm which is oscillating between a minimum of 989.9mm to a maximum of 1655.21mm. The rainfall distribution is highly variable both spatial and temporal scale. Most precipitation occurs in the wet season called Kiremt, a rainy season, (June through September), and the remaining precipitation occurs in the dry season called Bega which goes from October to January. Similarly, there is a mild season called Belg (from February to May) where a small amount of precipitation falls. These small rains originate from the Indian Ocean and are brought by south-east winds, while the heavy rains in the wet season are driven by south-west winds from the Atlantic Ocean (BCEOM, 1998).

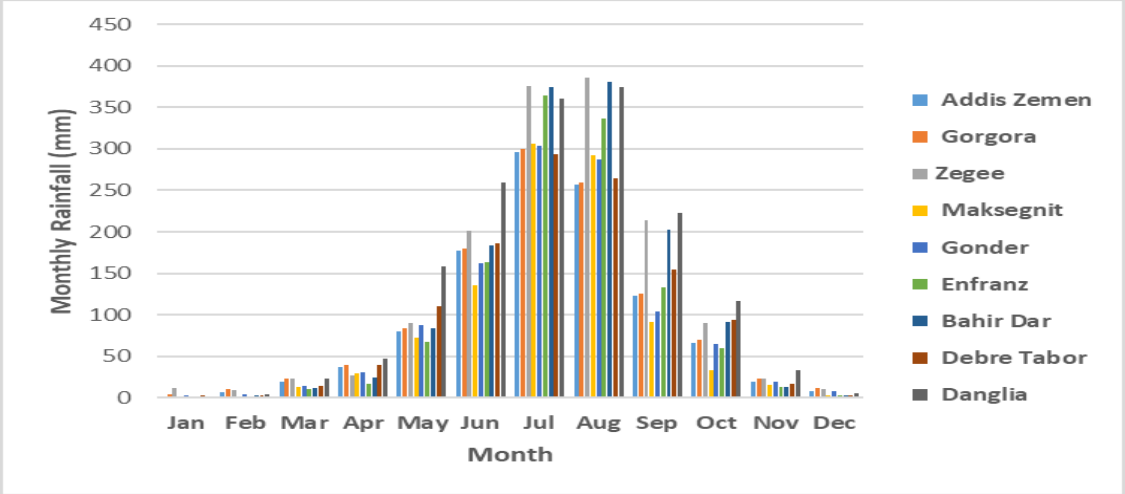

Figure 3. 5: Monthly Average Rainfall of Selected Stations in the Study Area (mm/month)

3.2 Material

Material used to achieve the objective of the study

- ❖ Arc GIS 10.3
  - ✓ GIS software used for spatial analysis of hydrological and physical parameters.
- ❖ SWAT 2012
  - ✓ A GIS interface of soil and water assessment tool used for simulation.
- ❖ SWAT-CUP

  A sensitivity analysis program interface of SWAT and used for calibration, sensitivity analysis, Uncertainty measure and Validation.
- ❖ Climate Model data for hydrologic modeling (Cmhyd)
  - ✓ A climate data analysis tool which is used to extract and bias correct data obtained from Global and Regional climate model
- ❖ DEM(30m*30m)
  - ✓ Digital Elevation Model (30m*30m) spatial resolution for stream delineation.
- ❖ Spatial Data
  - ✓ Soil and Land Use / Land cover data to create Hydrologic Response Units and simulate the model.
- ❖ Hydrological Data
  - ✓ Streamflow data, for the purpose of the model Calibration and Validation.
- ❖ Metrological Data
  - ✓ Rainfall, Temperature, Solar Radiation, Wind speed, and Relative Humidity
  - ✓ It is used as an input data for SWAT simulation.
- ❖ Soil map
  - ✓ The soil map of the study area is taken from the soil Maps prepared by MWIE.
  - ✓ Input data for SWAT model simulation.
- ❖ CORDEX_ Ethiopia RCPs dataset (IWMI)
  - ✓ Coordinated Regional Climate Downscaling data.
  - ✓ It is used to obtain a downscaled historical and future climate data for Ethiopia and then extracted to Tana sub basin.

- ❖ AUTO-MK-Sen
  - ✓ To analysis seasonal Mann-Kendall test results of precipitation, maximum and minimum temperature of observed meteorological data
- ❖ Kendall
  - ✓ To analysis the regional trend test of observed meteorological data (minimum and maximum temperature and precipitation)

3.3 Methodology

The general methodology of this study was depending on the data which are collected from different organization. In order to achieve the objectives of the study, all the necessary data were collected from meteorological stations, hydrological stations, and respective organizations and prepared DEM for the study area.

3.3.1 Trend analysis

For this study, trend analysis was done using non-parametric Mann-Kendall (MK) test, Seasonal Mann-Kendall Test and Regional Mann-Kendall Test. This is a statistical test widely used for the analysis of the trend in climatological variables (Mavromatis and Stathis, 2011) and in hydrologic time series analysis (Yue and Wang, 2004). There are two advantages of MK test. First, it is a non-parametric test and does not require the data to be normally distributed. Second, the test has low sensitivity to abrupt breaks due to inhomogeneous time series (Tabari et al., 2011). Any data reported as non-detects are included by assigning them a common value that is smaller than the smallest measured value in the data set (Karmeshu, 2012). According to this test, the null hypothesis Ho assumes that there is no trend (the data is independent and randomly ordered) and this is tested against the alternative hypothesis H, which assumes that there is a trend (Onoz and Bayazit, 2012)

3.3.1.1 Mann-Kendall Tests for Trends

Mann-Kendall describes a nonparametric test for looking at trends in time series which is robust even for highly skewed hydro meteorological data. This test was later proven by Kendall as a special case for testing of correlation between two data series (Y, X) using Kendall's 0. For this reason, it is called the Mann-Kendall test and it measures whether data value (Y) tends to increase or decrease with time (T).

The original Mann-Kendall test assumes that the time series has no seasonal pattern. Later on (Hirsch et al. 1982) developed an extension of the Mann-Kendall test to allow for seasonal variations as they are existent in most hydro-meteorological time series.

3.3.1.2 Non-seasonal Mann-Kendall Test

The null hypothesis (Ho) and the alternative hypothesis (H) are stated as:

Ho: No trend exists i.e. the variation of the data is random

H: A trend exists that can be either positive or negative

No assumption of normality is required but the data must not be serially correlated for the computed p value to be taken as correct. This test is also invariant (monotonic) to any power transformation (such as, square roots and logarithms) which are often made to transform highly skewed data to more normally looking distributions.

To perform the test, Kendall's S statistic is computed from (T, Y) data pairs.

$$S = \sum_{i=1}^{n-1} \sum_{i=1}^{a} sng(Yj - yi)) \qquad [3\text{-}1]$$

$$sng(Yj - yi = \begin{cases} 1\ if\ (yj - yi) > 0 \\ 0\ if (yj - yi) = 0 \\ -1\ if (yj - yi) < 0 \end{cases}$$

It can be simplified

$$S_g = P - M$$

Where:

Tj>Ti

P= the number of times the Y's increase Yj>Yi

M= the number of times the Y's decrease Yj>Yi

For all i=1, n-1 and j= i+1, n. Hence, there will be n(n-1)/2 possible comparisons to be made along the n data pairs.

If Y increases as T increases, S= + of n(n-1)/2 then the correlation τ =+1.

If Y decreases as T increases, S= - of n(n-1)/2 then the correlation τ =-1

It can be shown that S is asymptotically normally distributed Hipel and McLeod, (1993) with mean E(S) = 0 and standard deviation (= (variance$^{1/2}$) F given by (Helsel and Hirsch, 2002; Helsel and Frans, 2006):

$$\delta s=\sqrt{\frac{n}{18}[(n-1)(2n+5)-\sum_{t=i}^{g} ti(ti-1)(2ti+5)]} \qquad [3\text{-}2]$$

Where:

g is the number of tied groups and t_i is the number of ties of extent i.

The normality distribution of S is even guaranteed for small numbers of data points (n<10) if one -use the standardized variable Z defined as

$$Z=\begin{Bmatrix}\frac{s+1}{\delta s}\ if\ S<0\\ 0\ if\ S=0\\ \frac{s-1}{\delta s}\ if\ S>0\end{Bmatrix} \qquad [3\text{-}3]$$

For n ≤ 10, given the level of significance (α) determine the critical Z directly from the table of any standard statistical book. But for n > 10 and with the presence of ties, since the tied values of Yi and Yj produces 0 instead of +1 or -1 hence ties do not contribute to either P or M. Kendall's τ can be defined as:

$$\tau = S/D \qquad [3\text{-}4]$$

where: D is the maximum possible value of S, when all data points are monotonically increasing and is given in (Hipel and McLeod, 1993). When no ties exist, D is a constant, so that the statistics of S and τ are the same.

The null hypothesis H stated above (no trend exists) is tested through the significance of S or 0, being significantly different from zero, i.e. the null hypothesis is rejected at a significant level X (significant trend exist in the time series) if the computed value $|Z_S|>Z_{1-\alpha/2}$

Where:

$Z_{1-\alpha/2}$ is the value of the standard normal distribution with the probability of exceedance of α/2. For 5% significance level, the critical Z1-α/2 value which is computed from any standard normal distribution table is 1.96

3.3.1.3 Seasonal Mann-Kendall Test

The seasonal Mann-Kendall trend test avoids the shortcomings of the regular Mann-Kendall test in the presence of seasonal data. (Hirsch et al,1982) developed this test which consists mainly by computing the regular Mann-Kendall test separately for each season and to combine the results to get Kendall's 0 test statistic. Of course, depending on the nature of the time series a season could be a month or quarter of a year, a year or any combination of these. So for monthly "seasons", January data are compared only with January, February only with February, etc... so that, overall, there are m=12 seasons. No comparisons are made across season boundaries. Here, S' is the sum of Kendall's S, computed as discussed in the previous section for each season g.

$$S' = \sum_{g=1}^{m} Sg \qquad [3\text{-}5]$$

3.3.1.4 Regional Mann-Kendall (RMK) Test

The Regional Kendall test extends this concept to spatial locations rather than seasons. A Mann-Kendall test is computed for individual locations and results are combined into one overall test for consistent regional trend (Helsel and Frans,2006). The test is applicable to data where observations have been made annually at numerous locations, such as at water wells, and one overall test is desired to determine whether the same trend is evident across those locations.

In order to assess trends at a regional scale, the regional MK test was employed by to quantitatively combine results of the MK test for individual stations and to evaluate the regional trends (Hirsch et al,1982). In the regional MK test, the Sr of regional data is calculated as: -

$$Sr = \sum_{i=1}^{n} Si \qquad [3\text{-}6]$$

Where Sr is Kendall's S for the "ith" station in a region with m stations within the region. If Sr is estimated using independent identically distributed data, Sr is approximately normally distributed for large m with mean equal to 0 and the variance as noted below

$$(Var)Sr = \sum_{i=1}^{n} Var = \delta^2 \qquad [3\text{-}7\}$$

$$Zr = \begin{cases} \frac{Sr-1}{\delta} & for\ Sr > 0 \\ \frac{Sr+1}{\delta} & for\ Sr < 0 \\ 0 & for\ Sr = 0 \end{cases} \qquad [3\text{-}8]$$

.

3.4 Data Collection and Anaysis

The basic step to collect sufficient and quality data before undertaking and processing of any research. Therefore, the primary task of the study was getting relevant information and data of the study area. This section identifies and discusses the types and source of data required for the study, and their analysis.

For this study spatial data, meteorological data (Precipitation, minimum and maximum temperature, wind speed, relative humidity and solar radiation), hydrological data (stream flow data) and regionally downscaled climate data were required. Those meteorological data's collected from the National Meteorological Service Agency (NMSA) of Ethiopia. Hydrological data obtained from ministry of water, irrigation and electricity (MWIE). Regionally downscaled climate data also provided from International Water Management Institute (IWMI).

3.4.1 Observed meteorological data

Meteorological data are among the most important time series data necessary for hydrological design and analysis of water resources projects (Chow et al., 1988). The criterion for the selection of the Metrological data was based on the availability of data, the data quality and possibly weather the station is within the study area. The necessary long year daily precipitation, temperature relative humidity, sunshine hour and wend speed data were collected from nine meteorological stations such as Dangila, Bahir Dar, Zege, Gorgora, Debre Tabor, Addis Zemen, Enfranz, Gondar and Maksegnit. From those stations Gondar was the synoptic station. The 30 years' historical weather data for above nine stations were obtained from National Meteorological Service Agency (NMSA) from 1988 to 2017.

Table 3. 3: Meteorological Stations of Tana Sub-Basin with 30 Years' Average and Coefficient of variation

No	Station Name	Period	30 years average	CV	Northing/ Latitude	Easting/ Longitude	Elevation
1	Addis Zemen	1988-2017	1466.12	0.08	12.11652	37.77313	1940
2	Bahirdar	1988-2017	1412.97	0.11	11.595	37.385	1800
3	Dangila	1988-2017	3252.2	0.05	11.4337	36.846	2116
4	Debre Tabor	1988-2017	1185.94	0.09	11.8666	37.9954	2612
5	Enfranz	1988-2017	1165.45	0.12	12.25847	37.62593	1937

6	Gondar	1988-2017	1176.08	0.09	12.52115	37.4319	1973
7	Gorgora	1988-2017	941.79	0.10	12.25	37.3	1830
8	Maksegnit	1988-2017	993.10	0.12	12.3884	37.5551	1912
9	Zege	1988-2017	1582.62	0.11	11.68878	37.31243	1801

3.4.2 Hydrological data

Streamflow was used for calibrating and validating the SWAT model simulation. Daily streamflow data were obtained from Ministry of Water Irrigation and Energy (MWIE) for Gilgel Abay, Gummara, Ribb and Megech rivers from 1988 to 2008. But those four river are a tributary of Blue Nile river (Abay River) located at Bahirdar gauging station which is the outlet of Lake Tana. So in this study Blue Nile river flow for 1988-2008 used for calibration and validation by using SWAT-CUP.

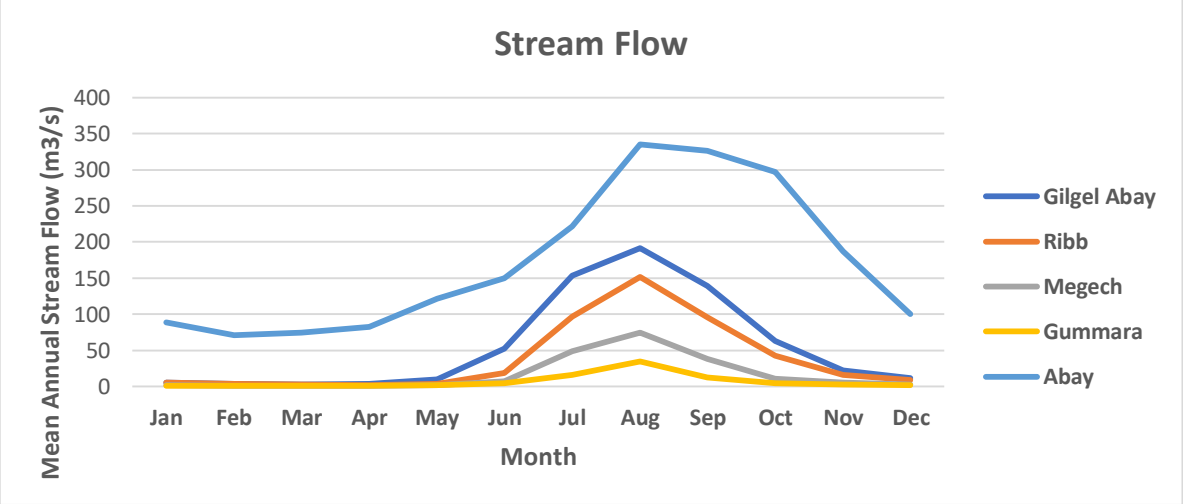

Figure 3. 6: Mean Monthly Streamflow Tana Sub-Basin

3.4.3 Spatial data

The DEM, soil and land use / land cover data were collected in shape file format from the GIS department of EMWR was obtained with a resolution of 30 m by 30 m. Digital elevation model (DEM), land use/land cover, and soil are spatial data inputs required by SWAT model. DEM describes the elevation of any point in a given area at a specific spatial resolution as a digital file. DEM is one of the essential inputs required by SWAT:

1. To delineate the watershed into a number of sub-watersheds or sub-basins and

2. To analyze the drainage pattern of the watershed, slope, stream length, width of the channel within the watershed.

3.4.4 Future climate projection

The Intergovernmental Panel on Climate Change (IPCC) Fifth Assessment Report (AR5) is due for publication in 2013-2014. Its findings will be based on a new set of scenarios that replace the Special Report on Emissions Scenarios (SRES) standards employed in two previous reports. The new scenarios are called Representative Concentration Pathways (RCPs) (Stocker TF et al., 2013). There are four pathways: RCP8.5, RCP6, RCP4.5 and RCP2.6. from those four Scenarios the medium and high emissions (RCP4.5 and RCP8.5 respectively) was selected for this study. The first scenario considers what the future climate will be under conditions with a representative concentration path (RCP) that assumes that radiative forcing will stabilize at 8.5 W/m-2 in 2100 (RCP8.5); the second less extreme scenario assumes that radiative forcing will stabilize at 4.5 W/m-2 15 (Teutschbein and Jan Seibert,2010).

Downscaled rainfall, and minimum and maximum temperatures for the period 1951-2100 have been obtained from CORDEX-Ethiopia with a spatial resolution of (approximately 50 km × 50 km) database /International Water Management Institute (IWMI) shown the table3.1 below in detail. This data is dynamically down scaled form regional climate model by nesting RCMs into GCMs under representative concentration pathways (RCP4.5, RCP8.5). The data correspond to RCP scenarios of RCP2.6, RCP6, RCP4.5, and RCP8.5. Because of time limitation, this study was considered only, RCP 4.5 and RCP 8.5 forced scenarios from 2020 to 2079 for the future prediction of the study area and down scaled CORDEX precipitation and temperature which ranges from 1988-2017 to historical periods. Outputs from GCM for the 1988–2017 (baseline), 2020–2049 and 2050–2080 used to generate climate change scenarios. The 2020–2049 and 2050–2080 correspond to near term and midterm future, respectively.

Table 3. 4: Sources of future climate data

Data source (RCM)	Project	Institute	GCM	Country	Scenarios
SMHI-RCA4	CMIP5	MOHC	HadGEM2-ES	UK	RCP(4.5,8.5)

3.5 Data Quality Checking

Before using the rainfall records of a station, it is necessary to check the data for continuity and consistency. The continuity of a record may be broken with missing data due to many reasons such as damage or fault in a rain gauge during a period of recording (K Subramanya,2008). So in order to the quality of data this study considered consistency and homogeneity test.

Before using the rainfall records of a station, it is necessary to first check the data for continuity and consistency. The continuity of a record may be broken with missing data due to many reasons such as damage or fault in a rain gauge during a period (K Subramanya,2008). Measured precipitation data are important to many problems in hydrologic analysis and design, because of the cost associated with data collection, it is very important to have complete records at every station. Obviously, conditions sometimes prevent this. For gages that require periodic observation, the failure of the observer to make the necessary visit to the gage may result in missing data. Vandalism of recording gages is another problem that results in incomplete data records, and instrument failure because of mechanical or electrical malfunctioning can result in missing data. Any such causes of instrument failure reduce the length and information content of the precipitation record.

3.5.1 Filling of missed data

There are a number of methods provided to fill the missing records of daily precipitation data. Among those methods, the Arithmetic average method is applied, if the average annual rainfall station to be filled is within 10% gap of annual rainfall of the adjoining stations. The station with missed data is filled in an estimate of simple average calculations of nearby stations.

Unlike the arithmetic method, the Normal ration method is applied when the percentage gap between the station to be filled and the adjoining station's annual rainfall is more than 10%. The station missed data is filled by estimating the rainfall with a weighted average of adjoining stations. The adjoining stations are weighted by the ratio of average annual rainfall of the station to be filled and by the adjoining stations. Considering easiness and the percentage gap of the annual average rainfall between the station to be filled and the adjoining stations are greater than 10%, in this study the arithmetic method and normal Ratio Method was selected to fill the missed records.

Arithmetic Mean Method: - used when the normal annual rainfall of the missing station is within 10% of the normal annual rainfall of the surrounding stations. This is the case in some of the stations near the study area. The method works based on a general formula.

$$P_x = \frac{1}{n}(P_1 + P_2 + ... + P_n) \quad [3\text{-}9]$$

Where P1, P2….. P_n are the precipitations of index stations and

Px is that of the missing station, n is the number of index stations

Normal Ratio Method: - is used when the normal annual precipitation of the index stations differs by more than 10% of the missing station. It is applicable for some stations near the study area. The general formula for computing missing precipitation by this method is:

$$P_x = \frac{N_x}{n}\left(\frac{P_1}{N_1} + \frac{P_2}{N_2} + ... + \frac{P_n}{N_n}\right) \quad [3\text{-}10]$$

Where P1, P2……Pn are the rainfall data of index stations,

N1, N2……Nn the normal annual rainfall of index stations,

Px and Nx the corresponding values for the missing station x in question and

n is the number of stations surrounding the station x

Table 3. 5: Percentage of missing precipitation data

SN	station	% of missing data	Filling method
1	Dangila	2.431	Arithmetic mean
2	Bahir Dar	5.678	Arithmetic mean
3	Gorgora	12.509	Normal Ratio
4	Zege	11.697	Normal Ratio
5	Debre Tabor	4.649	Arithmetic mean
6	Addis Zemen	1.548	Arithmetic mean
7	Enfranz	18.137	Normal Ratio
8	Gondar	0.978	Arithmetic mean
9	Maksegnit	13.496	Normal Ratio

3.5.2 Consistency test

Estimating missing data is one problem that hydrologists need to address. A second problem occurs when the catch at rain gages is inconsistent over a period of time and adjustment of the measured data is necessary to provide a consistent record. A consistent record is one where the characteristics of the record have not changed with time. Adjusting for gage consistency involves the estimation of an effect rather than a missing value. An inconsistent record may result from any one of a number of events; specifically, adjustment may be necessary due to changes in observation procedures, changes in exposure of the gage, changes in land use that make it impractical to maintain the gage at the old location, and where vandalism frequently occurs (McCuen, 19980).

Double-mass-curve analysis is the method that is used to check for an inconsistency in a gaged record. A double mass curve is a graph of the cumulative catch at the rain gage of interest versus the cumulative catch of one or more gages in the region that has been subjected to similar hydro meteorological occurrences and are known to be consistent. If a rainfall record is a consistent estimator of the hydro meteorological occurrences over the period of record, the double-mass curve will have a constant slope. A change in the slope of the double mass curve would suggest that an external factor has caused changes in the character of the measured values. If a change in slope is evident, then the record needs to be adjusted, with either the early or later period of record adjusted. Conceptually, adjustment is nothing more than changing the values so that the slope of the resulting double-mass curve is a straight line (McCuen, 19980).

The consistency of time series data analyzed based on the theory that a plot of two cumulative quantities that are measured for the same time period should be a straight line and their proportionality remain unchanged which is represented by the slope. To check the consistency of data, the double mass curve was used to correct rain gauge data for the given station.

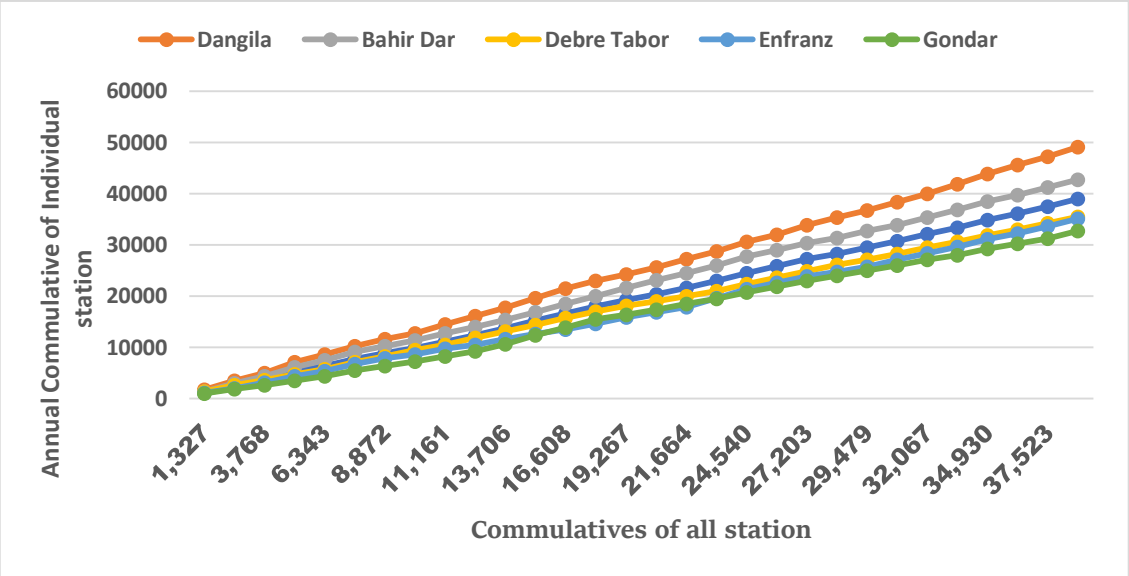

Figure 3. 7: Consistency Test Selected Stations of Tana Sub-Basin

3.5.3 Homogeneity test

Homogeneity analysis was used to separate a change in the statistical properties of the time series data which was caused by either natural or man-made like alterations to land use and relocation of the observation gauging station. Therefore, checking homogeneity of group stations is essential to select the representative meteorological station for the analysis of areal rainfall estimation. The homogeneity of the selected gauging stations daily rainfall records were carried out by non-dimensional equation. The non-dimensional observed precipitation data said to be homogeneous if the periodic data are proportional to an appropriate simultaneous period, method, materials, place, and environment (McCuen, 1998).

The restrictions of homogeneity assure that the observations are from the same population. The non-dimension of the month's values was calculated as;

$$Pi = \frac{Pix}{P1} * 100\% \qquad [3\text{-}11]$$

Where Pi:- is non-dimensional value of rainfall(month)

Pix: -is over year averaged monthly rainfall at the station i and

P1: - is the over year average yearly rainfall of the station.

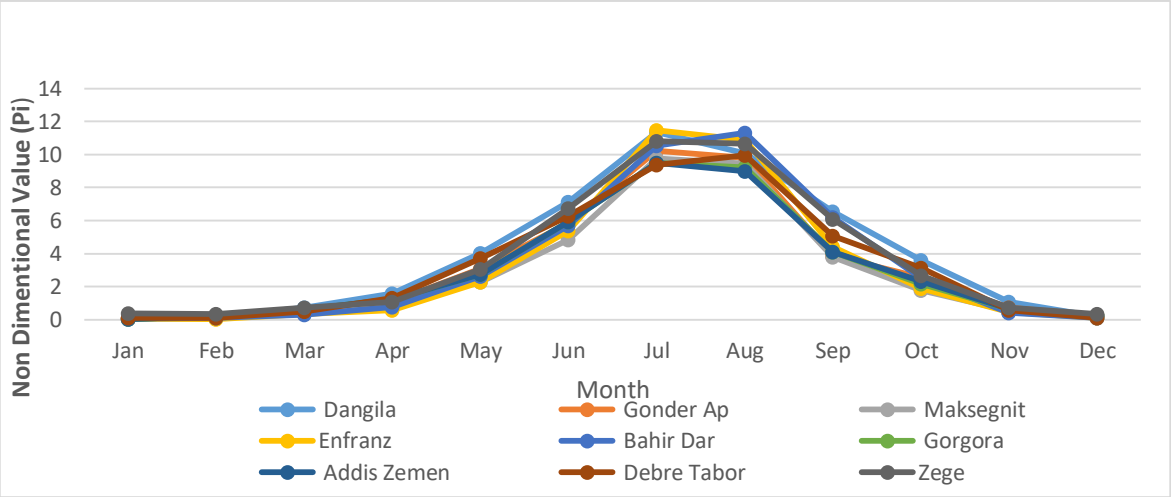

Figure 3. 8: Homogeneity Test Selected Stations of Tana Sub-Basin

3.5.4 Areal precipitation

Areal rainfall was deriving from the idea that evenly distributed rain gauge stations in a given drainage basin into sub-basins have their own point observation that may not be used as a representative value for the specified sub-basins. Hence, to get the representative record of those stations areal precipitation value in the specified basin is worked out. The most common methods used for areal parameter estimation are station-average method, arithmetic mean, grid point, Thiessen polygon method and Isohyetal method. The most common methods used for areal parameter estimation are station-average method, arithmetic mean, grid point, Thiessen polygon method and Isohyetal method.

For this study, Thiessen polygon method was used due to its sound theoretical basis, large differences in the basin at the rain gages and non-uniformly distribution of the rain gauges throughout the study areas. Thiessen area formed around each station by drawing the perpendicular bisectors of the lines joining adjacent stations using Arc GIS tool. The polygons areal contribution of the stations clipped using the shape of the catchments that includes stations of the selected ones for this study. If there are n-number of stations and n-polygons, the average depth of precipitation over the total area (A) is given by:

$$Pi = \frac{P1A1+P2A2+\cdots PnAn}{A1+A2+\cdots An} \quad [3\text{-}12]$$

Where,

Pi is average rainfall

P1, P2…Pn are the rainfall at each station and

A1, A2…. An are the area of polygons in the surrounding stations

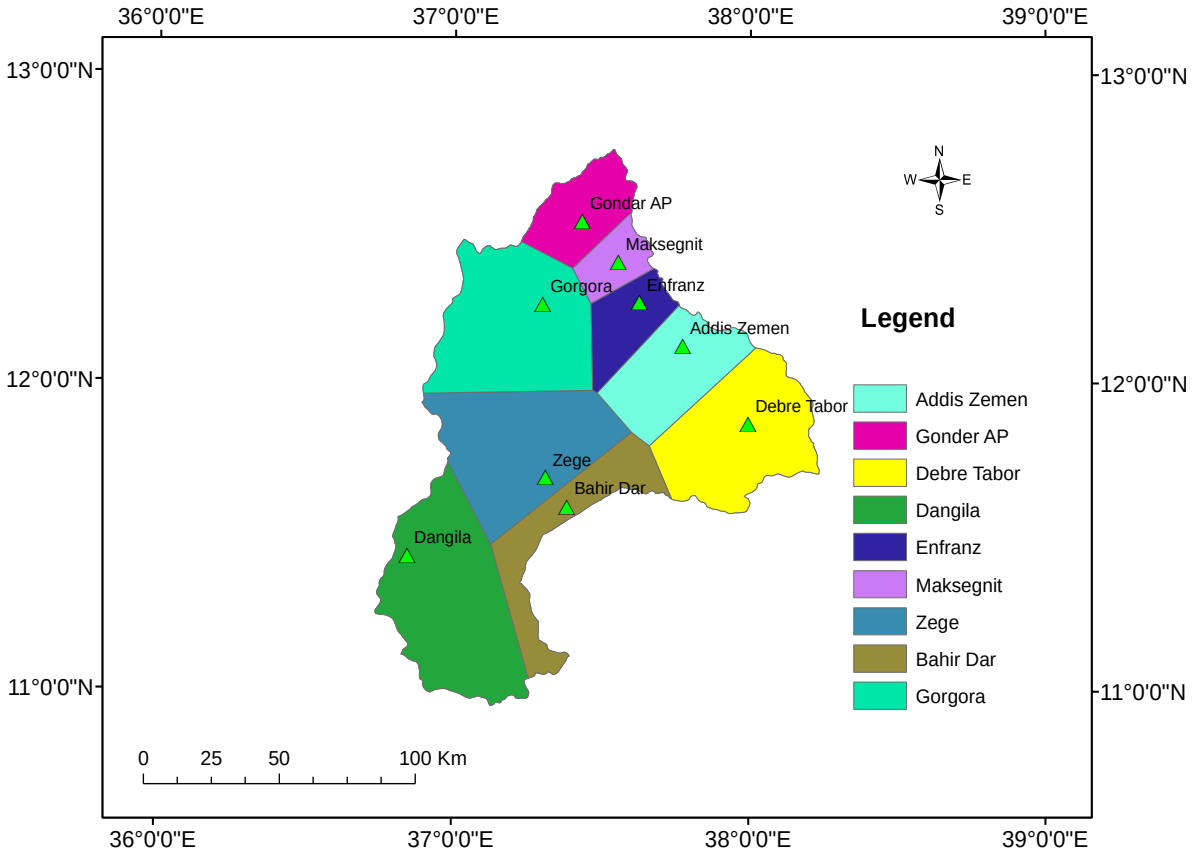

Figure 3. 9: Areal coverage of each Stations using Thiessen polygon

Table 3. 6: Areal Rainfall coverage of selected Stations

No	Sub-basin	Station	Area (km^2)	Area ratio (%)
1	Tana	Addis Zemen	1415.61	9.40
2		Gondar	964.40	6.40
3		Debre Tabor	2236.39	14.85
4		Dangila	2835.69	18.84
5		Enfranz	747.22	4.96
6		Maksegnit	489.30	3.25
7		Zege	2426.63	16.12
8		Bahir Dar	1302.38	8.65
9		Gorgora	2635.98	17.51
		Total Area (km^2)	15053.59	100.00

3.6 Climate Model Performance

Performance measure of climate model is used to test simulated precipitation and temperature datasets against observed precipitation datasets in terms of four performance measures and through visual inspection by plots of observed and simulated flow. The performance measures are statistically based and include Bias, Root Mean Square Error (RMSE) and Coefficient of Variation (CV) are described as follows. Bias indicates the systematic error in rainfall amount. A value of zero indicates no systematic difference between simulated and observed rainfall amounts where as large bias indicates that the RCP rainfall amount largely deviates from the observed rainfall amount. Negative bias indicates under estimation whereas positive bias indicates overestimation. RMSE has the same unit as the observed variable making its interpretation relatively easy. A RMSE value close to zero indicates favorable performance. Correlation is used to evaluate the linear relationship between the observed and modeled rainfall amounts with a value of 1.0 suggesting perfect linear relationship (Alemseged et al., 2015). Calculated CV for both the gauged and RCP simulated rainfall amounts to evaluate how well the rainfall variability by the network stations is captured and represented by the RCP.

$$\text{Bias} = 100 * \frac{\overline{R_{RCP} - R_{Observed}}}{\overline{R_{observed}}} \quad [3\text{-}13]$$

$$CV = 100 * \frac{\delta \mathrm{R_{RCP}}}{\delta \mathrm{R_{obs}}} \quad [3\text{-}14]$$

$$RMSE = \sqrt{\frac{\sum (R_{RCP} - R_{observed})^2}{N}} \quad [3\text{-}15]$$

$$Correl = \frac{\sum_{i=1}^{N} (R_{RCP} - \overline{R_{RCP}})(R_{Observed} - \overline{R_{Observed}})}{\sqrt{\sum_{i=1}^{N} (R_{RCP} - \overline{R_{RCP}}) \sum_{i=1}^{N} (R_{Observed} - \overline{R_{Observed}})}} \quad [3\text{-}16]$$

3.6.1. RCP bias correction using CMhyd

The downscaled RCPs data cannot be directly used for impact assessment as the computed variables may differ systematically from the observed ones. Bias correction is therefore-applied to compensate for any tendency to overestimate or underestimate the mean of downscaled variables.

Bias correction is all about identifying the biases between the observed and simulated historical climate variables to parameterize a bias correction algorithm for the simulated historical climate data. The correction algorithm and its parameterization for current climate

conditions are assumed to be valid for future conditions as well. In CMhyd, there are about 8 bias correction methods. Among these methods, based (Teutschbein and Seibert, 2010, 2012) on the recommendation this study was used the distribution mapping and variance scaling for the precipitation and temperature bias correction of RCPs data, respectively.

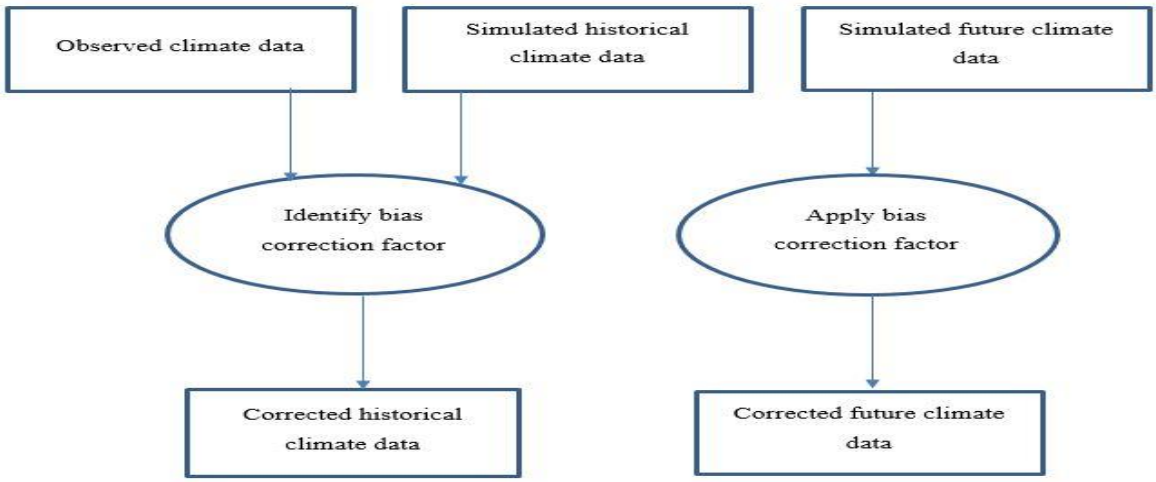

Figure 3. 10: Bias correction framework (source CMhyd manual, 2016)

Instead of choosing the nearest grid data to observation stations, precipitation and temperature scenarios from 1988–2017 and 2020-2079 with daily temporal resolution have been interpolated with bilinear interpolation from the four nearest grid points, as this method helps in conserving properties of robustness and eliminating unrealistic jumps (Abdella, 2013).

The equation 3-17 used for interpolation procedure is as follow.

$$\mathbf{P(x,y)} = \frac{(X_2-X)((Y_2-Y)}{(X_2-X_1)(Y_2-Y_1)}\mathbf{Q_{11}}+\frac{(X-X_1)(Y_2-Y)}{(X_2-X_1)(Y_2-Y_1)}\mathbf{Q_{21}}+\frac{(X_2-X)(Y-Y_1)}{(X_2-X_1)(Y_2-Y_1)}\mathbf{Q_{12}}+\frac{(X-X_1)(Y-Y_1)}{(X_2-X_1)(Y_2-Y_1)}\mathbf{Q_{22}} \quad [3\text{-}17]$$

Where: - P is one of observation point

Q11, Q12, Q21 and Q22 are RCP grid data

X, X_1, Y and Y_1 distance of these four stations relative to the observation stations

After selection of the grid point's bias correction for temperature and precipitation data for nine weather stations both RCP4.5 and RCP8.5 grid point. The corrected data divide three periods that means base period (1988-2017) and two future periods (2020-2049) short period & (2050-2079) long period. The table below shows all the selected grid points of the study area.

Table 3. 7: Selected Gird Point and Meteorological Stations of Tana Sub-Basin

Station Name		LAT	LONG	ELEV	Station Name		LAT	LONG	ELEV
Addis Zemen	GP112221	11.88	37.84	2104.16504	Enfranz	GP111221	11.88	37.4	1918.073
	GP112222	12.32	37.84	2036.58398		GP111222	12.32	37.4	1852.12097
	GP113221	11.88	38.28	2257.93408		GP112221	11.88	37.84	2104.16504
	GP113222	12.32	38.28	1987.70898		GP112222	12.32	37.84	2036.58398
Gondar	GP111222	12.32	37.4	1852.12097	Maksegnit	GP111222	12.32	37.4	1852.12097
	GP111223	12.76	37.4	1759.00806		GP111223	12.76	37.4	1759.00806
	GP112222	12.32	37.84	2036.58398		GP112222	12.32	37.84	2036.58398
	GP112223	12.76	37.84	2006.45605		GP112223	12.76	37.84	2006.45605
Debre Tabor	GP112220	11.44	37.84	2194.45605	Zege	GP110220	11.44	36.96	1853.245
	GP112221	11.88	37.84	2104.16504		GP110221	11.88	36.96	1643.979
	GP113220	11.44	38.28	2268.55688		GP111220	11.44	37.4	2092.95898
	GP113221	11.88	38.28	2257.93408		GP111221	11.88	37.4	1918.073
Dangila	GP109219	11.00	36.52	1574.35303	Bahir Dar	GP111220	11.44	37.4	2092.95898
	GP109220	11.44	36.52	1475.21802		GP111221	11.88	37.4	1918.073
	GP110219	11.00	36.96	1947.95203		GP112220	11.44	37.84	2194.45605
	GP110220	11.44	36.96	1853.245		GP112221	11.88	37.84	2104.16504
Gorgora	GP110220	11.44	36.96	1853.245					
	GP110221	11.88	36.96	1643.979					
	GP111220	11.44	37.4	2092.95898					
	GP111221	11.88	37.4	1918.073					

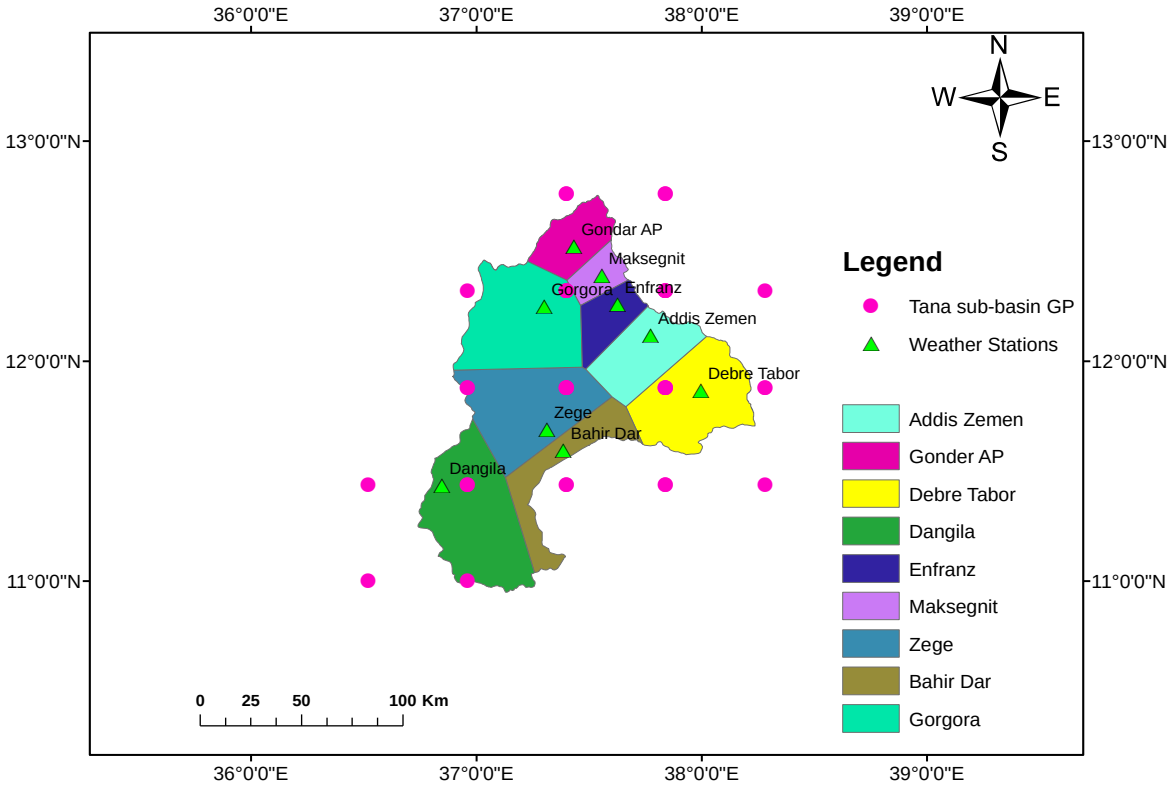

Figure 3. 11: Selective grid points of Tana Sub-Basin

3.6.2 Bias correction performance evaluation

The performance of the bias correction method will be evaluated using the root means square error (RMSE), the mean absolute error (MAE) and the Relative Error (RE) (Shamarokh A, 2012). These will be calculated using the following equations.

$$\text{RMSE}= \sqrt{\sum_{i=1}^{n}(Yi - Ymean)^2} \quad [3\text{-}18]$$

$$\text{RAE}=\frac{1}{N}\sum_{i=1}^{N}(Yi - Ymean) \quad [3\text{-}19]$$

$$\text{RE}= \frac{1}{n}\sum_{i=1}^{n}(Yi - Ymean) \quad [3\text{-}20]$$

Where Yi is the observed value at time step i, Yi is simulated value at time step i, Ymean is the mean of observed values, and N is the number of observations.

3.7 SWAT Model Description

Selecting the best and appropriate model is an essential part in any research work. There are various criteria to choosing the correct hydrological model for specific problem. These criteria are always research dependent, since every research has its own specific

requirements and needs. One commonly accepted approach to estimate the effects of climate change in reservoirs or water resources is with watershed or hydrological simulation models.

The criteria of Cunderlik and Simonovic (2007) used for selecting the hydrological model are:

- ✓ Required output of the model
- ✓ Availability of input data
- ✓ Prices and availability of the model
- ✓ The model structure

The model has been used to predict streamflow, which were compared favorably with measured data for a variety of basin and sub-basin scales, and to predict the effect of climate change on hydrology. According to the published reports, SWAT is a continuous time distributed hydrological model at a daily time step. It is considered to be versatile tool for watershed assessments. It can simulate many processes within the basin, including rainfall-runoff and plant growth processes. This model comprises many components, including hydrology, climate, soils, land management, plant growth, pesticides, and nutrients. It is also widely used, with high efficiency for simulating and assessing hydrological processes under changing environments (Breuer et al., 2009). Because of the above criteria, SWAT model was selected for this study.

3.7.1 SWAT model sensitivity analysis

The Soil and Water Assessment Tool (SWAT) is a physically based and computationally efficient hydrological model, which allows a number of different physical processes to be-simulated in a watershed based on specific information about weather, soil properties, topography, vegetation and land management practices. The physical processes associated with water movement, sediment movement, crop growth…etc. are directly modeled by SWAT using these input data.

In the SWAT modeling approach, a watershed is divided in to a number of sub-basins. Each sub basin is then further divided into groups of similar soil- and land cover areas, which because they are supposed to give similar hydrological responses are called HRUs (Neitsch et al., 2005).

2.7.2 Hydrological component of SWAT

The SWAT hydrological compartment in a watershed consists of a land phase and a water routing phase. The land phase of the hydrologic cycle controls the amount of water, sediment and pesticide loadings to the main channel in each sub-basin, whereas the routing phase of the hydrologic cycle shows the movement of water, sediment, nutrients, etc., through the channel network of the watershed and then to the outlet (Neitsch et al., 2005).

$$SWt = \mathrm{So} + \sum_{i=1}^{t}(\mathrm{Rday} - \mathrm{Qsurf} - \mathrm{Ea} + \mathrm{Qseep} - \mathrm{Qgw}) \quad [3\text{-}21]$$

Where; SWt= the final water content (mm H2O)

Swo= the initial soil water content on day i (mm H2O), t = time

Rday= is the amount of precipitation on day i (mm H2O)

Qsurf = is the amount of surface runoff on day i (mm H2O)

Ea= is the amount of evapotranspiration on day i (mm H2O)

Wseep = is the amount of water entering the vadose zone from the Soil profile on day i (mm H2O)

Qgw= is the amount of ground water flow on day i (mm H2O)

Surface runoff occurs whenever the rate of precipitation exceeds the rate of infiltration. SWAT provides two methods for estimating surface runoff: the SCS curve number procedure. Using daily or sub daily rainfall, SWAT simulates surface runoff volumes and peak runoff rates for each HRU.

For these research work SCS curve number method has been used to estimate surface runoff. The CN method was used for this study. The CN method assumes CN I at wilting point, CN II at field capacity and a CN III of 100 at saturation point (Arnold et al., 2000), and CN is modified daily based on soil moisture.

The surface runoff is calculated by

$$Qsurf = \frac{Rday - Ia}{Rday - Ia + S} \quad [3\text{-}22]$$

Where Qsurf is the accumulated precipitation excess (mmday-1); Rday is the precipitation depth for the day (mmday-1); Ia is the initial abstraction which includes surface storage,

infiltration and infiltration prior to runoff (mmday-1) and S is the retention parameter (mmday-1). The retention parameter varies spatially due to changes in soils, land use management and slope, and temporarily due to changes in the soil water content.

The retention parameter(S): -

$$SS = 24.5(\frac{100}{CN} - 10) \quad [3\text{-}23]$$

Where CN is curve number for the day and this curve number is based on the areas, hydrologic group, land use and hydrologic condition. The initial abstractions, Ia, is commonly approximated as 0.2S and then the above equation becomes:

$$Qsurf = \frac{(Rday - 025S)^2}{Rday + 0.5S} \quad [3\text{-}24]$$

Runoff will only occur when Rday > Ia.

3.7.2 SWAT model setup

1. SWAT project Setup

   It is the first step of SWAT project to specify the Directory and the File name of the Project.

2. Watershed delineation

   The first step to watershed delineation. At this stage, the following activities were performed.

A. The Digital Elevation Model (DEM) is selected.
B. DEM based flow direction and accumulation is done.
C. Stream network is carried out
D. After manually specifying outlet, the watershed of the study area is delineated.
E. Finally, the sub basin parameter calculation is done and saved in the predefined directory. The delineated watershed with sub basin is displayed in the Arc Map window.

3. Hydrologic Response Unit (HRU) analysis

At this step data like Land use and Soil either in polygon shape file or grid form along with their look up table and slope (from DEM) feed to SWAT to be created HRU.

Input data imported to the SWAT one by one.

A. Land use of the study area classified into six groups and correlated with SWAT Crop database.
B. Soil type of the study area first defined based on FAO classification and grouped into twelve type of dominant soil group. The FAO soil classification, further classified in to two based on their dominant Texture in order to correlate with SWAT user soil Database. For this sake user soil database is prepared and imported to SWAT database prior to model setup.
C. Classify slope

The HRU of the basin defined in different threshold values. For this study, 5% (land), 10% (soil) and 15 % (slope) threshold values are selected. The maximum numbers of HRU are selected by thinking the basin with more HRU.

The final process of this step is overlay the input parameters and prior to that create HRU feature class and create overlay report should be checked.

4. Write Input Tables Menu
   Here all weather Data and station location including the Weather Generator written to SWAT database. After weather station, writing, other SWAT input tables were written.
5. Edit Input SWAT Menu
   At this stage, SWAT model database is edited. For instance, CN adjustment for slope >5% and channel routing method is changed into Muskingum and its corresponding values were edited.
6. SWAT Simulation Menu

This is the final step of SWAT model to produce the specified output.

3.8 Evapotranspiration and Evaporation

3.8.1 Evapotranspiration

There are different methods to estimate potential evapotranspiration (ETO) using observed and predicted climatological data for the study area for each month of the year. However, the methods vary based on climatic variables required for calculation. For this specific study Penman-Monteith method is adopted to calculate the daily potential evapotranspiration for the base period to use during SWAT model calibration and validation. The potential evapotranspiration for different stations depending on the sub-basin locations were used for

model input. However, for the future time periods Hargreaves potential evapotranspiration method is adopted since the existing data are the down-scaled precipitation, minimum and maximum temperature. Future potential evapotranspiration over the study area has also been predicted in the name study of Elshamy et al. [2009]. For 2090s-decade increases of the potential evapotranspiration in a range from 2% to a 14%, depending on the type of GCMs, are obtained which most likely is due to an increase of temperature.

A. Penman-Monteith evapotranspiration

The Potential evapotranspiration is computed by using ET_O calculator software from meteorological data which uses FAO Penman-Monteith method equation (FAO, 1988).

The equation is given by:-

$$\text{ETopm} = \frac{0408\Delta(Rn-G)+\gamma\left(\frac{900}{T}+273\right)U2(es-ea)}{\Delta+\gamma(1+0.34U2)} \quad [3\text{-}25]$$

Where; ETopm = reference evapotranspiration by Penman-Monteith [mm day-1],

Rn = net radiation at the crop surface [MJ m-2 day-1],

G =soil heat flux density [MJ m^{-2} day^{-1}],

T = mean daily air temperature at 2 m height [°C],

U_2= wind speed at 2 m height [m s^{-1}],

e_s=saturation vapor pressure [kPa],

e_a= actual vapor pressure [kPa],

e_s-e_a= saturation vapor pressure deficit [kPa],

Δ= slope vapor pressure curve [kPa °C-1],

γ= psychometric constant [kPa °C-1].

B. Hargreaves potential evapotranspiration

Due to lack of climate data such as solar radiation, relative humidity, and wind speed data for future time periods, Hargreaves method ((Hargreaves et al., 1985) was adopted for PET estimation given by: -

$$ET_o\ hg = 0.0023(T\ mean + 17.8)(Tmax - Tmin)^{0.5}Ra \quad [3\text{-}26]$$

Where,

ET_ohg=Hargreaves potential evapotranspiration;

Ra=Extraterrestrial radiation (calculated from latitude and time of year);

T_{mean}= Mean temperature;

T_{min}= Minimum temperature; and

T_{max}= Maximum temperature.

3.8.2 Lake Evaporation

Evaporation from lakes and reservoirs cannot be measured directly, it should be determined indirectly by one or more of several methods, such as water balance, energy budget, Penman Monteith's formula using FAO CROPWAT software, pan evaporation technique. In this study, the Penman Monteith method was used to estimate monthly evapotranspiration. The FAO ETo calculator, which was developed to estimate evapotranspiration from a reference surface (Reference evapotranspiration ETo) was used to calculate open water evaporation from reservoir by applying an aridity correction factor (FAO, 1988). According to FAO Irrigation and Drainage paper 56 (FAO,1988) the conversion of ETo to open water evaporation with depth higher than 5 m, clear of turbidity, in temperate climate would be varied between 0.65 and 1.25. For Ethiopia, as stated in the feasibility study of lake Tana sub-basin dam project, the dryness correction factor was estimated to be 1.2 (WWDSE, 2008).

3.9 General Methodology

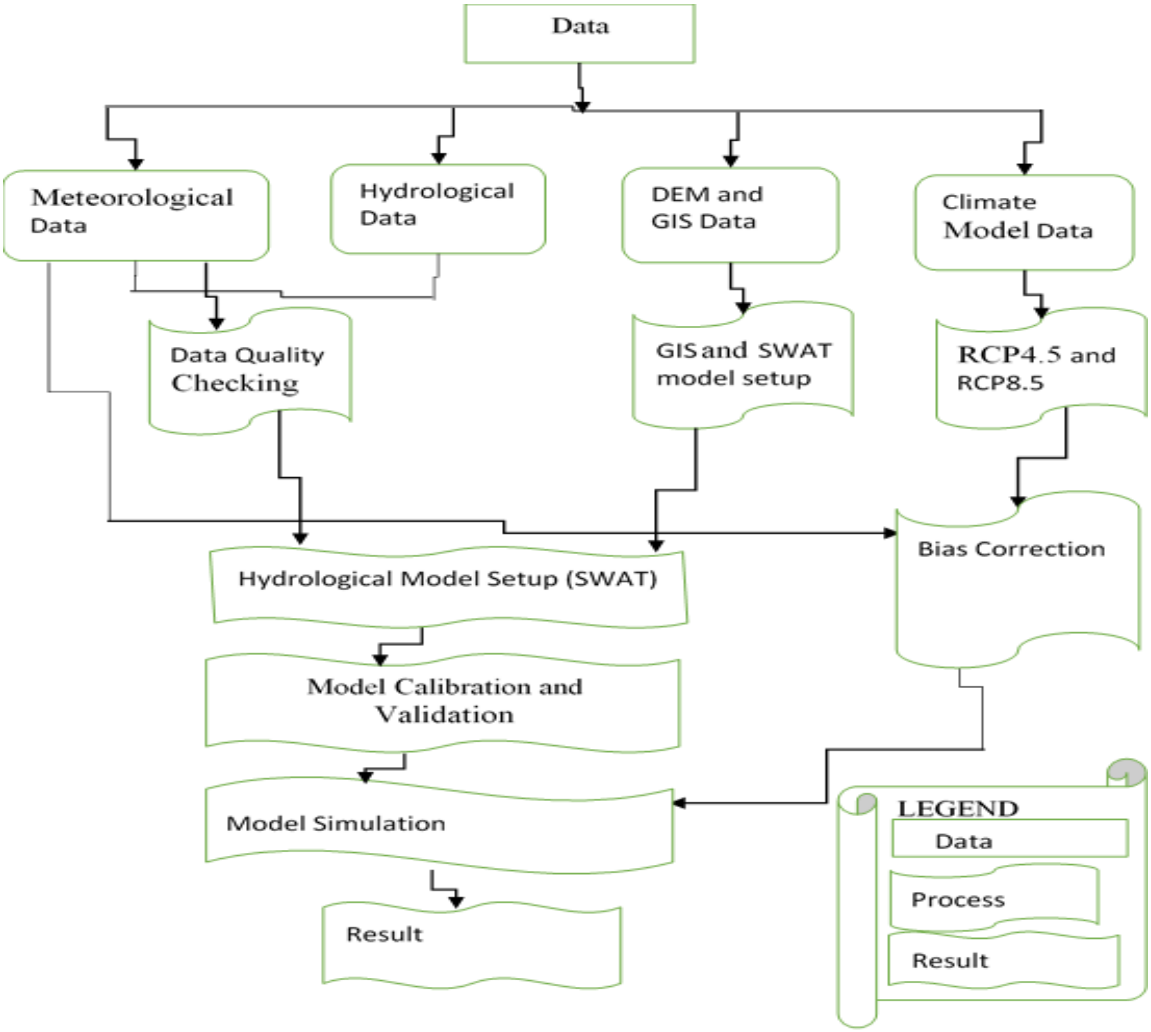

Figure 3. 12: General Framework

4. RESULTS AND DISCUSSIONS

4.1 Trends in the observed Tana Sub-Basin Meteorological Data

4.1.2 Results of the trend analyses

The trend test result shows that among the 9 stations of Tana sub-basin only three stations show the presence of a statistically significant trend in the precipitation. Similarly, four stations show a statistically significant trend in the maximum temperature. However, the minimum temperature three stations show statistically significant trend, Finally, three stations show significant a trend in the minimum temperature is observed.

Table 4. 1: Mann-Kendall trend test of precipitation, maximum and minimum temperature

S/N	Tana Sub-Basin (Stations)	PCP	MK-test(Z-test)	Tmax	MK-test(Z-test)	Tmin	MK-test(Z-test)
1	Addis Zemen	NO	0.05	NO	1.24	Sign(+)	1.79
2	Bahir Dar	NO	0.22	NO	1.22	NO	0.12
3	Dangila	Sign(+)	1.78	Sign(+)	3.57	NO	0.59
4	Debre Tabor	NO	1.22	Sign(+)	4.17	NO	1.07
5	Enfranz	Sign(+)	2.34	NO	0.40	Sign(+)	4.97
6	Gondar	NO	0.35	NO	0.36	NO	1.47
7	Gorgora	NO	1.35	NO	1.33	NO	0.09
8	Maksegnit	Sign(-)	-1.98	Sign(+)	1.97	Sign(+)	3.05
9	Zege	NO	0.98	Sign(-)	-2.97	NO	0.45

“No” implies there is no statically significant trend, “Sign” represents the presence of statically significant trend, and (+) increasing trend and (-) decreasing trend with the values of Y which is the time series.

Table 4. 2: Seasonal Mann-Kendall test results of precipitation, maximum and minimum temperature

SN	Tana-Sub-Basin (Stations)	PCP	MK-test (Z-test)			Tmax	MK-test(Z-test)			Tmin	MK-test(Z-test)		
			Rainy	*dry*	*mild*		Rainy	dry	mild		Rainy	dry	Mild
1	Addis Zemen	NO	-0.23	1.01	0.98	NO	0.31	1.22	1.2	NO	0.69	0.9	0.7
2	Bahir Dar	NO	-0.05	0.07	-1.32	NO	1.52	1.07	1.4	NO	-0.07	1.03	
3	Dangila	NO	0.46	0.36	-0.25	(+ve)	3.28	2.7	2.7	(+ve)	5.32	1.98	2.09
4	Debre Tabor	NO	-0.43	1.0	-1.23	NO	1.3	1.2	1.3	NO	-0.54	-1.04	-0.39
5	Enfranz	NO	1.02	1.21	-0.61	(+ve)	3.0	1.75	2.3	NO	1.07	1.22	1.22
6	Gondar	NO	0.29	-0.29	-0.32	(+ve)	1.89	2.2	1.8	NO	1.48	1.22	1.14
7	Gorgora	NO	-0.32	0.71	-0.11	NO	0.9	0.39	-0.3	(-ve)	-2.46	-3.1	-1.79
8	Maksegnit	No	0.61	0.25	-0.51	No	1.03	-0.46	0.24	No	1.02	1.26	-0.12
9	Zege	NO	-1.46	1.36	0.04	NO	0.2	-0.3	-0.4	NO	1.36	0.21	1.14

The annual observed time series of precipitation, maximum and minimum temperature constructed for the Tana Sub-Basin are shown in the Figure 4.1 The annual observed time series of precipitation, maximum and minimum temperature constructed Tana Sub-Basin is shown in- figures below respectively.

Annual Observed Precipitation

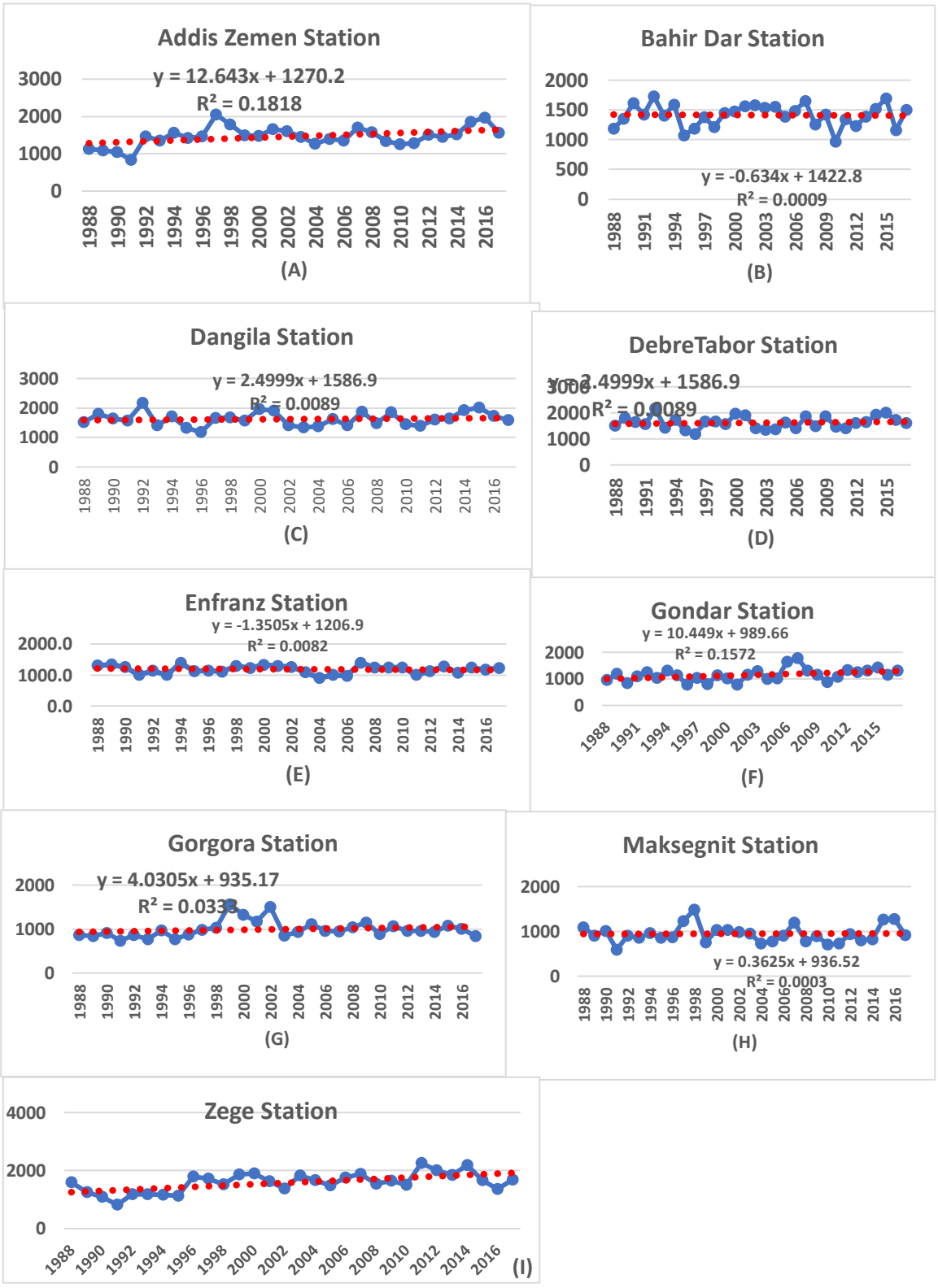

Annual Observed Minimum Temperature

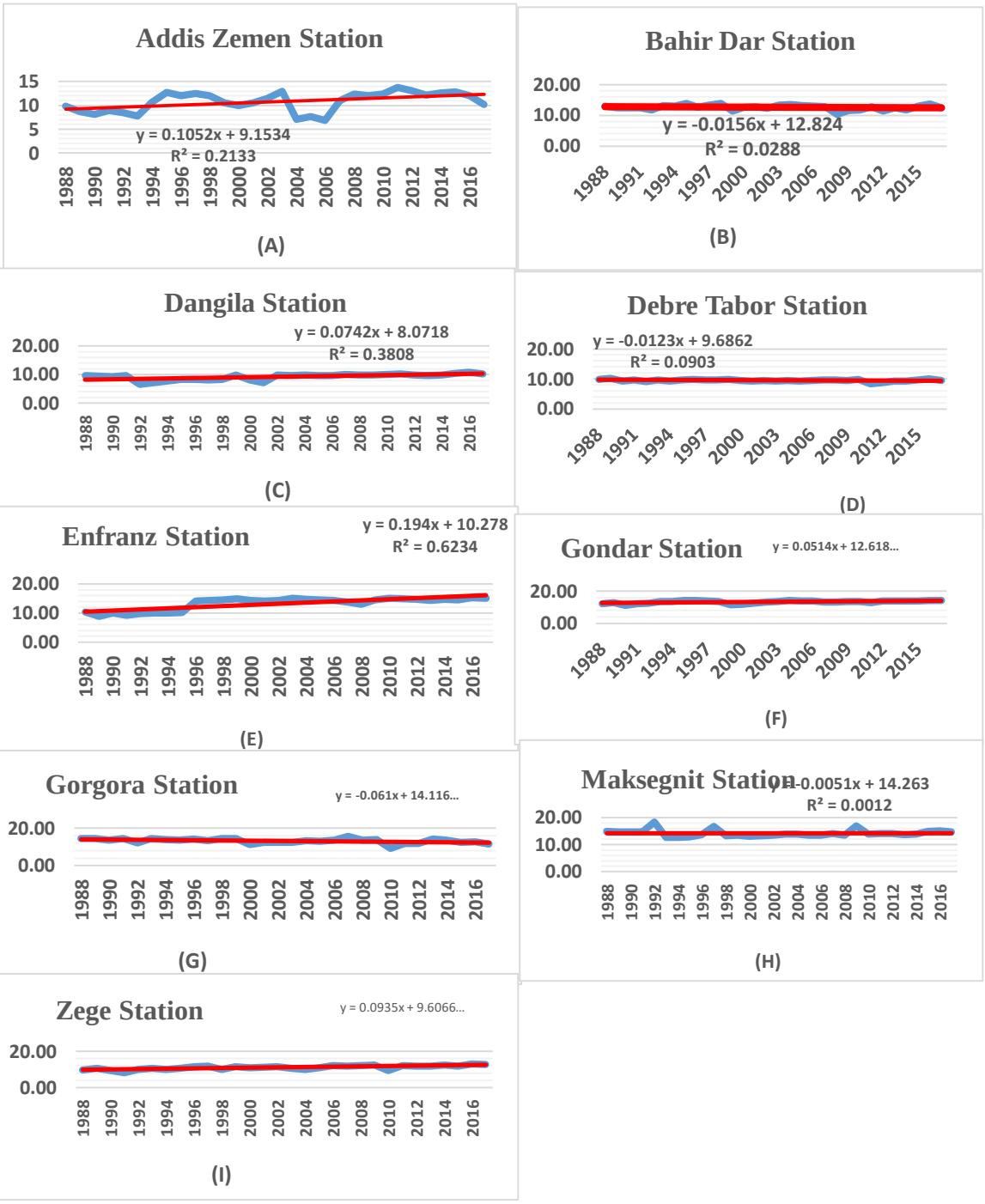

Annual Maximum Temperature

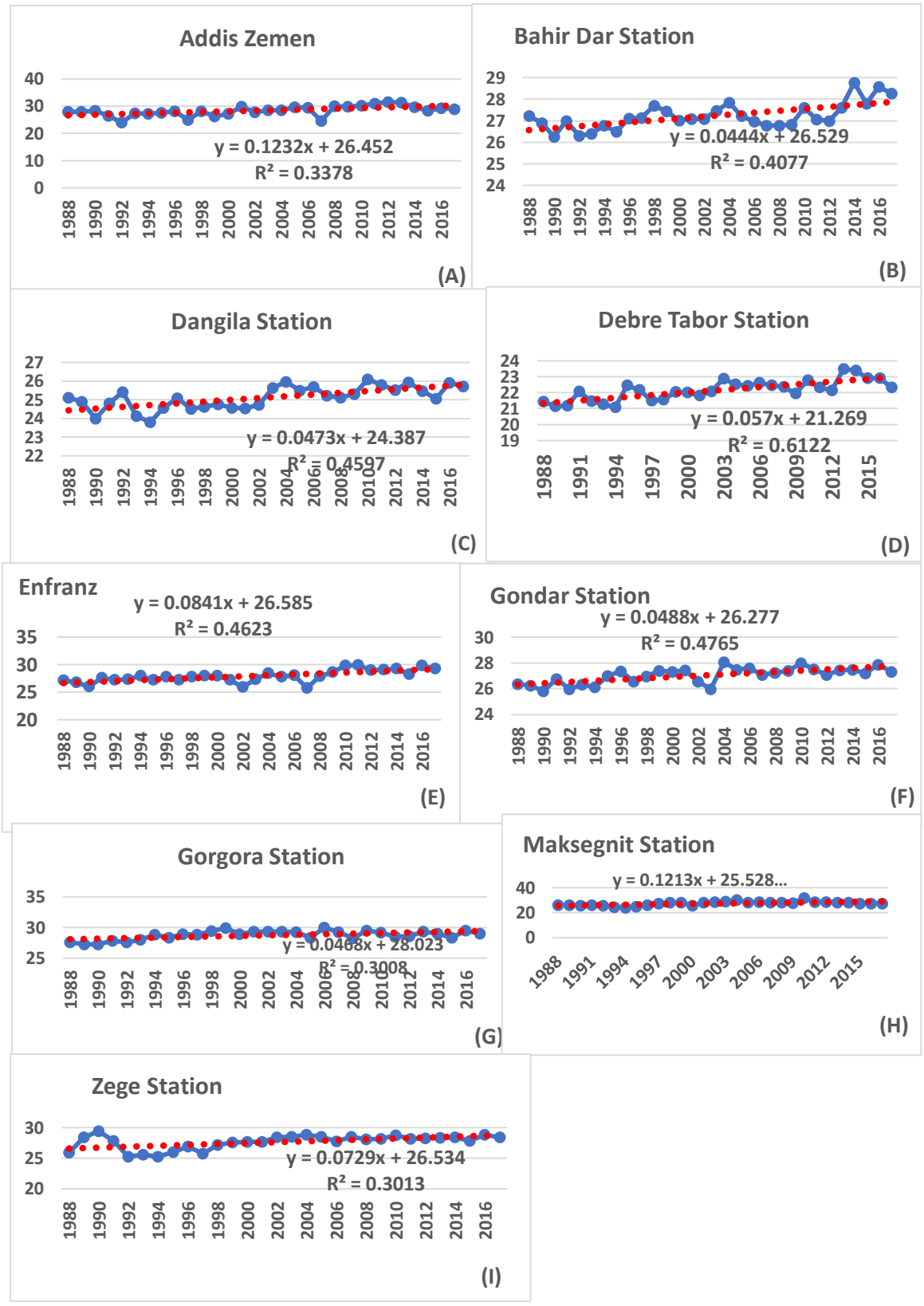

Figure 4. 1: Annual observed Precipitation, Minimum and Maximum Temperature

4.1.3 Result of Regional Mann-Kendall Test

The test is applicable to data where observations have been made annually at numerous locations. To determine whether to reject or not the null hypothesis of no trend, and test statistic Zr is assessed against the critical value Zcrit corresponding to the specific significance level α of the test. For the two-tailed test, the critical value is defined as $\Phi^{-1}(1-\frac{\alpha}{2})$, where Φ is cumulative distribution function of standard normal distribution, Helsel and Hirsch, (2002). The null hypothesis is rejected and the trend is considered significant statistically if the value of |Zr|≥ Zcrit. When the |Zr|≥1.96 there was a trend either increasing or decreasing but if |Zr|< 1.96 the trend analysis was rejected. In this study used 9 stations to analysis the regional Mann-Kendall test. The table below shown the result of the test of precipitation, minimum and maximum temperature.

Table 4. 3: Regional Mann-Kendall test results of precipitation, minimum and maximum temperature

Precipitation		Minimum Temperature		Maximum Temperature	
S	522	S	909	S	1787
Z	3.098	Z	5.401	Z	10.624
P	0.0019	P	0.000	P	0.000

The trend test result shown that among the 9 stations of Tana sub-basin only three stations show the presence of a statistically significant trend in the precipitation during none seasonal trend. Similarly, four stations show a statistically significant trend in the maximum temperature. Finally, three stations show significant trend in the minimum temperature was observed (show table 4.1). But during seasonal Mann-Kendall test there was no significant trend on precipitation, however three stations shown significant trend maximum temperature and two stations in minimum temperature (show table 4.2). Whereas the Regional Mann-Kendall trend test shown increasing trend as shown table 4.3.

4.2 Climate Model Performance Evaluation

Climate data performance evaluation is needed earlier to use in different hydrological models for any climate data when it was dynamically or statically downscaled from climate data set. The RCP data performance evaluation indicates how far adjustment should be care to secure the variation in estimated precipitation data by using bias correction method.

4.2.1 Scenarios developed for the base period

In this study for Tana sub-basin, bias corrected RCP emission scenario with a grid resolution of 0.5^0*0.5^0 used for analysis. Period from 1988-2017 taken as a baseline while the time periods from 2020-2049 and 2050-2079 are considered for impact study. Base period Scenarios are generated to compare the observed, RCP bias corrected and RCP bias uncorrected

4.2.2 Bias correction of precipitation

The result of bias correction between observed and down scaled precipitations at monthly level, as shown in the figure 4.1 below, indicates some are overestimated especially the six months May, June, July, August, October and November which are found in the main rainy season and Autumn (October & November) compare to observed rainfall. Whereas, January, February, March, April, May, September and December are underestimated. This result indicated that using down scaled RCP scenarios output directly without doing bias correction may lead to massive uncertainty of hydrological analysis. So before doing hydrological analysis downscaled climate data must be corrected.

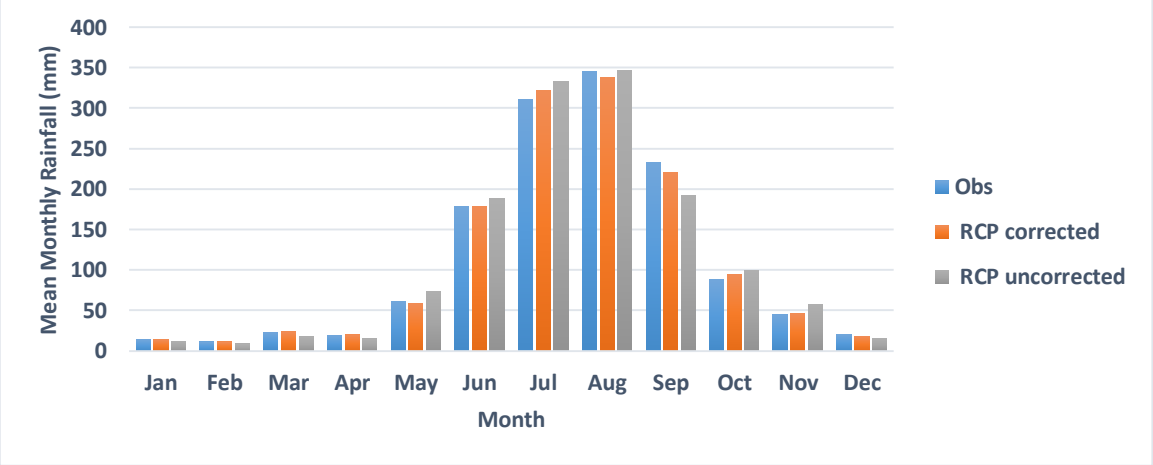

Figure 4. 2: Mean monthly rainfall distribution of observed PCP and RCP

4.2.3 Bias correction of temperature

A. Maximum Temperature

Bias corrected mean monthly maximum temperature tells good quality relations with the observed temperature for the baseline period. When down scaled mean monthly maximum temperature compared to observed mean maximum temperature, there are overestimation shown during March, April, May, June, October, November and December. During July

and August underestimation shown while for January, February and September there are good relationship between observed and RCP data (both RCP corrected &uncorrected). This result indicates that using the RCP data output without doing bias correction may lead to vast uncertainty of hydrological analysis.

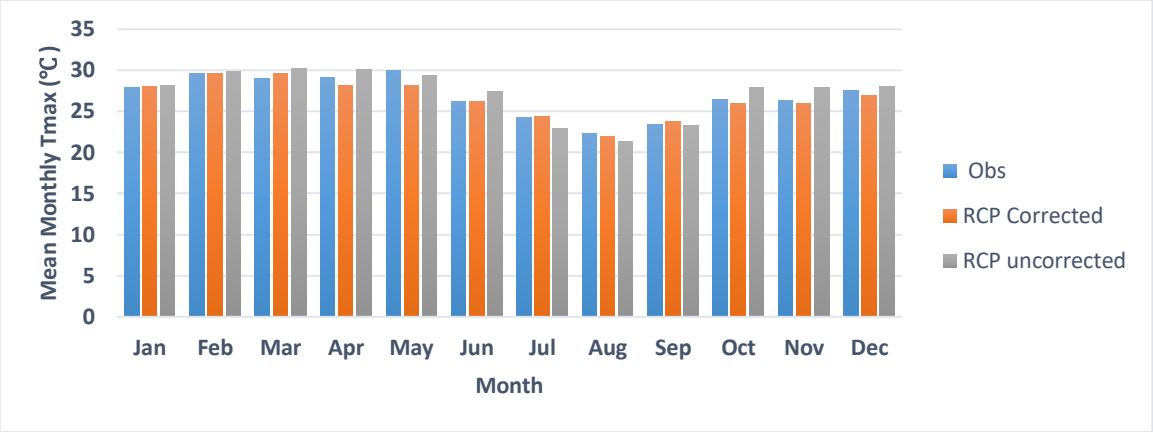

Figure 4. 3: Mean Monthly Observed and RCP Maximum Temperature

B. Minimum Temperature

Like Bias corrected mean monthly maximum temperature, bias corrected mean monthly minimum temperature shows a reasonably good similarity with the observed mean monthly minimum temperature for the baseline period. When down scaled mean monthly minimum temperature compared to observed mean monthly minimum temperature, considerable underestimation shown during June, July, August and December while considerable overestimation shown during September, April, May and September.

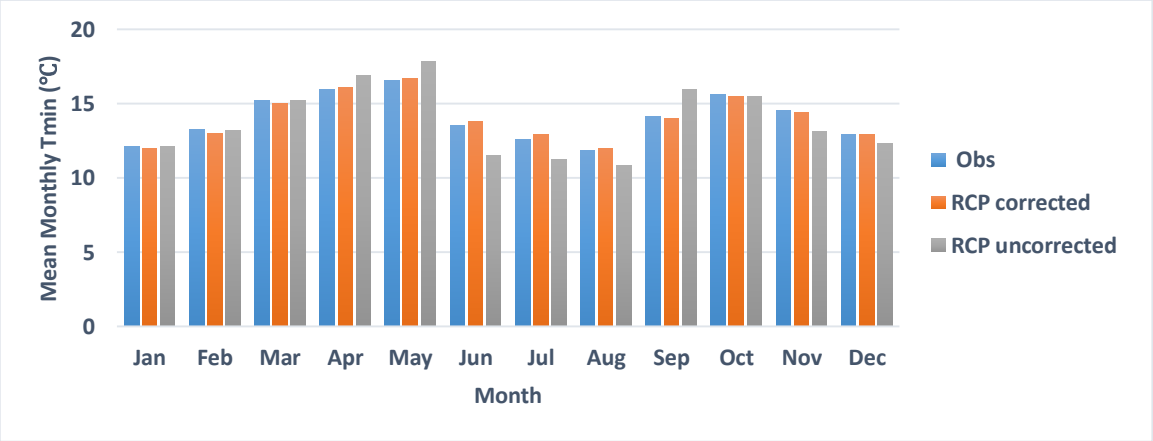

Figure 4. 4: Mean monthly minimum temperature for observed, bias corrected and uncorrected

4.3. Climate projection (2020-2079)

The future climate pattern includes precipitation, minimum temperature and maximum temperature was analyzed under RCP 4.5 and RCP 8.5 scenarios for Tana sub-basin. To simulate the future flow, the future climate projection carried out with down scaled and bias corrected RCP precipitation. The Comparison was made between the baseline 1988-2017 period and two consecutive 30 years' future periods: 2020-2049 and 2050-2079 respectively

4.3.1 Precipitation projection

The analysis of mean monthly distribution of rainfall in the Tana sub-basin provides relatively shown in decreasing change of rainfall pattern relative to the observed rainfall. The figure 4.5 presents the overall pattern of mean monthly precipitation in the Tana sub-basin for future periods under RCP 4.5 and RCP 8.5 scenarios. As shown the figure below the future projection of precipitation declines 2020-2049 +23.955% to 2050-2079 -47.466% for RCP4.5 and 2020-2049 -30.733% to 2050-2079 +2.091% for RCP8.5.

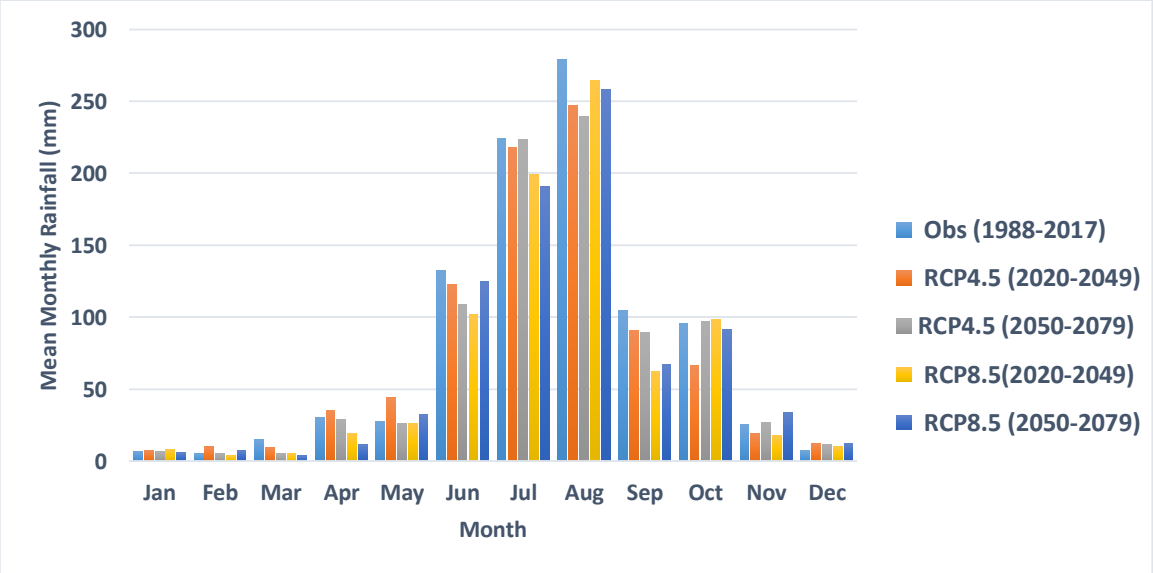

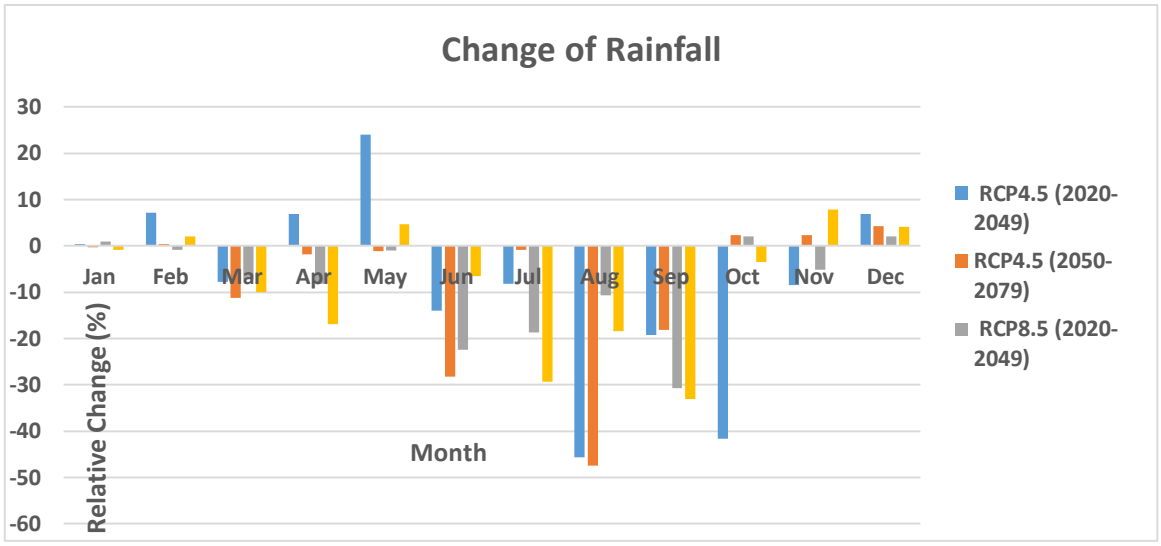

Figure 4. 5: Mean monthly and Relative change (%) future rainfall for Tana sub-basin

4.3.2 Maximum temperature projection

The projected maximum temperature has generally shown an increasing for both the future time periods 2020 – 2049 and 2050 – 2079 as compared to the base periods 1988-2017 for-RCP4.5 and RCP8.5 scenarios. Maximum temperature changes for RCP 4.5 shown in the figure below increases by 0.25°C to 1.6°C and 0.1°C to 1.91°C having 1.12°C and 1.15°C mean monthly maximum temperature change for 2020 – 2049 and 2050 – 2079 time periods with reference to the baseline periods respectively. For RCP 8.5 the maximum temperature shows increment between 0.11°C to 1.92°C and 0.19°C to 2.17°C having 1.16°C and 1.21°C of mean monthly maximum temperature change for 2020 – 2049 and 2050 – 2079 time periods as compared to the baseline periods respectively. Figure 4.6 below presents the future mean monthly maximum temperature fluxes as compared to the baseline periods under both RCP scenarios for future periods.

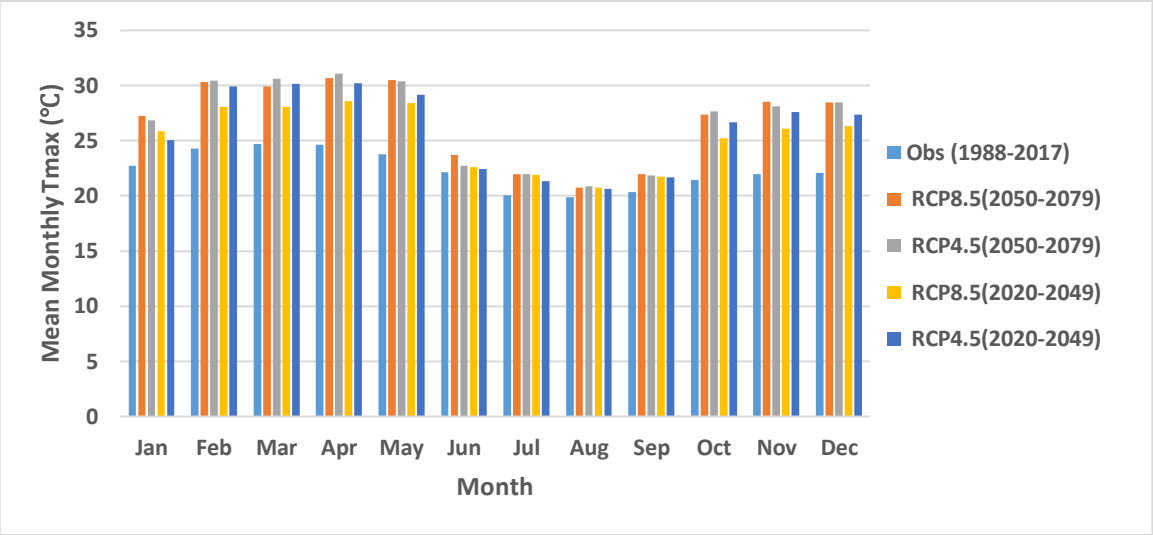

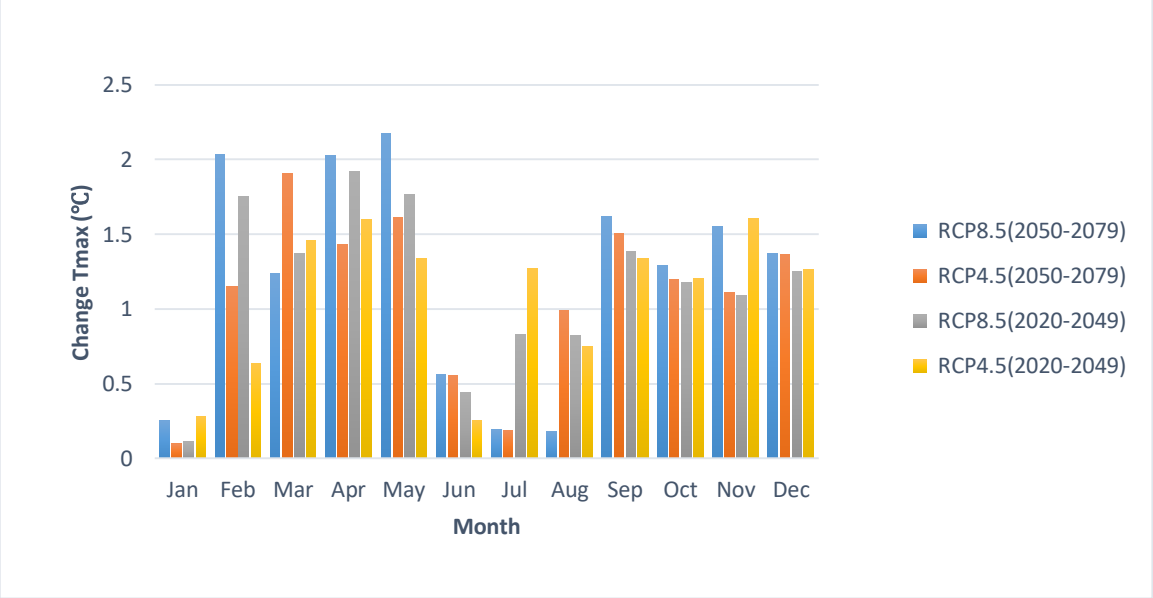

Figure 4. 6: Average monthly bias corrected and Percentage change of maximum temperature

4.3.3 Minimum temperature projection

Like to maximum temperature mean monthly minimum temperature shown an increasing from baseline to the future climate projection for both RCP scenarios (RCP4.5 and RCP8.5). Minimum temperature changes for RCP 4.5 shows increment by 0.26°C to 1.065°C and 0.45°C to 2.77°C mean monthly minimum temperature change for 2020 – 2049 and 2050 – 2079 time periods with respect to the baseline periods respectively. For RCP 8.5 the minimum temperature shows increasing by 0.145°C to 1.58°C and 1.02°C to 2.68°C mean monthly minimum temperature change for 2020 – 2049 and 2050 – 2079 time periods as

related to the baseline periods respectively. Figure 4.6 below shows future change in mean monthly minimum temperature to the baseline periods under both RCP scenarios.

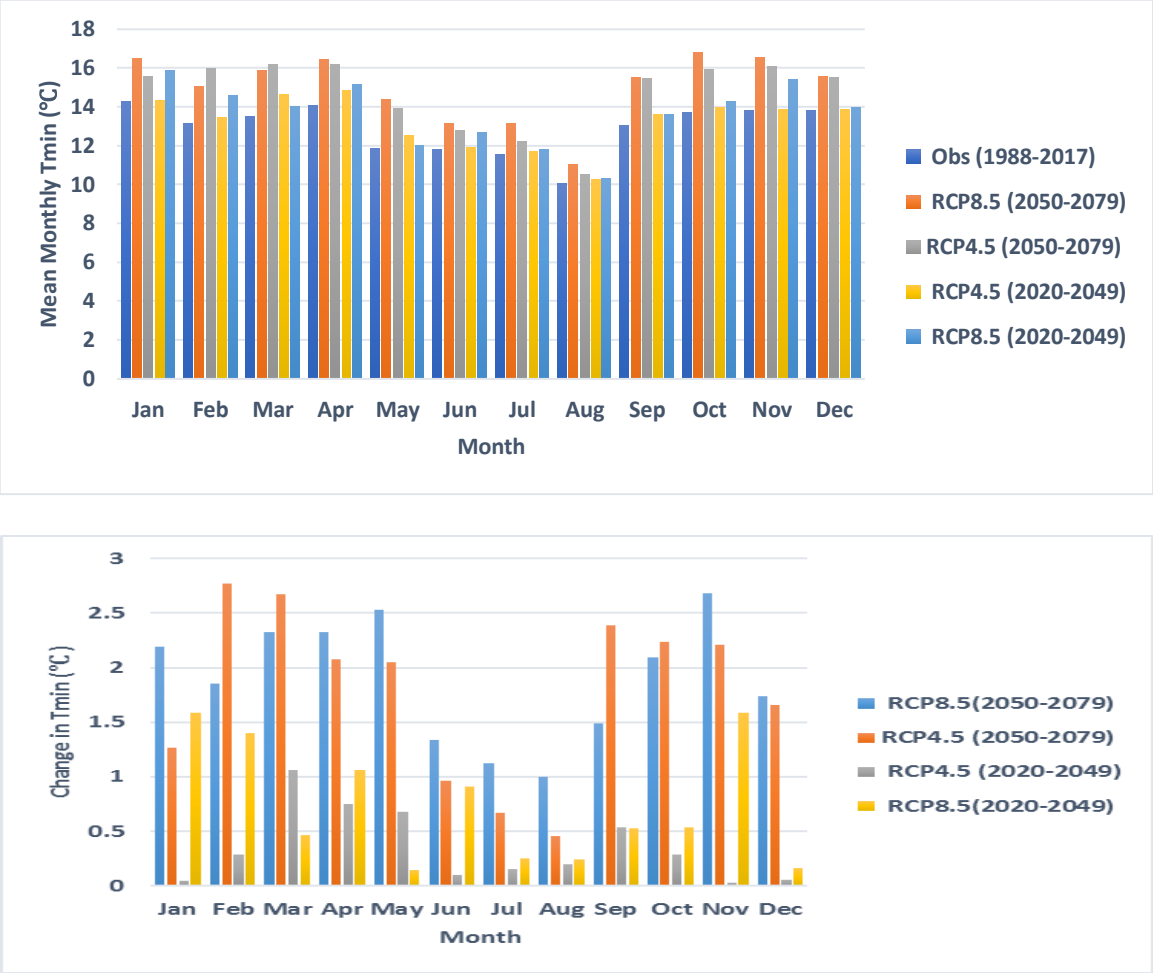

Figure 4. 7: Average monthly bias corrected and Percentage change of minimum temperature

Generally, both scenarios shown an increasing projection of minimum and maximum temperature RCP4.5 and RCP8.5 is slight over estimated. This result of the increase in minimum and maximum temperature is in agreement with IPCC 5th Assessment Reports (Niang et al,2014). The projected both minimum and maximum temperature over the study area will end up in warming, attributed to be the direct effect of continued increasing in CO2 emission during the 21st century, when the CO2 concentration is projected to be increased above 650ppm (IPCC,2014). This is in close agreement with the finding that have shown, there will be a warming over East Africa (Waithaka et al,2013).

4.4 SWAT Model Performance

After all the required inputs for the model were analyzed and prepared according to the model format, the watershed delineation was conducted from 30*30 DEM resolution and the model delineates an area of 14845 km2, provided that the outlet location is at Bahir Dar gauging station. The land use, soil and slope map of Tana Sub-Basin were over lay to produce a hydrologic response assembly by setting a threshold value of 5%, 20% and 20%. The land use/Cover, soil and slope domination to which land use percentage over the sub basin, soil over the land use and slope class percentage over the land use respectively selected by considering the effect of on the preparation of hydrologic response in the stream flow and for making the HRU formulation in a controllable amount. Accordingly, 43 sub basins having 273 HRUs created in the Tana sub basin of UBNRB.

4.4.1 Sensitivity analysis

Sensitivity analysis is a technique of identifying the responsiveness of different parameters involving in the simulation of a hydrological process. Hydrological models like SWAT, which involves a wide range of data and parameters in the simulation process, calibration is quite a cumbersome task. Hence, sensitivity analysis is a method of minimizing the number of parameters to be used in the calibration step by making use of the most sensitive parameters largely controlling the performance of the simulated process. Sensitivity of a model to a particular input or calibration parameter is defined as the ratio of the relative change of model output to the relative change of that parameter (Khari et al.,2016) Sensitivity analysis then shows the impact of input parameters on the objective function.

Before running the calibration, the sensitivity of the parameters was carried out using the Latin hypercube one-factor-at-a-time (LH-OAT) method of SWAT (van Griensven et al.,2006). This approach combines the advantages of global and local sensitivity analysis methods and can efficiently provide a rank ordering of parameter importance.

The sensitivity analysis is done on 23 SWAT model parameters that may have the potential effect on the stream flow of the sub-basin. The ranges of parameter variation are based on the SWAT manual (Abbaspour et al, 2004). After sensitivity analysis more sensitive SWAT parameters are identified based on their p-value of statistical significance for the Sub-Basin. After setting up the SWAT-CUP using SWAT model outputs and combining all input parameters, simulations were carried out with SUFI-2 by running 500 simulations and the Sensitivity analysis was carried out for both the calibration and warming up periods 1990-2001. The table below shows the SWAT model parameter used for this study.

Table 4. 4: SWAT Model Parameters for Calibration and Validation

SN	Parameter	Descriptions
1	CH-K2.rte	Effective hydraulic conductivity in main channel alluvium.
2	GW_DELAY.gw	Groundwater delay (days)
3	CN2.mgt	SCS runoff curve number
4	Alpha_BF.gw	Base flow alpha factor(days)
5	SOL_AWC.sol	Available water capacity of the soil layer
6	SLOP_CON hru	Soluble phosphorus concentration un runoff, after urban BMP is applied
7	ESCO.bsn	Soil evaporation compensation factor
8	EPCO.bsn	Plant uptake compensation factor
9	SOL_K.sol	Saturated hydraulic conductivity
10	WG_REVAP.wg	Ground water “revap” coefficient
11	OV_N.hru	Manning's "n" value for overland flow
12	USLE_K.sol	USLE equation soil erodibility (K) factor.
13	SURLAG.bsn	Surface runoff lag time
14	RCHARG_DP.gw	Deep aquifer percolation fraction.
15	REVAPMN.gw	Threshold depth of water in the shallow aquifer for "revap" to occur (mm).
16	SLSUBBSN.hru	Average slope length
17	SOL_ALB.sol	Moist soil albedo
18	SOL_CBN.sol	Organic carbon content
19	SOL_BD.sol	Moist bulk density

20	GW_QMN.gw	Threshold depth of water in the shallow aquifer required for return flow to occur (mm).
21	CANMX. hru	Maximum canopy storage
22	SOL.ZMX.sol	Maximum rooting depth of soil profile
23	IGRO.mgt	Land cover status code

Out of those twenty-three parameters used for the sensitivity analysis, only 10 Parameters were significant effect on the monthly flow simulation of Tana Sub-Basin stream flows. The sensitive parameters selected based on P-value and t-stat. The P-value closer to zero indicates more significance parameters and the absolute value of t-stat far from zero the parameters were most sensitive. The figure and table below shows rank of the sensitive parameters during calibration and validation of stream flow.

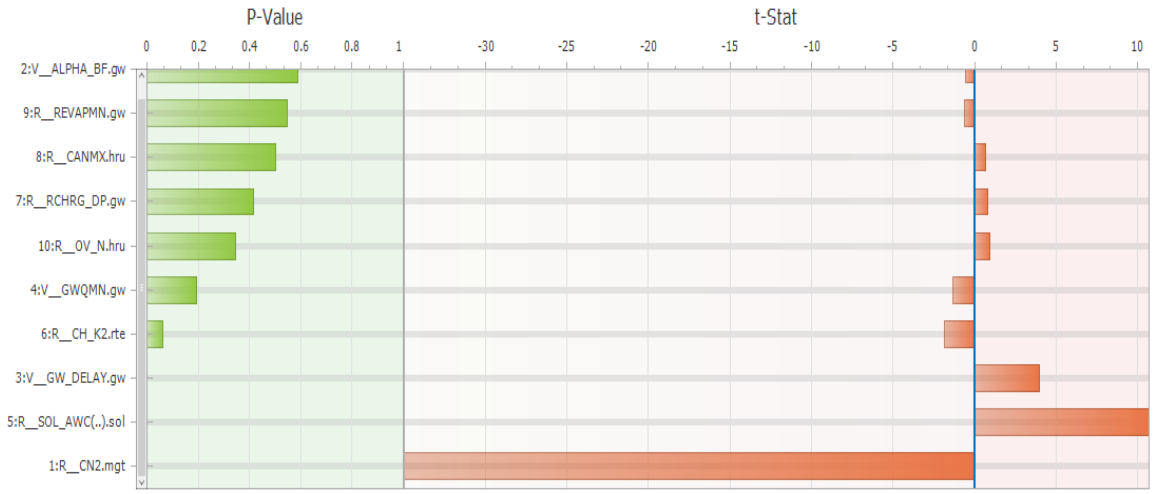

Figure 4. 8: Global Sensitivity Results Giving to P-value and T-Stat

Table 4. 5: Hydrologic calibration parameters values with their fitted value

Rank	Parameters	SWAT Default		Fitted Value
		Low boundary	Upper boundary	
1	R__CN2.mgt	-0.2	0.2	-0.102000
2	V__ALPHA_BF.gw	0	1	0.40500
3	V__GW_DELAY.gw	30	450	439.500000
4	V__GWQMN.gw	0	2	0.938000
5	R__SOL_AWC.sol	0	1	0.963000
6	R__CH_K2.rte	-0.01	500	175.493515
7	R__RCHRG_DP.gw	0	1	0.151000
8	R__CANMX.hru	0	100	65.300003
9	R__REVAPMN.gw	0	500	61.500000
10	R__OV_N.hru	0.01	30	16.594471

4.4.2 Calibration, Validation and Uncertainty analysis

Flow calibration has done for a period of fourteen years from January 1, 1988 to December 31, 2002 using the sensitive parameters recognized. However, flow was simulated for 21 years from January 1, 1988 to December 31, 2008, within which the first two years was considered as a warm up period. Flow validation was performed for a period of six years from January 1,2003 to December 31, 2008.

The parameters were allowed to vary during the calibration process within acceptable ranges until an acceptable fit between the measured and simulated values was obtained at watershed outlet; no changes were made to the calibrated parameters during the six-year of validation. Hydrologic calibration parameters and their fitted values for the gauged stations are shown in Table 4.5 The calibration and validation results for the gauged station in Table 4.6 show that there is a good agreement between the monthly simulated and observed flows. The

general performance rating of recommended statistics for monthly time step as suggested by (Moriasi et al.,2015) indicates R^2>0.6, ENS>0.5 and PBIAS<±25, based on the recommendation, the present result shows acceptable performance.

Table 4. 6: Calibration, Validation and Uncertainty Analysis Results

Criteria	Calibration (1988-2002)	Validation (2003-2008)
R^2	0.87	0.84
NSE	0.61	0.6
P-Bias	-23.1	-24.1
P-factor	0.6	0.78
R-factor	1.36	1.86

Uncertainty analysis was also done using SWAT-CUP linked to SUFI-2 on measured stream flow data. The degree to which all uncertainties are accounted for quantified by a measure referred to as the P-factor, which is the percentage of measured data bracketed by the 95% prediction uncertainty (95PPU) and another measure quantifying the strength of a calibration/uncertainty analysis is the R-factor, which is the average thickness of the 95PPU band divided by the standard deviation of the measured data. The results of P-factor and R-factor for monthly discharge are also shown in Table 4.6 above.

Gauging station at Bahir Dar monthly discharge, 60% of the observed data is bracketed by the 95PPU (P-factor) and the thickness of the 95PPU (R-factor) had a value of 1.36 during calibration, which is a good result. The smaller R-factor value, the smaller the uncertainties and the better is the calibration work. A value close to 1 is highly desirable for R-factor with a P-factor also close to 1.

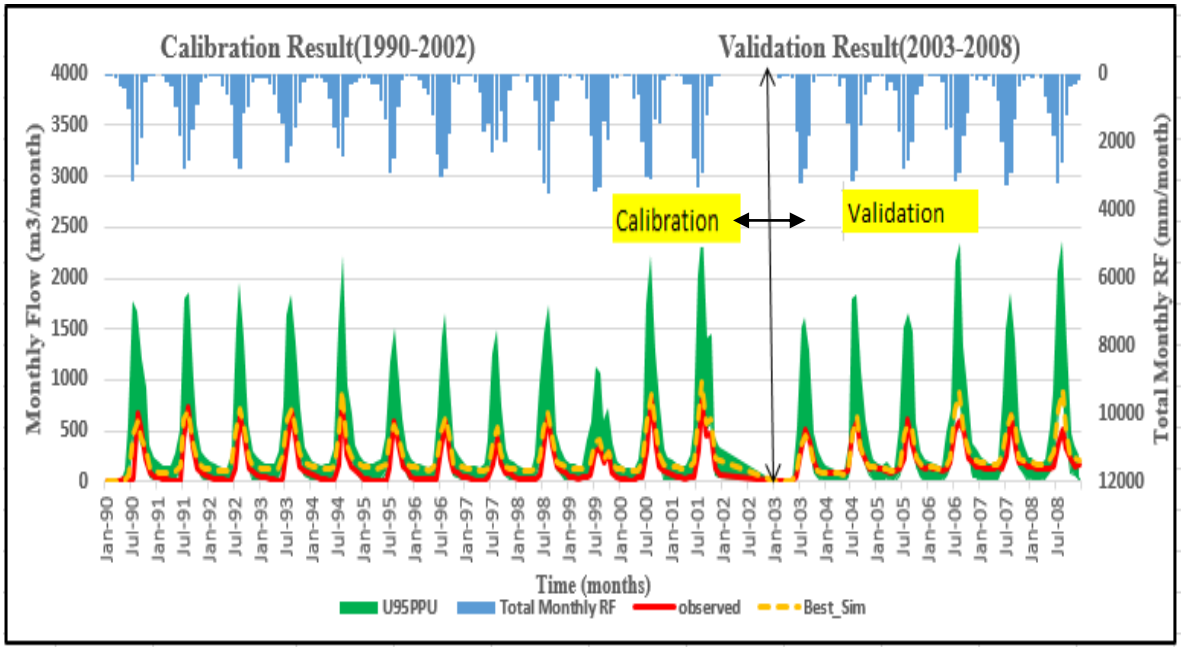

Figure 4. 9: Observed and Simulated Monthly Streamflow For Calibration and Validation

4.4.3 Climate change impact on the streamflow

The key objective of downscaling is to generate a reliable estimation of meteorological variables corresponding to given scenario of the future climate consequently these meteorological variables will be used as basis for different types of impact studies. Therefore, after calibration and validation of hydrological models with historical record, the next step is to simulate stream flows in the sub-basin of Tana corresponding to future climate conditions by using the downscaled daily precipitation and temperature in to SWAT model. Such simulation supports to identify the hydrological response impacts affected by climate change. The future climate variables that are downscaled precipitation and temperature originated as an output from the RCPs scenarios' and corrected RCPs were given as an input to the SWAT model. Then simulation results corresponding to each of downscaling scenario time period (baseline 1988-2017, and future 2020-2049 and 2050-2079 were analyzed for all RCP4.5 and RCP8.5 scenarios.

4.3.4 Climate change impact on monthly streamflow of Tana Sub-Basin

Climate change impact on monthly streamflow was evaluated by relating base period stream flow with the future flows for the 2020-2049 and 2050- 2079 for both RCP4.5 and RCP8.5 scenarios. As shown in the figure below the future streamflow shows increment and decrement trends for both RCP4.5 and RCP8.5 scenarios.

In the periods 2020-2049 & 2050-2079 for the RCP4.5 scenarios, the streamflow may shown

an increment and decrement for the given months. In 2020-2049 the future streamflow 1.57% to 32.46% in the months of April and December and 2050-2079 the future streamflow increases 5.74% to 16.87% in the months of may and April respectively. However, the future streamflow in the period 2020- 2049 1.23% to 44.38% decreases in the months of January and June and 2050-2079 0.91% to 38.73% decreases in the months of January and June respectively. Increase and decrease streamflow may be observed in months which shown an increasing and decreasing in monthly precipitation.

In the periods 2020-2049 & 2050-2079 for the RCP8.5 scenarios, the simulated future streamflow shown an increment and decrement trend for the given months. In 2020-2049 the future streamflow 3.33% to 11.04% in the months of Junuary and December and 2050-2079 the future streamflow will be increased 2.52% to 21.29% in the months of March and may respectively.

And also, the simulated streamflow will be decreased 2.84% to 68.15% in the periods of 2020-2049 in the months of May and July and 2.8% to 57.86% in the periods of 2050-2079 in the months of January and July respectively.

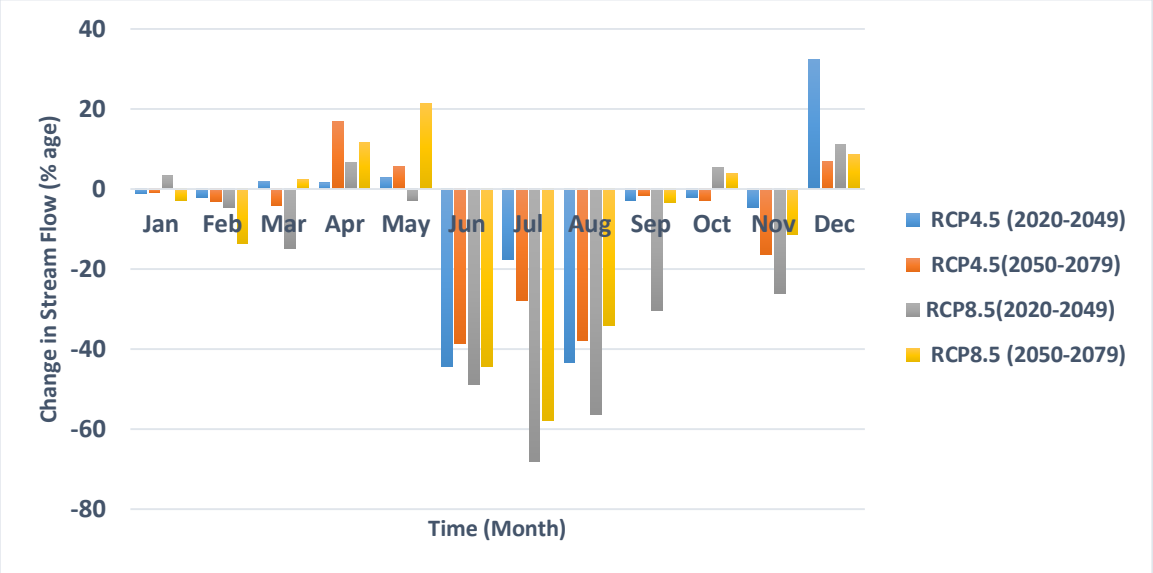

Figure 4. 10: Monthly Observed and Simulated future streamflow change in percentage (RCP4.5 and RCP8.5)

Generally, the pattern of steam flow projection in Tana sub-basin follows increasing and decreasing as compared to baseline period shown in the figure above. Those increasing and decreasing future stream flow will have affected the existing and the future projects in the study area. Therefore, to reduce the impact of climate change on hydrology of the study area

of future stream flow different measurements must be taken. Water resource is projected to be increase in east Africa including Ethiopia by 10% at the end of 21st century (UNECA, 2011). The projected stream flow of Tana sub-basin will be increased and decreased in both future time periods under both RCP scenarios. Therefore, water resource planners and users should be connected the existing water resource for developmental purpose like irrigation project and others taking into account mitigation and adaptation strategies due to changing climate projected over the study area.

4.4 Future Projection of Evapotranspiration

In this study, Evapotranspiration was calculated using both penman and Hargreaves method for baseline to develop correction factor between penman and Hargreaves method for future projection. To be well-suited with the method adopted during model calibration, and validation a regression equation was developed and correct by correction factor to estimate the Penman- potential Evapotranspiration from Hargreaves potential evapotranspiration used for Future period analysis.

Therefore, the developed equation between Penman and Hargreaves method for this study is shown below: -

Future ETo =Hargreaves*0.459 [4-1]

The average monthly evapotranspiration shown increase trend for future scenarios for the study area under both RCP scenarios. The rate of monthly evapotranspiration is found to be increase during all months of both RCP 4.5 and RCP 8.5 for future projections. Under RCP 4.5 mean monthly evapotranspiration increased by 2.71% and 3.98% for 2020 – 2049 and 2050 – 2079 time periods respectively. Whereas, for RCP 8.5 the increase reaches 5.87% and 9.13% for 2020 – 2049 and 2050 – 2079 time periods respectively. The rate of monthly evapotranspiration is found to increase comparatively at higher degree during the months of January , March, May and December for both future- projections under all RCP scenarios.

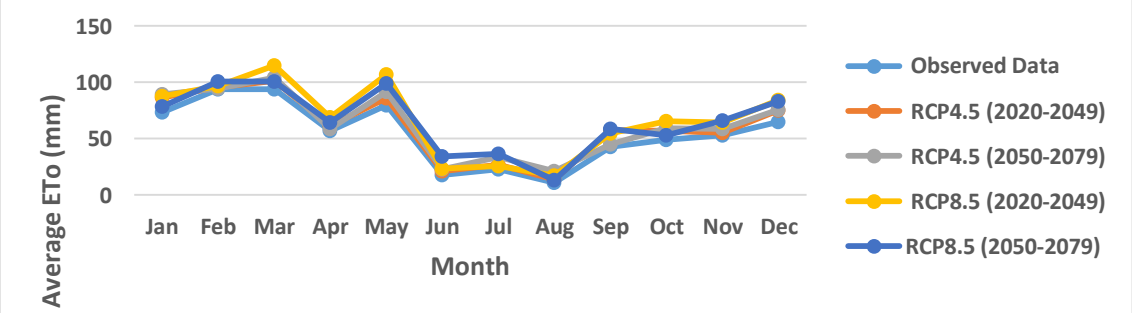

Figure 4. 11: - Average Monthly Evapotranspiration for the Tana sub-basin

4.5 Future Projection Evaporation

The results of modeled lake evaporation in the present day scenario exposed that the reservoir has a variable trend. The maximum and minimum net evaporation rate were recorded for the month November and Julay respectively. The average monthly evaporation shown increasing by 3.81% and 5.98% for the year 2020– 2049 and 2050 – 2079 under RCP 4.5 scenario respectively. Whereas, for RCP 8.5 spreads up to 4.89% and 6.45% for the year 2020 – 2049 and 2050 – 2079 respectively.

The rate of monthly evaporation is found to increase comparatively at higher rate during the months of January , March and may in 2020 – 2049 and 2050 – 2079 time periods under both RCP scenarios. This indicates that, the increase in temperature will also increases the average lake evaporation under the climate change scenario.

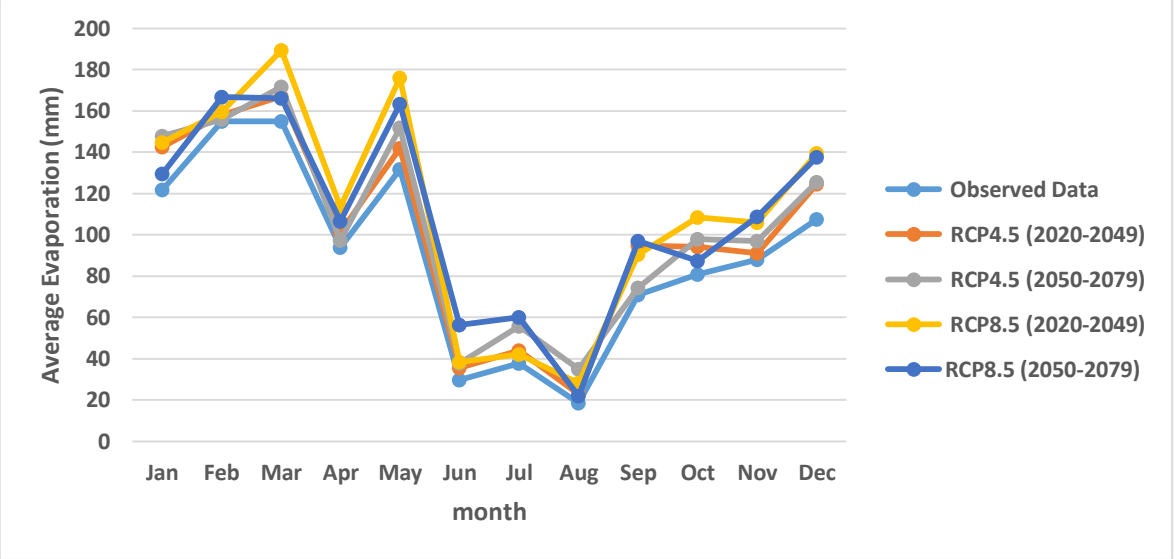

Figure 4. 12: - Average Monthly Evaporation for the Lake Tana

5. SUMMERY AND CONCLUSION

5.1 SUMMERY

Climate change has potential impacts on future hydrological and meteorological variables due to increased greenhouse gas emissions which are associated with increasing temperature of the globe. The presence of potential trends test for precipitation, maximum and minimum temperature in the Tana Sub-Basin was checked at each stations using the concepts of the Mann-Kendall and the seasonal Mann-Kendal tests by using XLSTAT statistical software and all stations by using Regional Mann-Kendall trend test.

The result of climate projection reveals that the CORDEX-Africa data outputs of HadGEM2-ES under representative concentration pathways (RCP4.5 and RCP8.5) scenarios has very good ability to replicate the historical maximum and minimum temperature for the observed period; but The replication of precipitation was poor. The bias correction of dynamically downscaled raw RCPs data was corrected using CMhyd tool successfully as the bias-corrected climate variables produced consistent results with the historical records. The corrected and historical monthly values were smaller than the raw RCP and historical monthly values of precipitation and temperature. The bias correction methods performance estimation for precipitation, minimum temperature and maximum temperature, was also performed and better improvement was increased after bias correction. So it can be concluding that the bias correction method used was accurate for downscaled climate variables to replicating the main features of the observed data.

The future impact of climate change on hydro meteorological characteristics of the basin has been studied such as precipitation, Minimum and Maximum Temperature for the two future time periods 2020-2049 and 2050-2079 using CMIP5 projection output. SWAT 2012 hydrological model was used to study impacts of climate change on Tana Sub-Basin Streamflow.

The climate projection analysis indicated of mean monthly distribution of precipitation in the Tana sub-basin provides relatively shown in decreasing and decreasing pattern relative to the observed rainfall in different months.

The overall pattern of mean monthly precipitation in the Tana sub-basin for future periods under RCP 4.5 and RCP 8.5 scenarios expected to declines by 30.73%-47.46% and will have increased 2.09%-23.96% for 2020-2049 and 2050-2079 respectively.

The projected maximum temperature has shown an increasing change for both the future time periods 2020 – 2049 and 2050 – 2079 as compared to the base periods (1988-2017) For RCP4.5 and RCP8.5 scenarios will have increased by 0.25℃ to 1.6℃ and 0.1℃ to 1.91℃ and 0.11℃ to 1.92℃ and 0.19℃ t0 2.17℃ respectively. And Minimum temperature shown an increasing change from baseline period to the future climate projection of both RCP 4.5 and RCP 8.5 scenarios could have increased by 0.26℃ to 1.065℃ and 0.45℃ to 2.77℃ and 0.145℃ to 1.58℃ and 1.02℃ to 2.68℃ for 2020-2049 and 2050-2079 respectively.

The result of SWAT model calibration and validation indicates that the SWAT model simulated the stream flow considerably very good for this study area. The model performance criterion which is used to evaluate the model result indicated that Nash and Sutcliffe efficiency criteria ($R^{2)}$ were 0.87 and 0.84 and 0.61.and 0.6 during calibration and validation period respectively.

Climate change impact on monthly streamflow was evaluated by relating base period stream flow with the future flows for the 2020-2049 and 2050- 2079 for both RCP4.5 and RCP8.5 scenarios. The future streamflow expected to show increment and decrement for both RCP4.5 and RCP8.5 scenarios. The future stream flow of Tana Sub-Basin in RCP4.5 and RCP8.5 scenarios 3.65% to 24.67% averagely will be increased and decreased 1.07% to 41.42% and 2.93% to 16.17% increased and 2.84% to 63.00% decreased for both 2020-2047 and 2050-2079 periods respectively.

The results of this study confirmed that in the future streamflow will have increased and decreased due to climate change at the outlet of Tana sub-basin in the Blue Nile River at Bahirdar gauging stations. The increases future stream flow will play significant benefits for small and large scale projects in the study area. Whereas the decreases of future stream flow due to climate change will have negative impacts on those small and large scale projects.

Generally, the stream flow of Tana Sub-Basin which is the sources of Blue Nile river basin and highly vulnerable to climate change which causes high temporal variation of stream. So it needs serious measures to climate change impacts on the stream flow of the basin. Moreover, the results shown in this study would provide valuable insight to decision makers and stack holders on the degree vulnerability of Blue Nile river basin to climate change which is important to design, appropriate adaptation and mitigation measures and strategies.

5.2 CONCLUSION

There are many sources of uncertainty in the hydrological impact scenarios that are in the climate change study modelling the mothed used for transferring the climate signal to meteorological stations and in the hydrological modelling the model simulations have not well-thought-out the land use land cover changes. It is expected that changes in land use land cover may relate with climate change impact important to different projections of future hydrological conditions. Therefore, the results of this study should be taken with upkeep and be considered as indication future change rather than the actual prediction.

The land use land cover and Soil activity will also contribute excessive impact on rainfall runoff process. This study considers the climate variable by assuming land use land cover and soil constant. Soil and water conservation activities and Soil moisture improvement techniques including afforestation should get high concern to compensate the projected climate change impact. Therefore, future researcher should focus on land use land cover and soil variability.

The current study indicates that there exists a difference in the result found between SRES scenarios of previous research work and the RCPs (RCP 4.5 and RCP 8.5) in the current study. therefore, further analysis can be assumed with more RCPs and more bias correction method to give a perfect result for policy makers.

Water resources are inseparably linked with climate change; the view of global climate change has a serious implication for water resources. as water recourse stresses become severe in the future as result of climate change impacts, there will be increasing conflict between the environment and humans living around there. As we have seen the result of this study the future stream flows shown decreasing and increasing trends in different months. So thus decreasing and increasing future stream flow will be caused drought and flooding due to climate change on hydrology of the study area. Therefore, to reduce drought and flooding the respective bodies must practice good environmental managements like afforestation, methods of farming, decreasing cattle grazing, decreasing the users of firewood and aware stakeholders in and around the Tana sub-basin.

REFERENCES

Abayneh, A. (2011). Evaluation of Climate Change Impact on Extreme Hydrological Event on Upper Blue Nile basin. Addis Ababa University, Addis Ababa

Abbasnia, M.; Toros, H. Future changes in maximum temperature using the statistical downscaling model (SDSM) at selected stations of Iran. Model. Earth Syst. Environ. 2016

Abdella, K. (2013). The Effect of Climate Change on Water Resources Potential of Omo-Gibe Basin, Ethiopia. Universität der München. PhD Dissertation.

Abeyou., W. W., Dile, Y. T., Ayana, E. K., Jeong, J., Adem, A. A., & Gerik, T. (2018). Impact of climate change on streamflow hydrology in headwater catchments of the Upper Blue Nile Basin, Ethiopia. Water, 10(2), 120. (accessed on 1/22/2019

Alemseged, T. H., & Tom, R. (2015). Evaluation of regional climate model simulations of rainfall over the Upper Blue Nile basin. Atmospheric research, 161, 57-64.

Antonia Longobardi and Paolo Villani (2009) Trend analysis of annual and seasonal rainfall time series in the Mediterranean area Department of Civil Engineering, University of Salerno, Via Ponte Don Melillo, 84084 Fisciano (SA), Italy, accessed date 23/9/2019

BCEOM (1998) Abbay River Basin Integrated Development Master Plan Project Phase 2, Data Collection and – Site Investigation Survey and Analysis, Section II, - Sectoral Studies, Volume XIV – Demography and Sociology. The Federal Democratic Republic of Ethiopia, Ministry of Water Resources.

Breuer, L.; Huisman, J.; Willems, P.; Bormann, H.; Bronstert, A.; Croke, B.; Frede, H.G.; Graff, H.T.; Jakeman, L. Assessing the impact of land use change on hydrology by ensemble modeling (LUCHEM). I: Model inter comparison with current land use. Adv. Water Resource. 2009, 32, 129–146

Brown, C., Greene, A, Block, P. and Giannini, A. (2008). Review of downscaling methodologies for Africa climate applications. International Research Institute for Climate and Society Columbia University.

Chow, V. T., Maidment, D. R., & Mays, L. W. (1988). Applied hydrology McGraw-Hill International editions. New York, USA.

Claudia Teutschbein and Jan Seibert: Regional Climate Models for Hydrological Impact Studies at the Catchment Scale: A Review of Recent Modeling Strategies, Department of Physical Geography and Quaternary Geology, Stockholm University, 2010,834-860 accessed date,8/20/2019

Climate Change National Adaptation Programmer of Action (NAPA) OF ETHIOPIA, Addis Ababa Ethiopia,2007, accessed date 8/20/2019

Conway D, Schipper EL (2011) Adaptation to climate change in Africa: Challenges and opportunities identified from Ethiopia. Glob Environ Chang 21: 227-237.

Elshamy, M. E., I. A. Seierstad, A. Sorteberg (2009). Impacts of climate change on Blue Nile flows using bias-corrected GCM scenarios, Hydrol. Earth Syst. Sci., 13, 551–565.

Emerta, A. (2013) climate change, growth, and poverty in Ethiopia. The Roberts. Strauss center, working paper No.3

Feyissa, G., Zeleke, G., Bewket, W., & Gebremariam, E. (2018). Downscaling of future temperature and precipitation extremes in Addis Ababa under climate change. Climate, 6(3), 58.

Gelete, G., Gokcekus, H., & Gichamo, T. (2019). Impact of climate change on the hydrology of Blue Nile basin, Ethiopia: A review. Journal of Water and Climate Change.

Getnet et al (2018) Downscaling of Future Temperature and Precipitation Extremes in Addis Ababa under Climate Change, Department of Geography and Studies, Addis Ababa University,2018 accessed date 12/4/2018

Hayelom, B., Chen, Y., Marsie, Z., & Negash, M. (2017). Temperature and precipitation trend analysis over the last 30 years in Southern Tigray Regional State, Ethiopia.

Hirsch, R. M., Slack, J. R., & Smith, R. A. (1982). Techniques of trend analysis for monthly water quality data. Water resources research, 18(1), 107-121.

Intergovernmental Panel on Climate Change. Climate Change (2014): Impacts, Adaptation, and Vulnerability WGII AR5 for.2014. (accessed on 12/15 2018).

IPCC (2007) Climate Change- The Physical Science Basis. The contribution of Working Group I to the Fourth Assessment Report of the Intergovernmental Panel on Climate Change [Solomon, S., Qin, D., Manning, M. et al., (eds)]

Contribution of Working Group I to the Fourth Assessment Report of the Intergovernmental Panel on Climate Change. Cambridge University Press, Cambridge, UK.

IPCC (2008a) Special report on Climate Change and Water. A Special Report of Working Group II of the Intergovernmental Panel for Climate Change. Cambridge University Press, Cambridge.

IPCC (2013). Climate Change- The Physical Science Basis. The contribution of Working Group I to the Fifth Assessment Report of the Intergovernmental Panel on Climate Change [Stocker, T.F., D. Qin, G. - K. Plattner, M. Tignor, S.K. Allen, J. Boschung, A. Nauels, Y. Xia, V. Bex and P.M. Midgley (eds.)]. Cambridge University Press, Cambridge, United Kingdom and New York, NY, USA, 1535 pp.

IPCC .(2014). Climate change 2014: mitigation of climate change. The contribution of Working Group III to the Fifth assessment report of the Intergovernmental panel on climate change. Cambridge University Press, Cambridge, United Kingdom and New York, NY, USA

IPCC Technical Summary, (2001). Climate Change (2001): The Scientific Basis. Technical Summary of the Working Group I Report [Houghton, J.T., Y. Ding, D.J. Griggs, M. Noguer, P.J. van der Linden, X. Dai, K. Maskell, and C.A. Johnson (eds.)]. Cambridge University press, Cambridge United Kingdom and New York, NY, USA.

IPCC- TGICA, (2007): General Guidelines on the Use of Scenario Data for Climate Impact and Adaptation Assessment. Version 2. Prepared by T.R. Carter on behalf of the Intergovernmental Panel on Climate Change, Task Group on Data and Scenario Support for Impact and Climate Assessment, 66 pp)

K. Subramanya (2008). Engineering Hydrology, Tata McGraw-Hill. New Dehli.

Kebede, A.; Diekkruger, P.; Moges, S.A. (2013) An assessment of temperature and precipitation change projections using a regional and a global climate model for the Baro-Akobo Basin, Nile Basin, Ethiopia. J. Earth Sci. Clim. Chang. 2013.

Khairi Khalida, Mohd Fozi Alib, Nor Faiza Abd Rahmanc, Muhamad Radzali Mispand, Siti Humaira Harone, et al, (2016): - Sensitivity analysis in watershed model using SUFI-2 algorithm, a Faculty of Civil Engineering, Universiti

Teknologi MARA Pahang, Bandar Jengka, Pahang, Malaysia 162 (2016) 441 – 447 accessed date 16/10/2019.

Moriasi, D. N., Gitau, M. W., Pai, N., & Daggupati, P. (2015). Hydrologic and water quality models: Performance measures and evaluation criteria. Transactions of the ASABE, 58(6), 1763-1785.

Netsanet, Z. C. (2013). Downscaling and modeling the effects of climate change on hydrology and water resources in the upper Blue Nile river basin, Ethiopia (Doctoral dissertation, Universitätsbibliothek Kassel). (accessed on 12/7/2018)

Rathjens, H., Bieger, K., Srinivasan, R., Chaubey, I., & Arnold, J. G. (2016). CMhyd User Manual.

SMEC, I.P(2007). Hydrological study of Tana beles sub basin part I.

Solomon, A.; Rao, P.; Rao, M.N. (2013) Statistical downscaling of daily temperature and rainfall data from global circulation models: In South Wollo zone, North Central Ethiopia. J. Res. Sci. Tech. 2013.

Stocker, T. ed., (2014). Climate change 2013: the physical science basis: Working Group I contribution to the Fifth assessment report of the Intergovernmental Panel on Climate Change. Cambridge University Press.

Teutschbein and Jan Seibert (2010): Regional Climate Models for Hydrological Impact Studies at the Catchment Scale, Department of Physical Geography and Quaternary Geology, Stockholm University,2010 accessed data 8/20/2019, 834–860.

Tocker TF, Qin D, Plattner GK, Tignor M, Allen SK, et al. (2013) Climate Change 2013: The Physical Science Basis. Contribution of Working Group I to the Fifth Assessment Report of the Intergovernmental Panel on Climate Change. Cambridge University Press, Cambridge, United Kingdom and New York, NY, USA, p: 1535.

United Nation Economic Commission for Africa (UNECA); African Climate Policy Center (ACPC). (2011). Climate Change and water resource of Africa: Challenges and opportunities and impacts; Working Paper 5; UNECA: Addis Ababa, Ethiopia.

Van Griensven, A., Meixner, T., Grunwald, S., Bishop, T., Diluzio, M., Srinivasan, R. 2006. A global sensitivity analysis tool for the parameters of multi-variable catchment models. Journal of Hydrology, 324, pp. 10-23.

van Roosmalen, L., Sonnenborg, T. O., & Jensen, K. H. (2009). Impact of climate and land use change on the hydrology of a large-scale agricultural catchment. Water Resources Research, 45(7). accessed date 12/4/2018.

Van Vuuren D.P., Edmonds J., Thomson A., Riahi K., Kainuma M., Matsui T., Hurtt G.C., Lamarque J- F., Meinshausen M., Smith S. (2016). Representative concentration pathways: an overview. In: Climatic Change, 109, 5- 31.

Vörösmarty, C. J., Douglas, E. M., Green, P. A., & Revenga, C. (2005). Geospatial indicators of emerging water stress: an application to Africa. AMBIO: A journal of the Human Environment, 34(3), 230-236.Getachew, B. (2017). Trend analysis of temperature and rainfall in south Gonder zone, Ethiopia. Journal of Degraded and Mining Lands Management. ISSN, 5, 1111-1125.

Wurbs, R. A.; Muttiah, R. S.; Felden, F. 2005. Incorporation of climate change in water availability modeling. Journal of Hydrologic Engineering

WWDSE, T. (2008). Lake Tana sub-basin four dams project, final feasibility report for Ribb irrigation project, volume III: hydrological report. WaterWorks Design and Supervision Enterprise and TAHAL.

Zeray, L., Roehrig, J., & Dilnesaw, A. C. (2006). Climate change impact on Lake Ziway watershed water availability, Ethiopia. In Paper Presented at the Conference on International Agricultural Research for Development.

APPENDICES

Appendix: - A Meteorological data

Table: - A1 Location of selected Meteorological stations of Tana Sub-Basin

STATION	STATION NAME	LONGITUDE	LATITUDE	ELEVATION
1	Addis Zemen	37.77313	12.11652	1940
2	Gondar	37.4319	12.52115	1973
3	Dangila	36.846	11.4337	2116
4	Bahir Dar	37.385	11.595	1800
5	Debre Tabor	37.9954	11.8666	2612
6	Enfranz	37.62593	12.25847	1937
7	Maksegnit	37.5551	12.3884	1912
8	Zege	37.31243	11.68878	1801
9	Gorgora	37.3	12.25	1830

Table: - A2 Selected Annual Precipitation of Tana Sub-Basin Stations.

Year	Dangila	Bahir Dar	Zege	Gorgora	Debe-Tabar	Addis Zemen	Maksegnit	Enfranz	Gonder
1988	1797.2	1355.5	1253.6	1093.2	1346.9	1093.2	927.4	1187.4	949.1
1989	1646.2	1621.1	1094.1	1052.9	1263.7	1052.9	645.5	844.9	958.1

1990	1563.8	1422.3	823.8	843.8	1009.0	843.8	692.3	1096.5	777.1
1991	2164.1	1734.8	1184.0	1078.8	1138.7	1078.8	844.3	1259.3	862.8
1992	1413.1	1403.4	1174.5	920.3	1011.9	920.3	628.3	1035.9	850.4
1993	1715.6	1591.5	1162.1	1131.2	1395.4	1130.7	724.6	1303.6	1066.6
1994	1317.9	1076.5	1125.9	990.3	1126.6	990.0	649.5	1146.8	905.2
1995	1184.6	1186.4	1782.9	904.2	1154.8	904.2	663.5	791.5	896.5
1996	1654.7	1380.0	1718.4	1698.3	1108.3	1698.3	1474.8	1047.1	1041.4
1997	1667.2	1217.5	1517.1	1336.8	1301.6	1336.8	1512.0	796.2	924.9
1998	1568.9	1448.3	1854.1	1084.3	1228.1	1084.3	1360.7	1145.8	1427.8
1999	1959.4	1477.6	1896.9	1058.9	1333.9	1058.9	1611.8	1016.3	1726.5
2000	1895.7	1563.8	1632.6	1193.3	1290.0	1193.3	1332.1	788.4	1458.9
2001	1411.1	1585.4	1381.2	1194.9	1270.1	1194.9	1687.8	1162.3	1709.9
2002	1349.8	1534.9	1826.9	1059.5	1092.4	1059.5	777.4	1293.3	882.7
2003	1369.4	1560.9	1659.0	820.1	911.5	820.1	922.0	998.0	956.0
2004	1627.9	1388.2	1487.8	1004.9	1010.6	1004.9	952.3	1025.2	1137.3
2005	1405.4	1488.4	1756.8	989.9	978.6	989.9	922.0	1640.3	986.2
2006	1869.0	1655.7	1880.5	1172.6	1403.9	1172.6	1172.1	1780.4	1174.6
2007	1478.7	1260.0	1537.6	1150.8	1245.7	1150.8	1007.9	1316.4	1143.7
2008	1858.1	1428.5	1645.0	955.1	1245.1	955.1	1191.6	1160.4	1177.8
2009	1454.6	971.2	1496.2	839.5	1247.9	839.5	746.9	887.6	951.3
2010	1392.3	1344.7	2264.4	867.6	1009.4	867.6	901.7	1068.8	1050.9
2011	1599.2	1228.3	1998.9	1034.5	1128.1	1034.5	1033.1	1331.8	989.6
2012	1640.4	1391.9	1847.9	942.1	1284.6	942.1	920.8	1247.5	1099.8

2013	1920.4	1522.3	2193.7	1048.8	1078.2	1048.8	900.4	1310.4	917.4
2014	2008.2	1693.5	1661.9	1366.0	1243.8	1366.0	941.9	1423.9	1198.0
2015	1731.0	1162.2	1361.7	1478.6	1178.9	1478.6	854.3	1161.8	1027.8
2016	1595.5	1502.6	1675.0	1400.2	1234.2	1400.2	1043.9	1310.8	1057.2
2017	1903.2	1596.7	1712.7	1031.8	1205.0	1031.8	887.1	1580.5	1387.4

Table: - A3 Selected Annual Minimum Temperature of Tana Sub-Basin Stations

year	Dangila	Bahir Dar	Zege	Gorgora	Debre Tabor	Addis Zemen	Maksegnit	Enfranz	Gonder AP
1988	9.4	12.4	10.5	14.5	10.3	8.7	14.8	8.8	12.8
1989	9.2	12.5	9.5	13.4	9.3	8.1	14.6	10.0	11.2
1990	9.6	12.4	8.2	14.6	9.7	8.9	14.6	9.3	12.3
1991	6.7	11.7	10.0	12.0	9.1	8.4	18.3	9.9	12.8
1992	7.2	13.1	10.5	14.3	9.7	7.8	13.2	10.0	13.8
1993	7.7	13.0	10.0	13.9	9.4	10.6	12.6	10.1	13.7
1994	8.4	13.8	10.6	13.4	9.6	12.7	12.9	10.3	14.2
1995	8.4	12.6	11.4	14.2	9.9	12.0	13.7	14.1	14.4
1996	8.1	13.3	11.8	13.2	9.6	12.5	11.9	14.3	14.0
1997	8.2	13.8	10.0	14.5	9.7	12.1	13.4	14.5	13.7
1998	9.9	11.4	11.4	14.5	9.9	10.5	13.4	14.9	11.8
1999	8.2	12.6	10.9	11.3	9.4	10.0	13.1	14.3	11.9
2000	7.1	12.8	11.2	12.4	9.3	10.6	13.2	14.2	12.7
2001	9.8	12.3	11.4	12.5	9.5	11.5	13.4	14.3	13.2
2002	9.7	13.4	10.6	12.3	9.4	13.0	13.9	15.1	13.8

2003	9.8	13.5	9.9	13.1	9.4	7.1	13.8	14.8	14.2
2004	9.6	13.1	10.9	12.8	9.4	7.7	13.9	14.6	13.9
2005	9.6	12.9	12.0	13.6	9.4	6.9	13.4	14.4	14.1
2006	9.9	12.9	11.7	14.1	9.6	11.0	14.0	13.9	13.4
2007	9.9	10.3	12.2	13.7	9.6	12.4	13.6	13.0	13.2
2008	9.8	11.6	12.4	13.8	9.5	12.1	13.8	14.6	13.7
2009	10.0	11.8	12.0	12.0	9.9	12.4	13.8	15.0	13.5
2010	10.3	12.8	12.1	11.8	8.4	13.8	14.0	15.0	13.1
2011	9.8	11.5	11.7	11.9	8.8	13.1	14.0	14.7	14.1
2012	9.6	12.4	11.9	14.0	9.3	12.2	13.6	14.4	14.1
2013	9.8	11.7	12.3	13.7	9.3	12.6	14.4	14.8	14.1
2014	10.3	12.9	11.9	12.2	9.6	12.8	14.9	14.6	13.8
2015	10.7	13.8	13.1	12.6	10.0	12.0	15.1	15.2	14.4
2016	10.2	12.4	12.6	11.6	9.4	10.2	14.7	15.0	14.3
2017	10.1	13.7	11.8	13.2	9.4	9.2	14.6	14.0	14.4

Table: - A4 Selected Annual Maximum Temperature of Tana Sub-Basin Stations

year	Dangila	Bahir Dar	Zege	Gorgora	Debre Tabor	Addis Zemen	Maksegnit	Enfranz	Gonder AP
1988	24.9	26.9	28.4	27.3	21.1	28.1	26.0	26.7	26.2
1989	24.0	26.2	29.4	27.3	21.2	28.3	25.6	26.0	25.8
1990	24.8	27.0	27.9	27.8	22.1	26.5	26.1	27.5	26.8
1991	25.4	26.3	25.2	27.6	21.5	24.1	25.6	27.2	26.0
1992	24.1	26.4	25.5	28.0	21.3	27.4	24.5	27.3	26.3
1993	23.8	26.8	25.2	28.8	21.1	27.3	24.0	27.9	26.1

1994	24.6	26.5	26.0	28.3	22.5	27.7	24.9	27.2	27.0
1995	25.1	27.1	26.9	28.9	22.1	28.1	26.0	27.8	27.3
1996	24.5	27.1	25.7	28.8	21.5	26.4	27.2	27.3	26.6
1997	24.6	27.7	27.2	29.4	21.6	28.2	28.0	27.8	27.0
1998	24.8	27.4	27.5	29.9	22.0	26.3	28.1	27.9	27.4
1999	24.6	27.0	27.7	28.9	22.0	27.2	27.9	27.9	27.3
2000	24.5	27.1	27.6	29.3	21.8	29.9	28.2	27.2	27.4
2001	24.7	27.1	28.4	29.3	22.1	27.8	28.5	25.9	26.6
2002	25.6	27.5	28.5	29.3	22.9	28.5	29.1	27.3	26.0
2003	26.0	27.9	28.9	29.2	22.5	28.5	29.1	28.4	28.1
2004	25.5	27.2	28.5	28.3	22.4	29.6	28.4	27.8	27.5
2005	25.7	27.0	27.8	30.0	22.6	29.5	28.6	28.0	27.6
2006	25.2	26.8	28.5	29.3	22.5	29.8	28.0	25.7	27.1
2007	25.1	26.8	28.1	28.2	22.3	30.1	28.3	27.8	27.2
2008	25.3	26.8	28.1	29.5	21.9	29.8	27.9	28.6	27.4
2009	26.1	27.6	28.8	29.1	22.8	30.3	29.2	29.8	28.0
2010	25.8	27.1	28.1	28.5	22.3	30.9	28.7	29.8	27.5
2011	25.5	27.0	28.2	28.6	22.1	31.7	28.6	28.9	27.1
2012	25.9	27.6	28.3	29.4	23.5	31.4	28.0	29.0	27.4
2013	25.5	28.8	28.4	29.0	23.4	29.7	28.0	29.2	27.5
2014	25.1	27.8	27.9	28.3	22.9	28.4	27.3	28.3	27.2
2015	25.9	28.6	28.8	29.5	22.9	29.3	27.5	29.8	27.9
2016	25.7	28.3	28.4	29.0	22.3	29.0	27.4	29.2	27.3
2017	25.2	27.8	28.9	28.3	22.4	28.6	27.2	27.7	27.7

Appendix: - B Data Quality Test

Table: - B1 Homogeneity test of Tana Sub-Basin Stations

Month	Dangila	Gonder	Maksegnit	Enfranz	Bahir Dar	Gorgora	Addis Zemen	Debre Tabor	Zege
Jan	0.07471	0.10714	0.04006	0.06608	0.05316	0.04240	0.0424	0.1079	0.3685
Feb	0.14878	0.17016	0.06176	0.03923	0.09926	0.23143	0.2314	0.0919	0.3387
Mar	0.73707	0.49898	0.42383	0.34380	0.31529	0.62029	0.6203	0.4852	0.7398
Apr	1.59409	1.08567	0.98204	0.55225	0.76519	1.22678	1.2268	1.3001	1.0933
May	4.03091	3.07778	2.29235	2.29127	2.60582	2.75008	2.7501	3.7291	3.0547
Jun	7.12737	5.84291	4.85094	5.37728	5.67119	5.93684	5.9368	6.2844	6.7199
Jul	11.34570	10.21986	9.74402	11.4558	10.5277	9.49910	9.4991	9.3895	10.8013
Aug	10.07643	9.79695	9.44121	10.87308	11.31471	9.21064	8.9821	9.9465	10.6403
Sep	6.52403	3.87866	3.80175	4.40247	6.19044	4.09703	4.0970	5.0704	6.0734
Oct	3.57833	2.53017	1.76410	1.90584	2.50846	2.16165	2.3162	3.1235	2.6785

Nov	1.05817	0.71160	0.51756	0.44908	0.42928	0.66575	0.6657	0.5610	0.7375
Dec	0.17971	0.26558	0.10959	0.10166	0.10937	0.26192	0.2619	0.1018	0.3452

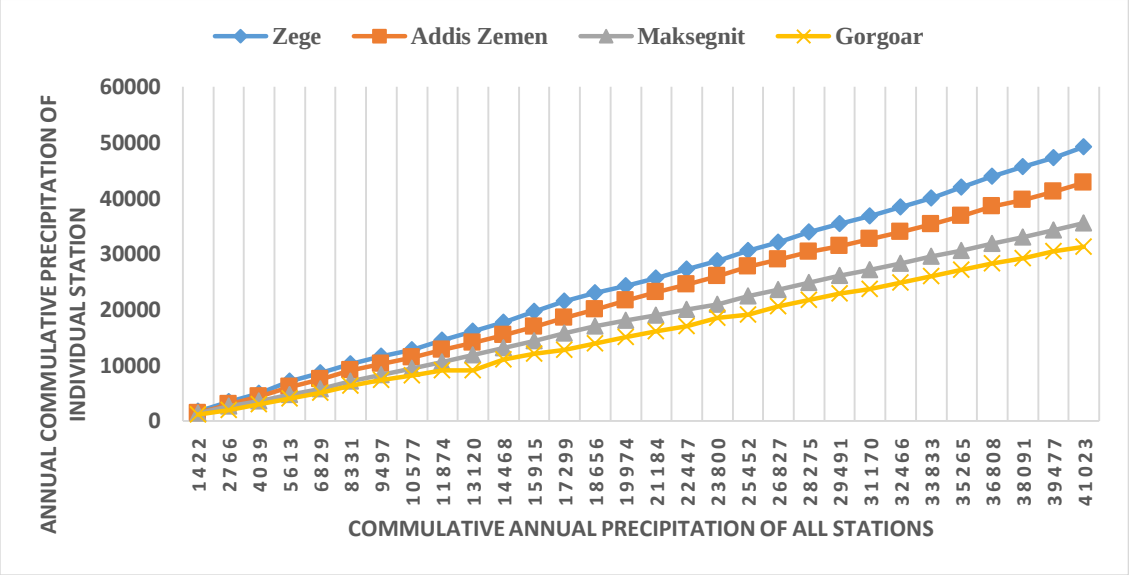

Figure: - B2 Consistency test of the remaining stations of Tana Sub-Basin

Appendix: - C Hydrological Data

Table: - C1 Annual Stream Flow of Tana Sub-Basin

Year	Gilgel Abay	Abbay	Gummara	Ribb	Megech
1988	21214.795	66674.336	14909.933	6799.747	2419.965
1989	21124.598	42342.632	11687.205	4184.164	873.982
1990	14862.343	24465.713	11469.26	4628.667	1070.338
1991	21676.555	56924.567	11727.714	9748.457	1019.561
1992	19706.088	43727.766	11009.633	7757.983	1487.319
1993	22805.24	55668.356	12283.055	5100.894	1787.134
1994	17328.431	55668.356	14127.611	6882.738	2173.288
1995	16260.352	21845.235	11631.969	4447.197	2106.075

1996	27237.653	50700.675	19686.77	6873.122	2246.002
1997	20847.927	49255.193	18082.85	4374.667	1827.751
1998	10705.035	43925.708	4400.731963	2232.069	1146.819
1999	14228.608	49188.517	7249.300667	5457.105	2318.961
2000	22130.613	63959.009	13460.45333	5638.763	2795.271
2001	19276.459	63761.2	12285.85	5636.338	3160.899
2002	15432.199	49632.766	11911.023	3324.713	1634.634
2003	19331.919	30241.776	19331.919	5389.087	2724.087
2004	17086.434	27862.575	17065.568	4064.234	2723.593
2005	15070.858	32172.043	15037.009	5497.118	3404.221
2006	26619.4901	55423.527	13891.37369	7079.726	4828.394
2007	21468.525	71221.0039	12099.19267	7948.686	6148.7

Appendix: - D Soil Lookup Table

OBJECTID	MUID	SEQN	SNAM	S5ID	CMPPCT	NLAYERS	HYDGRP	SOL_ZMX	ANION_EXCL	SOL_CRK	TEXTURE
1	VT029	1	chromic luvisols	VT0041	16	3	B	1800	0.5	0.5	C
2	VT027	2	eutric cambisols	VT0017	42	2	B	600	0.5	0.5	L
3	VT023	3	Eutric Fluvisols	NY0006	3	4	B	736.6	0.5	0.5	SIL-CN--SIL-CNV-SIL-UWB
4	VT021	4	Eutric Leptosols	ME0044	0	2	C	650	0.5	0.5	CL
5	ET022	5	Eutric Regosols	VT0012	1	3	A	1000	0.5	0.5	lomy sand
6	VT021	6	Eutric Vertisols	NY0096	0	7	C	2422.4	0.5	0.5	C
7	ET077	7	Haplic Alisols	ME0021	0	1	B	600	0.5	0.5	LS
8	VT021	8	Haplic Luvisoils	ET019	0	3	D	1400	0.5	0.5	C
9	VT021	9	Haplic Nitisols	VT0007	5	3	C	1651	0.5	0.5	LFS-S-VFSL
10	VT023	10	Lithic Leptosols	VT0018	1	4	D	1574.8	0.5	0.5	C-C-C-C
11	VT091	11	URBAN LAND	DC0035	8	1	D	152.4	0.5	0.5	VAR
12	VTW	12	WATER	DC0038	3	1	D	25.4	0.5	0.5	

SOL_Z1	SOL_BD1	SOL_AWC1	SOL_K1	SOL_CBN1	CLAY1	SILT1	SAND1	ROCK1	SOL_ALB1	USLE_K1	SOL_EC1
250	1.22	0.11	2.64	3.77	56.91	32.64	10.45	0	0.13	0.18	0.09
250	1.3	0.12	2.44	4.2	47.07	28.29	24.62	0.03	0.11	0.15	0.09
279.4	1.25	0.19	26	3.49	11.5	56.14	32.36	7.51	0.01	0.32	0
200	1.1	0.11	25	2	50	34	17	5	0.13	0.22	0
100	1.62	0.15	360	0.58	8	12	80	18	0.321	0.157739	0.1
181.68	1.1	0.11	4.34	1.47	60.6	23.3	16.1	0	0.09	0.2	0
600	1.5	0.06	68.22	1.87	8.5	11.68	79.82	0	0.28	0	0.16
200	1.23	0.1	3.17	5.54	54.37	30.7	14.94	0	0.07	0.16	0.09
203.2	1.7	0.14	700	1.74	3	16.7	80.3	1.94	0.01	0.24	0
177.8	1.35	0.19	1.7	5.81	62.5	26.24	11.26	0	0.01	0.49	0
152.4	1.5	0.1	500	0	15	30	55	20	0.23	0.28	0
25.4	1.72	0	260	0	0	0	0	0	0.23	0	0

SOL_Z2	SOL_BD2	SOL_AWC2	SOL_K2	SOL_CBN2	CLAY2	SILT2	SAND2	ROCK2	SOL_ALB2	USLE_K2	SOL_EC2
650	1.17	0.1	1.34	1.74	65.69	25.58	8.74	0	0.3	0.17	0.06
900	1.33	0.13	1.75	2.3	47.03	30.71	22.27	0	0.24	0.15	0.07
457.2	1.35	0.14	15	0.29	11.5	56.14	32.36	20.93	0.13	0.28	0
650	1.23	0.1	13	1.1	66	14	20	0.01	0.13	0.22	0
300	1.2	0.098	18.76	1.6	26	22	52	0	0.0224	0.2814	0
363.4	1.27	0.11	4.54	1.37	60.6	18.6	20.8	0	0.09	0.2	0
0	0	0	0	0	0	0	0	0	0	0	0
650	1.17	0.09	1.26	2.43	67.95	23.03	9.03	0	0.23	0.16	0.06
812.8	1.7	0.06	600	0.58	3	1.51	95.49	1.94	0.08	0.24	0
914.4	1.38	0.13	0.14	0.58	75	17.58	7.42	0	0.08	0.49	0

0	0	0	0	0	0	0	0	0	0	0	0
0	0	0	0	0	0	0	0	0	0	0	0

SOL_Z3	**SOL_BD3**	**SOL_AWC3**	**SOL_K3**	**SOL_CBN3**	**CLAY3**	**SILT3**	**SAND3**	**ROCK3**	**SOL_ALB3**	**USLE_K3**	**SOL_EC3**
1600	1.13	0.1	0.98	0.46	68.38	22.37	9.26	0	0.5	0.16	0.06
0	0	0	0	0	0	0	0	0	0	0	0
711.2	1.83	0.09	6.8	0.29	11.5	56.14	32.36	51.86	0.13	0.2	0
0	0	0	0	0	0	0	0	0	0	0	0
1000	1.3	0.098	13.01	0.9	26	21	52	0	0.0863	0.2814	0
847.85	1.28	0.11	5.16	1.41	62.6	17	20.4	0	0.09	0.3	0
0	0	0	0	0	0	0	0	0	0	0	0
1400	1.14	0.1	0.95	0.89	68.01	21.99	9.99	0.01	0.42	0.16	0.07
1651	1.6	0.13	54	0.19	10.5	25.49	64.01	0	0.16	0.43	0
1168.4	1.38	0.12	0.1	0.19	75	17.58	7.42	0	0.16	0.49	0
0	0	0	0	0	0	0	0	0	0	0	0
0	0	0	0	0	0	0	0	0	0	0	0

SOL_Z4	**SOL_BD4**	**SOL_AWC4**	**SOL_K4**	**SOL_CBN4**	**CLAY4**	**SILT4**	**SAND4**	**ROCK4**	**SOL_ALB4**	**USLE_K4**	**SOL_EC4**
0	0	0	0	0	0	0	0	0	0	0	0
0	0	0	0	0	0	0	0	0	0	0	0
736.6	2.5	0.01	500	0.1	5	25	70	98	0.19	0	0
0	0	0	0	0	0	0	0	0	0	0	0
0	0	0	0	0	0	0	0	0	0	0	0
1029.54	1.22	0.11	4.24	0.88	62.8	8.4	28.8	0	0.09	0.3	0
0	0	0	0	0	0	0	0	0	0	0	0
0	0	0	0	0	0	0	0	0	0	0	0
0	0	0	0	0	0	0	0	0	0	0	0
1574.8	1.4	0.11	0.07	0.06	75	17.58	7.42	0	0.2	0.49	0

0	0	0	0	0	0	0	0	0	0	0	0
0	0	0	0	0	0	0	0	0	0	0	0

SOL_Z5	**SOL_BD5**	**SOL_AWC5**	**SOL_K5**	**SOL_CBN5**	**CLAY5**	**SILT5**	**SAND5**	**ROCK5**	**SOL_ALB5**	**USLE_K5**	**SOL_EC5**	**SOL_Z6**	**SOL_BD6**	**SOL_AWC6**	**SOL_K6**
0	0	0	0	0	0	0	0	0	0	0	0	0	0	0	0
0	0	0	0	0	0	0	0	0	0	0	0	0	0	0	0
0	0	0	0	0	0	0	0	0	0	0	0	0	0	0	0
0	0	0	0	0	0	0	0	0	0	0	0	0	0	0	0
0	0	0	0	0	0	0	0	0	0	0	0	0	0	0	0
1392.9	1.13	0.11	4.34	1.17	62.6	9.4	28	0	0.09	0.3	0	1635.15	1.1	0.11	4.24
0	0	0	0	0	0	0	0	0	0	0	0	0	0	0	0
0	0	0	0	0	0	0	0	0	0	0	0	0	0	0	0
0	0	0	0	0	0	0	0	0	0	0	0	0	0	0	0
0	0	0	0	0	0	0	0	0	0	0	0	0	0	0	0
0	0	0	0	0	0	0	0	0	0	0	0	0	0	0	0
0	0	0	0	0	0	0	0	0	0	0	0	0	0	0	0

SOL_CBN6	**CLAY6**	**SILT6**	**SAND6**	**ROCK6**	**SOL_ALB6**	**USLE_K6**	**SOL_EC6**	**SOL_Z7**	**SOL_BD7**	**SOL_AWC7**	**SOL_K7**	**SOL_CBN7**	**CLAY7**	**SILT7**	**SAND7**
0	0	0	0	0	0	0	0	0	0	0	0	0	0	0	0
0	0	0	0	0	0	0	0	0	0	0	0	0	0	0	0
0	0	0	0	0	0	0	0	0	0	0	0	0	0	0	0
0	0	0	0	0	0	0	0	0	0	0	0	0	0	0	0
0	0	0	0	0	0	0	0	0	0	0	0	0	0	0	0
1.24	60	12.7	27.3	0	0.09	0.2	0	2422.44	1.2	1.1	0.09	4.04	0.34	63.6	16.6
0	0	0	0	0	0	0	0	0	0	0	0	0	0	0	0

0	0	0	0	0	0	0	0	0	0	0	0	0	0	0	0
0	0	0	0	0	0	0	0	0	0	0	0	0	0	0	0
0	0	0	0	0	0	0	0	0	0	0	0	0	0	0	0
0	0	0	0	0	0	0	0	0	0	0	0	0	0	0	0
0	0	0	0	0	0	0	0	0	0	0	0	0	0	0	0

ROCK7	**SOL_ALB7**	**USLE_K7**	**SOL_EC7**	**SOL_Z8**	**SOL_BD8**	**SOL_AWC8**	**SOL_K8**	**SOL_CBN8**	**CLAY8**	**SILT8**	**SAND8**	**ROCK8**	**SOL_ALB8**	**USLE_K8**	**SOL_EC8**
0	0	0	0	0	0	0	0	0	0	0	0	0	0	0	0
0	0	0	0	0	0	0	0	0	0	0	0	0	0	0	0
0	0	0	0	0	0	0	0	0	0	0	0	0	0	0	0
0	0	0	0	0	0	0	0	0	0	0	0	0	0	0	0
0	0	0	0	0	0	0	0	0	0	0	0	0	0	0	0
19.8	0	0.09	0.3	0	0	0	0	0	0	0	0	0	0	0	0
0	0	0	0	0	0	0	0	0	0	0	0	0	0	0	0
0	0	0	0	0	0	0	0	0	0	0	0	0	0	0	0
0	0	0	0	0	0	0	0	0	0	0	0	0	0	0	0
0	0	0	0	0	0	0	0	0	0	0	0	0	0	0	0
0	0	0	0	0	0	0	0	0	0	0	0	0	0	0	0
0	0	0	0	0	0	0	0	0	0	0	0	0	0	0	0

SOL_Z9	**SOL_BD9**	**SOL_AWC9**	**SOL_K9**	**SOL_CBN9**	**CLAY9**	**SILT9**	**SAND9**	**ROCK9**	**SOL_ALB9**	**USLE_K9**	**SOL_EC9**	**SOL_Z10**	**SOL_BD10**	**SOL_AWC10**	**SOL_K10**
0	0	0	0	0	0	0	0	0	0	0	0	0	0	0	0
0	0	0	0	0	0	0	0	0	0	0	0	0	0	0	0

0	0	0	0	0	0	0	0	0	0	0	0	0	0	0	0
0	0	0	0	0	0	0	0	0	0	0	0	0	0	0	0
0	0	0	0	0	0	0	0	0	0	0	0	0	0	0	0
0	0	0	0	0	0	0	0	0	0	0	0	0	0	0	0
0	0	0	0	0	0	0	0	0	0	0	0	0	0	0	0
0	0	0	0	0	0	0	0	0	0	0	0	0	0	0	0
0	0	0	0	0	0	0	0	0	0	0	0	0	0	0	0
0	0	0	0	0	0	0	0	0	0	0	0	0	0	0	0
0	0	0	0	0	0	0	0	0	0	0	0	0	0	0	0
0	0	0	0	0	0	0	0	0	0	0	0	0	0	0	0

SOL_CBN10	**CLAY10**	**SILT10**	**SAND10**	**ROCK10**	**SOL_ALB10**	**USLE_K10**	**SOL_EC10**	**SOL_CAL1**	**SOL_CAL2**	**SOL_CAL3**	**SOL_CAL4**	**SOL_CAL5**	**SOL_CAL6**	**SOL_CAL7**	**SOL_CAL8**
0	0	0	0	0	0	0	0	0	0	0	0	0	0	0	0
0	0	0	0	0	0	0	0	0	0	0	0	0	0	0	0
0	0	0	0	0	0	0	0	0	0	0	0	0	0	0	0
0	0	0	0	0	0	0	0	0	0	0	0	0	0	0	0
0	0	0	0	0	0	0	0	0	0	0	0	0	0	0	0
0	0	0	0	0	0	0	0	0	0	0	0	0	0	0	0
0	0	0	0	0	0	0	0	0	0	0	0	0	0	0	0
0	0	0	0	0	0	0	0	0	0	0	0	0	0	0	0
0	0	0	0	0	0	0	0	0	0	0	0	0	0	0	0
0	0	0	0	0	0	0	0	0	0	0	0	0	0	0	0
0	0	0	0	0	0	0	0	0	0	0	0	0	0	0	0
0	0	0	0	0	0	0	0	0	0	0	0	0	0	0	0

SOL_CAL9	SOL_CAL10	SOL_PH1	SOL_PH2	SOL_PH3	SOL_PH4	SOL_PH5	SOL_PH6	SOL_PH7	SOL_PH8	SOL_PH9	SOL_PH10
0	0	0	0	0	0	0	0	0	0	0	0
0	0	0	0	0	0	0	0	0	0	0	0
0	0	0	0	0	0	0	0	0	0	0	0
0	0	0	0	0	0	0	0	0	0	0	0
0	0	0	0	0	0	0	0	0	0	0	0
0	0	0	0	0	0	0	0	0	0	0	0
0	0	0	0	0	0	0	0	0	0	0	0
0	0	0	0	0	0	0	0	0	0	0	0
0	0	0	0	0	0	0	0	0	0	0	0
0	0	0	0	0	0	0	0	0	0	0	0
0	0	0	0	0	0	0	0	0	0	0	0
0	0	0	0	0	0	0	0	0	0	0	0

Appendix: - E Observed and Simulated stream flow and SWAT-CUP model calibration and validation result

Table: - E1 Annual stream flow of observed and simulated stream flow.

year	Observed	Simulated
1990	2248.5313	5105.43
1991	2866.3401	6037.61
1992	2633.16	6395.77
1993	2226.2673	4991.9
1994	2626.2673	4945.26
1995	2316.2255	4970.92

1996	3054.0831	6309.36
1997	2587.1225	5650.18
1998	3414.9339	7213.9
1999	4013.8571	7742.5
2000	3566.9853	7451.5
2001	3451.654	6398.92

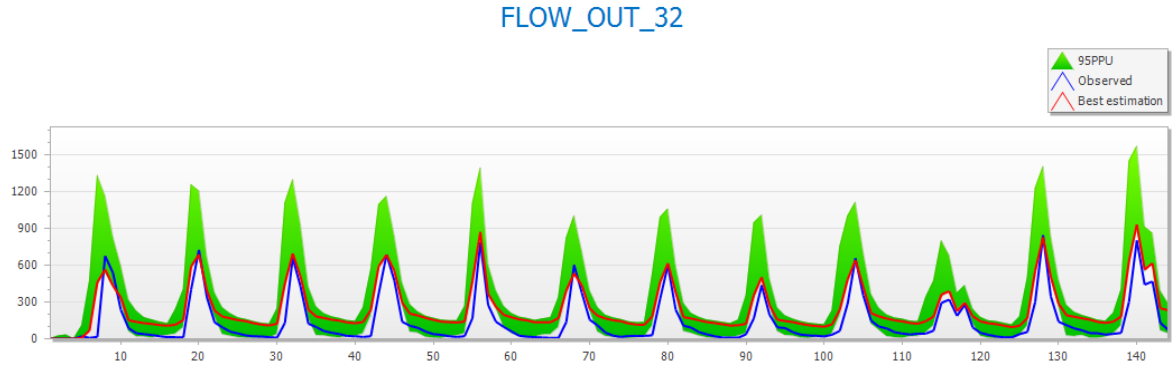

Figure: - E2 Observed and simulated monthly flow hydrograph during calibration

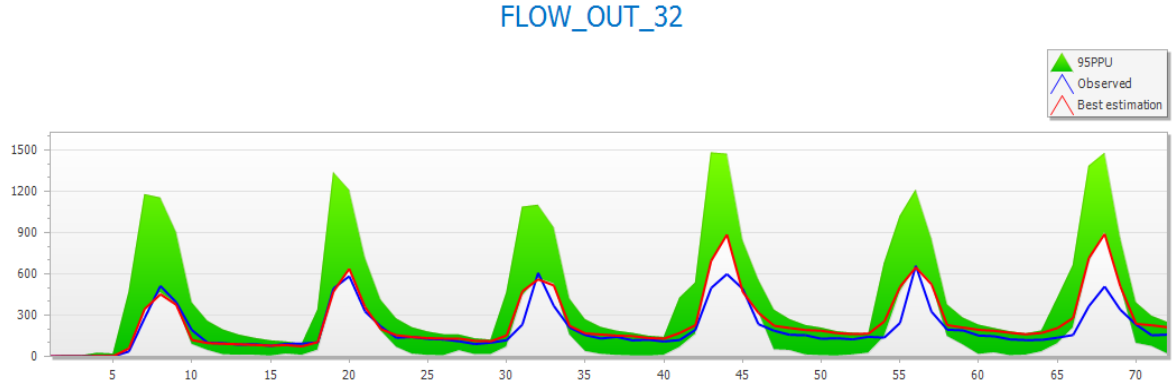

Figure: - E3 Observed and simulated monthly flow hydrograph during validation

Appendix: - F future climate change and stream flow analysis

Table: - F1 Future Climate Change projection relative to observed data in precipitation, temperature and future stream flow values for;(A) Precipitation, (B) and (C) Temperature and (D) stream flow

A. Two Future scenario periods Percentage change in precipitation relative to baseline period

MONTH	RCP4.5 (2020-2049)	RCP4.5(2050-2079)	RCP8.5(2020-2049)	RCP8.5 (2050-2079)
Jan	-1.231847965	-0.912716453	3.331317717	-2.807701701
Feb	-2.056705865	-3.096389767	-4.550778563	-13.46459014
Mar	2.040163664	-4.079326369	-14.84023843	2.525491585
Apr	1.570561129	16.86933614	6.692351954	11.60907475
May	2.716505702	5.742543976	-2.843620458	21.29695389
Jun	-44.38277386	-38.73039015	-48.8708962	-44.48937089
Jul	-17.52073209	-27.83049015	-68.15429677	-57.86030515
Aug	-43.33273406	-37.8679333	-56.35051743	-34.19233866
Sep	-2.882814589	-1.484946244	-30.35377389	-3.480103378
Oct	-2.019012412	-2.905161876	5.396291149	3.945617005
Nov	-4.635556075	-16.31866159	-26.20613143	-11.42167514
Dec	32.46069936	7.023707566	11.04604054	8.705288314

B. Change in minimum (℃) temperature relative to baseline period

month	RCP4.5 (2020-2049)	RCP4.5 (2050-2079)	RCP8.5 (2020-2049)	RCP8.5 (2050-2079)
Jan	0.0448	1.2663	1.5822	2.1898
Feb	0.2829	2.7743	1.3966	1.8576
Mar	1.0655	2.6679	0.4687	2.3276
Apr	0.7498	2.0752	1.0608	2.3268
May	0.6745	2.0536	0.1465	2.5259
Jun	0.1030	0.9672	0.9088	1.3352
Jul	0.1572	0.6693	0.2552	1.1258
Aug	0.2026	0.4526	0.2423	1.0021
Sep	0.5364	2.3838	0.5295	1.4889
Oct	0.2861	2.2320	0.5329	2.0977

Nov	0.0261	2.2139	1.5830	2.6828
Dec	0.0540	1.6584	0.1631	1.7344

C. Change in maximum (℃) temperature relative to baseline period

Month	RCP4.5 (2020-2049)	RCP4.5 (2050-2079)	RCP8.5 (2050-2079)	RCP8.5 (2020-2049)
Jan	0.2836	0.0969	0.2527	0.1125
Feb	0.6398	1.1466	2.0324	1.7494
Mar	1.4583	1.9109	1.2360	1.3753
Apr	1.5963	1.4342	2.0253	1.9188
May	1.3414	1.6114	2.1744	1.7654
Jun	0.2562	0.5584	0.5631	0.4406
Jul	1.2697	0.1889	0.1935	0.8313
Aug	0.7485	0.9877	0.1859	0.8267
Sep	1.3350	1.5089	1.6174	1.3856
Oct	1.2094	1.1945	1.2883	1.1784
Nov	1.6049	1.1085	1.5516	1.0861
Dec	1.2641	1.3629	1.3756	1.2490

D. Change in future stream flow

Month	RCP4.5 (2020-2049)	RCP4.5 (2050-2079)	RCP8.5 (2020-2049)	RCP8.5 (2050-2079)
Jan	-1.2318	-0.9127	-8.3313	-22.8077
Feb	-2.0567	-3.0964	-42.5508	-13.4646
Mar	-2.0402	-4.0793	-14.8402	2.5255
Apr	1.5706	16.8693	6.6924	11.6091
May	2.7165	5.7425	-2.8436	21.2970
Jun	44.3828	38.7304	48.8709	44.4894
Jul	17.5207	27.8305	68.1543	57.8603
Aug	43.3327	37.8679	56.3505	34.1923
Sep	2.8828	1.4849	30.3538	3.4801
Oct	2.0190	2.9052	5.3963	3.9456
Nov	-4.6356	-16.3187	-26.2061	-11.4217
Dec	-4.4607	-7.0237	-81.0460	-31.7053